Exploring the Role of Endoplasmic Reticulum Calcium Dynamics in Maintaining Cholesterol Homeostasis

by

Wen-An Jennifer Wang

A thesis submitted in partial fulfillment of the requirements for the degree of

Doctor of Philosophy

Department of Biochemistry

University of Alberta

Abstract

Calreticulin is an endoplasmic reticulum (ER) protein chaperone and calcium (Ca^{2+}) binding protein and is therefore important for maintaining ER homeostasis. Calreticulin deficiency is embryonic lethal in mice due to inadequate inositol trisphosphate receptor ($InsP_3R$)-mediated Ca^{2+} signaling and Ca^{2+}/calcineurin-dependent activation of transcription factors involved in cardiogenesis. Cardiac-specific expression of constitutively active calcineurin allows for normal cardiac development of calreticulin-deficient mice and rescues embryonic lethality in mice. However, the rescued *Calr*$^{-/-}$ mice have disrupted energy metabolism, with a high concentration of triacylglycerols and cholesterol in the blood plasma indicating the existence of a link between lipid metabolism and calreticulin.

The objective of the research within this thesis was to explore the consequence of disrupted ER homeostasis in maintaining cholesterol homeostasis. Specifically, we investigated the consequence of the absence of calreticulin on cholesterol metabolism controlled through the sterol regulatory binding protein (SREBP) pathway. We discovered that in the absence of calreticulin, there was increased accumulation of lipids in *Calr*$^{-/-}$ cells and *Caenorhabditis elegans* and this increase was attributed to the increased activation of SREBP and *de novo* lipid biosynthesis. This increase in SREBP activity and lipid biosynthesis in the absence of calreticulin occur in the absence of cholesterol depletion and intracellular levels of unesterified cholesterol were abundant.

To unravel this conundrum, we investigated the effect of the chaperone activity of calreticulin on components of the SREBP processing pathway and found that the SREBP processing pathway was fully functional in the absence of calreticulin. Next, we investigated the Ca^{2+} binding

function of calreticulin and identified that in the absence of calreticulin Ca^{2+} binding, the reduction of ER Ca^{2+} stores caused a re-distribution of the intracellular unesterified cholesterol away from the sensing mechanism of the SREBP processing pathway. Therefore we were able to establish a link between ER Ca^{2+} and cholesterol homeostasis.

Having established the connection between of ER Ca^{2+} and cholesterol homeostasis, we next investigated the mechanism behind the role of ER Ca^{2+} in the distribution of intracellular cholesterol. ER Ca^{2+} dynamics is a tightly regulated event that involves the level of ER Ca^{2+} stores, ER Ca^{2+} release and ER Ca^{2+} refilling regulated by a process known as store-operated Ca^{2+} entry (SOCE). Therefore, we investigated the role of SOCE as a mechanism behind the observed redistribution of unesterified cholesterol and increased SREBP activity in the absence of calreticulin and reduced ER Ca^{2+} conditions. We discovered that the stromal interaction molecule 1 (STIM1), an integral ER membrane protein that senses ER Ca^{2+} levels and an important component of SOCE, and its recently discovered cholesterol binding domain plays an important role in intracellular unesterified cholesterol distribution and SREBP activity. We hypothesize that STIM1 may function in binding ER membrane unesterified cholesterol and play a role in the movement of cholesterol between the ER and plasma membrane. Furthermore, this movement and distribution of unesterified cholesterol may be affected by ER Ca^{2+} status and SOCE activity.

Preface

The literature review presented in chapter 1 of this thesis is my original work.

Chapter 2 and 3 have been published as W.A. Wang, W.X. Liu, S. Durnaoglu, S.K. Lee, J. Lian, R. Lehner, J. Ahnn, L.B. Agellon and M. Michalak, "Loss of Calreticulin Uncovers a Critical Role for Calcium in Regulating Cellular Lipid Homeostasis," *Scientific Reports*, vol. 7, issue 1, 5941-5955. The laboratory of Sun-Kyung Lee at the Research Institute of Natural Science in Hanyang University, Seoul, performed the experiments and analyzed the data presented in Figure 2.3 and Figure 2.9. I performed all other experiments and data analysis, and also prepared and edited the manuscript. M. Michalak was the supervisory author and was involved in manuscript preparation.

The data and analysis presented in chapter 4 are my original work, as is the concluding discussions presented in chapter 5.

Acknowledgments

My PhD degree would not have been the fulfilling journey that it was without the many individuals who I have the pleasure of calling mentor, friend and family. I would like to thank my supervisor Marek, for accepting me into the lab all those years ago as a young and naïve summer student. Thank you for your guidance and support these past 9 years. I have learned so much from your generous attitude towards life and your passion towards science and have enjoyed all of our conversations from science to politics to philosophy. Thank you for being an amazing boss.

To Jody, Asia, Alison and Ela, I want to thank you for all of your constant care and guidance, the stability that you provide and all of your advice in both science and life. To all former and present members of the Michalak lab, including Daniel, Qian, Wen-Xin, Dukgyu, Hector and Lauren, thank you for all the lovely lunch room conversations, I have learned so much from each of you and could not have asked for a more talented or friendly group of individuals to work with.

To my collaborators, Dr. Agellon, Dr. Lehner and Dr. Lee, thank you for your expertise and contribution throughout my research. To Russ and Jihong, thank you for your help with the many lipid pulse chase and extraction experiments. To my supervisory committee Dr. Young and Dr. Fahlman, thank you for all of your advice and guidance throughout my degree and for the abundant number of reference letters. To Dr. Sipione and Dr. Chen, thank you for agreeing and taking the time to serve as my PhD defence examiners. To Dr. Parrish, thank you for being such a great career mentor and for all your support in the GTL program.

I would also like to acknowledge the funding agencies, the Alberta Cancer Foundation and the Canadian Institutes of Health Research, for funding my research.

To all of my friends, thank you for your support these last few years and for being my source of distraction from the ups and downs that come with science. Firstly, I am grateful for my fellow yogi Emily, thank you for keeping me sane with all the food and shopping adventures. Thank you to my hiking/camping buddies Maryam, Chloe and Melanie for all of our conquered trips in the Rockies. Thank you to my climbing buddies Joe and Gareth for all the trips to the wall. Thank you to my friend Ply for all the random activities around the city. Lastly, I want to thank all my teammates who played with me on Eastern Bloc, Scibabes, Kiss My Fatty Acids and DiscTrick 12; it has been such a pleasure.

Finally, but most importantly, I would like to thank my mom and dad, Hsiang-Yun and Li-Fu, for blindly supporting me these 6 years, unsure of what my PhD was about or where it would lead. Thank you both for bringing me to Canada and then encouraging me to venture out freely and on my own despite the constant worries. You have always been my source of motivation and stability, thank you for being amazing parents.

Table of Contents

List of Tables

List of Figures

List of Abbreviations

ABCA3	ATP binding cassette class A 3
α-MHC	α-myosin heavy chain
ANOVA	analysis of variance
ApoB100	apolipoprotein B
ATF6	activating transcription factor 6
eIF2α	eukaryotic initiating factor 2α
Ca^{2+}	calcium
Calr	calreticulin
CHAPS	3-[(3-cholamidopropyl)dimethylammonio]-1-propanesulfonate
CMV	cytomegalovirus
Cre	cyclization recombination
DIC	differential interference contrast
DMEM	Dulbecco's Modified Eagle's Medium
EDTA	ethylenediaminetetraacetic acid
EGTA	ethylene-bis(oxyethylenenitrilo)tetraacetic acid
ER	endoplasmic reticulum
ERAD	ER associated degradation
ERSE	ER stress response element
E-SYT	synaptotagmin
FASN	fatty acid synthase
FBS	fetal bovine serum

GAPDH	glyceraldehyde 3-phosphate dehydrogenase
GP78	glycoprotein 78
GRP78	glucose-regulated protein 78
HDL	high-density lipoprotein
Hepes	4-(2-hydroxyethyl)-1-piperazineethanesulfonic acid
HMG-CoA	3-hydroxy-3-methylgluaryl-CoA
HRP	horseradish peroxidase
IDI1	isopentyl-diphosphate delta isomerase 1
IDL	intermediate-density lipoprotein
INSIG	insulin-induced gene
$InsP_3R$	inositol 1,4,5-trisphosphate receptor
IRE1α	inositol-requiring enzyme 1α
LDL	low-density lipoprotein
LDLR	LDL receptor
LSS	lanosterol synthase
MβCD	methyl-β-cyclodextrin
MCS	membrane contact site
mutSRE	mutated SRE
MVD	mevalonate pyrophosphate decarboxylase
NaDOC	sodium deoxycholate
nATF6	nuclear ATF6
Ni-NTA	nickel-nitrilotriacetec acid
NPC1	Niemann-Pick type C1

nSREBP	N-terminus of SREBP
OHT	4-hydroxytamoxifen
Orai1	calcium release activated channel 1
ORP	oxysterol-binding protein
PBS	phosphate-buffered saline
PDI	protein disulfide-isomerase
PERK	protein kinase RNA-like ER kinase
PFO	Perfringolysin O
PIP	phosphoinositide
$PI(4,5)P_2$	phosphatidylinositol (4,5) bisphosphate
PIPES	piperazine-N,N'-bis(2-ethanesulfonic acid)
RFP	red fluorescent protein
RI1	replication initiator 1
RIPA	Radioimmunoprecipitation
RT-qPCR	reverse transcriptase quantitative polymerase chain reaction
S1P	site-1 protease
S2P	site-2 protease
SCAP	SREBP cleavage activating protein
SDS-PAGE	sodium dodecyl sulfate polyacrylamide gel electrophoresis
SERCA	sarco-endoplasmic reticulum Ca^{2+} ATPase
SOAT	sterol O-acyltransferase
SOCE	store-operated Ca^{2+} entry
SQLE	squalene epoxidase

SRE	sterol regulatory element
SREBP	sterol regulatory element binding protein
STARD3	steroidogenic acute regulatory-related lipid transfer domain 3
STIM1	stromal interaction molecule 1
TG	thapsigargin
TLC	thin-layered chromatography
TPC	two-pore channel
TUN	tunicamycin
TRP	transient receptor potential
UBC7	ubiquitin-conjugating enzyme E2 7
UPR	unfolded protein response
VAP	vesicle-associated membrane protein
VCP	valosin-containing protein
VLDL	very-low-density lipoprotein
XBP1	X-box binding protein 1

Chapter One: General Introduction

The Endoplasmic Reticulum

The endoplasmic reticulum (ER) is a membranous organelle, accounting for 50% of an animal cell's total membrane surface. It is multifunctional and is involved in a wide variety of important cellular functions, notably the biosynthesis of lipids and proteins, and the storage of Ca^{2+} [1-3]. To maintain these numerous and distinct cellular functions and pathways, the ER is structurally and morphologically unique from other organelles and is constructed as a continuous heterogeneous network of membrane sheets and cisternae that extend from the nuclear envelope throughout the cytoplasm to the plasma membrane [4]. The ER sheets are flattened membrane-enclosed sacs and are stacked and concentrated close to the nucleus [5]. The cisternae are a network of tubular structures that vary in density throughout the cytoplasm, forming a polygonal network via three-way junctions [5, 6]. There are two types of ER, the "rough" and "smooth" ER. The "rough ER" is marked by the presence of membrane bound ribosomes on its outer cytosolic surface and is an important site for protein synthesis, folding, posttranslational modifications and secretion [6]. Conversely, the "smooth ER" is marked by the absence of ribosomes and is important for maintaining lipid homeostasis, playing an important role in lipid synthesis and generating and maintaining the cellular membranous network [6]. Due to its highly flexible and dynamic nature, the "smooth ER" also acts as a site for vesicular trafficking and make points of contact or interaction with other membranes and organelles through membrane contact sites (MCSs) [7].

Ca^{2+} Signaling

The ER is a major Ca^{2+} store and is therefore involved in numerous Ca^{2+} signaling events within the cell. The total concentration of total Ca^{2+} within the ER ranges from 0.4 – 1 mM, which is in

contrast to the low cytosolic Ca^{2+} concentration of ~100 nM [3, 8]. This large contrast in Ca^{2+} concentrations between the ER and the cytosol is achieved through the many Ca^{2+} buffering proteins and transporters within the ER. During a Ca^{2+} signaling event, activation of the inositol 1,4,5-trisphosphate receptor ($InsP_3R$), an ER membrane $InsP_3$-dependent Ca^{2+} channel, causes a rapid release of Ca^{2+} from the ER into the cytoplasm [9, 10]. The resulting increase in cytoplasmic Ca^{2+} is responsible for regulation of a variety of cellular processes, including cell proliferation, metabolism and apoptosis [8].

The depletion of total ER luminal Ca^{2+} triggers a process called store-operated Ca^{2+} entry (SOCE). SOCE is a process whereby, the depletion of ER Ca^{2+} stores triggers the influx of Ca^{2+} across the plasma membrane from the extracellular space to sustain cytoplasmic Ca^{2+} signaling and allow for ER Ca^{2+} store refilling [1]. Stromal interaction molecule 1 (STIM1) is an ER type I transmembrane protein that acts as an ER Ca^{2+} sensor [11-13]. The EF-hand of STIM1 binds Ca^{2+} (K_d = ~0.2 – 0.6 mM) within the lumen of the ER [14, 15] and upon ER Ca^{2+} depletion, STIM1 extends its conformation [16, 17], oligomerize [14, 18] and moves towards the plasma membrane to form ER-plasma membrane MCSs [19, 20]. At the plasma membrane, STIM1 interacts with the cytoplasmic domain of the Ca^{2+} release activated channel 1 (Orai1) [21-25], causing oligomerization and the formation of an active Ca^{2+} channel, allowing Ca^{2+} influx through the plasma membrane [26-30]. This influx of Ca^{2+} across the plasma membrane sustains the elevated cytoplasmic Ca^{2+} signal, important for a number of cellular processes such as T-cell activation, and allows for the refilling of ER Ca^{2+} stores through the sarco-endoplasmic reticulum Ca^{2+} ATPase (SERCA), which functions to continuously pump Ca^{2+} back into the ER at the expense of ATP [8].

Protein Folding and Quality Control

One important function of the ER is to regulate the quality, folding and secretion of newly synthesized proteins. Approximately 30% of cellular proteins are made in the ER, for this purpose, the ER contains many molecular chaperones and enzymes that bind to nascent proteins and allow them to reach their native conformation [31]. Some of these include the glucose-regulated protein 78 (GRP78), which recognizes and binds exposed hydrophobic regions of unfolded proteins; calreticulin and calnexin, which interact with nascent proteins by binding to their monoglucosylated glycans; and protein disulfide-isomerase A3 (PDIA3), a folding enzyme that assists in forming protein disulfide linkages [32, 33].

The calreticulin/calnexin cycle is a major protein folding quality control pathway within the ER and it regulates the folding of N-glycosylated proteins. Nascent proteins synthesized by ER ribosomes will translocate into the ER lumen, whereby a $Glc_3Man_9GlcNAc_2$ oligosaccharide is attached by an oligosaccharyltransferase to the asparagine amino acid residue on the consensus sequence Asn-X-Ser/Thr of the peptide, through an amide linkage [32]. Within the lumen of the ER, two terminal glucose residues are sequentially cleaved by glucosidase I and II, allowing the protein to be recognized by calreticulin and calnexin within the quality control cycle [23]. Once bound and properly folded, the monoglucosylated protein undergoes de-glucosylation by glucosidase II and is sent onwards to the secretory pathway. In the case where the protein is not folded properly, it is recognized by UDP-glucose:glycoprotein glucosyltransferase and re-glucosylated for prolonged interaction with calreticulin and calnexin. This is repeated until the glycoprotein is folded properly, however if the protein is terminally misfolded, the quality machinery then targets the protein for ER associated degradation (ERAD) [33].

ER Stress and the Unfolded Protein Response

The ER is a site for many processes that are essential for the proper functioning of the cell. These processes include protein synthesis, folding, posttranslational modifications, Ca^{2+} signaling, lipid synthesis, assembly and trafficking of membranes and proteins, regulation of gene expression and signaling to other membranes and organelles [3, 34-37]. Therefore, it is critical for cells to maintain ER homeostasis. In an ever changing environment however, many different factors can perturb this homeostasis, disrupt protein folding processes within the ER and induce ER stress responses to counteract the disturbance; a particularly important ER stress response is the unfolded protein response (UPR).

The UPR is composed of three different pathways that fall under the control of three respective ER transmembrane proteins: protein kinase RNA-like ER kinase (PERK), inositol-requiring enzyme 1α (IRE1α) and activating transcription factor 6 (ATF6) [38-40]. Under unperturbed conditions, the majority of PERK, IRE1α and ATF6 form stable complexes with the ER stress sensor GRP78 and remain in their inactive states [41]. GRP78 binds to the ER luminal domains of PERK and IRE1α and prevents homodimerization and activity [42, 43]. GRP78 binding to ATF6 blocks its Golgi-localization signals, prevents ER to Golgi transport and ATF6 processing and activation [40, 44].

In the presence of cellular stress, misfolded proteins accumulate in the ER, bind to GRP78 competitively and cause GRP78 to dissociate from PERK, IRE1α and ATF6, removing GRP78 inhibitory effects [41, 42, 44]. Upon dissociation of GRP78, PERK dimerizes, autophosphorylates its cytoplasmic domains and turns on its kinase activity [42]. The kinase subunit of PERK phosphorylates and inhibits the eukaryotic initiating factor 2α (eIF2α), turning

off protein synthesis but selectively increasing the expression of pro-survival transcription factor ATF4 [39, 42, 45]. Similarly, upon GRP78 release from IRE1α, IRE1α undergoes dimerization and autophosphorylation, activating its endonuclease activity for mRNA processing [42, 46-50]. A particularly important target of IRE1α is the mRNA encoding X-box binding protein 1 (XBP1). IRE1α splices a 26 base pair region from the intron of the XBP1 mRNA and produces an active XBP1 transcription factor that binds to the ER stress response element (ERSE) within promoters to upregulate genes encoding protein chaperones and proteins involved in ERAD [50]. In the case of ATF6, release of GRP78 binding unmasks its Golgi-localization signals, allowing ATF6 to translocate to the Golgi. ATF6 is then sequentially cleaved by Golgi localizing site-1 and site-2 proteases (S1P and S2P), releasing the N-terminal ATF6 fragment, an active transcription factor that also binds to ERSE on the promoters of genes and increases the expression of XBP1, protein chaperones and proteins involved in ERAD [44, 50, 51]. Altogether, the UPR serves as a pro-survival mechanism to return the cell to its state of homeostasis by turning off protein translation and production of further misfolded proteins, increasing ERAD and expression of protein chaperones.

Calreticulin

An important protein chaperone that is upregulated by the UPR during ER stress is calreticulin. Calreticulin was first discovered in 1972 as an important Ca^{2+} binding protein in the sarcoplasmic reticulum of skeletal muscle and later on also as a Ca^{2+} binding protein of the ER in non-muscle tissue [52, 53]. Following the initial discovery of calreticulin, subsequent studies have established the importance of this one ER protein in regulating intracellular Ca^{2+} homeostasis, protein folding and a wide variety of signaling processes and pathophysiological

conditions including cardiogenesis, adipocyte differentiation, cancer and cellular immunity [32, 54].

Structure and Function

Calreticulin contains a cleavable ER targeting sequence at the N-terminus and a KDEL ER retrieval signal at the C-terminus and following posttranslational modifications, it is a 46kDa protein composed of three distinct and functional domains (Figure 1.1). The N-domain of calreticulin is globular in shape, forming a stable core that contains a disulphide bond and binding sites for polypeptides, carbohydrates and Zn^{2+} [32, 55]. The P-domain is proline-rich, has an extended region that interacts with PDIA3 and binds Ca^{2+} with high affinity and low capacity [32, 55, 56]. Together, the N and P domains are the folding unit important for the chaperone activity of calreticulin within the calreticulin/calnexin cycle [57]. Lastly, the C-domain, the carboxyl terminal region of calreticulin, consists of negatively charged and acidic residues which are responsible for binding Ca^{2+} with high capacity (25 mol of Ca^{2+} per one mol of protein) and low affinity (K_d = 2 mM) [55, 56]. The C and P domains are essential for the Ca^{2+} binding function of calreticulin, enabling calreticulin to bind 50% of ER $Ca^{2+}$and therefore function in maintaining Ca^{2+} homeostasis [55, 56, 58].

Calreticulin has been shown to modulate ER Ca^{2+} signaling. Overexpression of calreticulin in cells increases total ER Ca^{2+}stores and reduces STIM1 Ca^{2+} sensitivity and SOCE activity [59, 60]. In addition, calreticulin has been shown to modulate Ca^{2+} release through $InsP_3R$ [61, 62]. Calreticulin deficiency reduces total ER Ca^{2+}, causes misfolding of the bradykinin receptor and therefore disrupts bradykinin-mediated activation of $InsP_3R$ and Ca^{2+} release from the ER [61,

62]. This disruption in Ca^{2+} signaling in the absence of calreticulin can be restored with the expression of the NP domain of calreticulin [61].

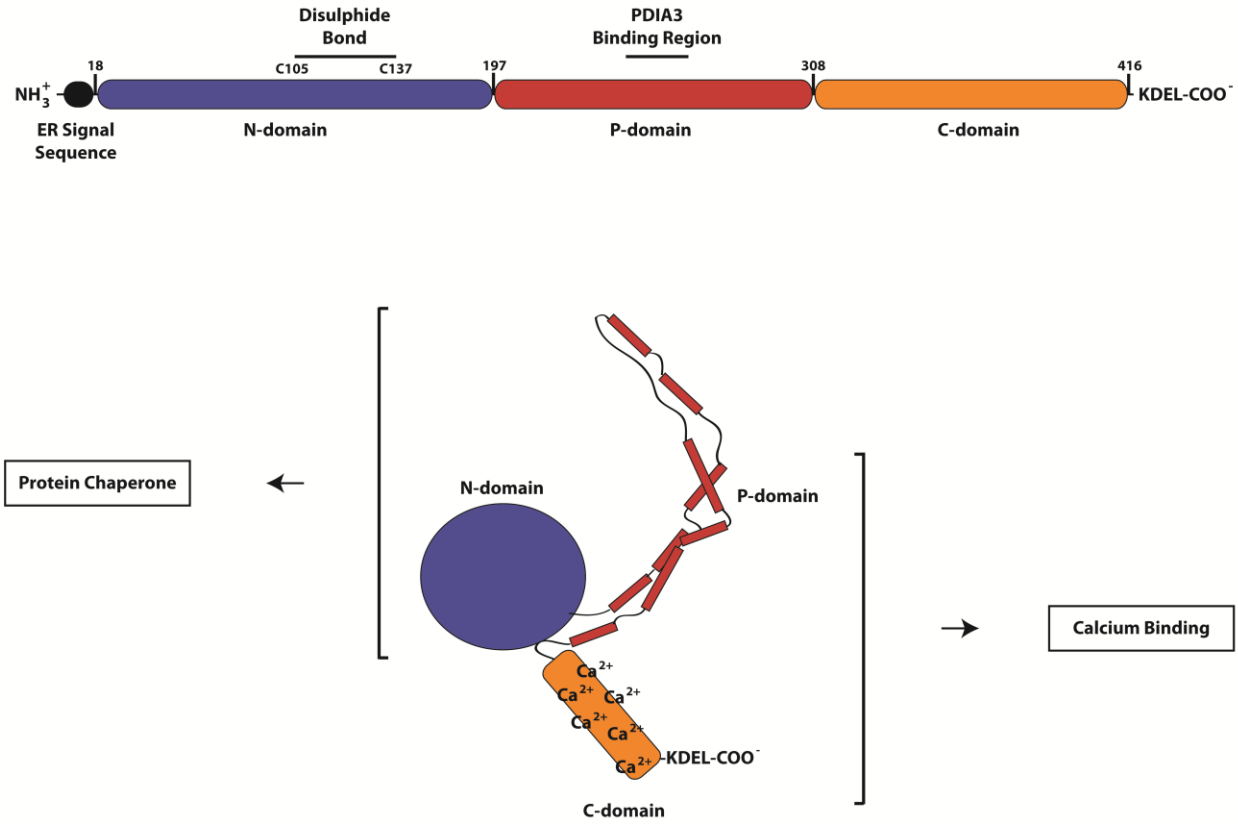

Figure 1.1 Structure and function of Calreticulin

A schematic representation of the domain and structure of calreticulin, in its linear (top) and folded (bottom) representations. Calreticulin is synthesized with a NH_3^+-terminal ER signal sequence, an N-globular domain (purple) that contains a pair of cysteines for disulphide bond formation, a P-domain (red) with a protein disulfide-isomerase A3 (PDIA3) interacting region, an acidic C-domain (orange) for binding Ca^{2+} with high capacity and lastly a COO^--terminal KDEL ER retrieval signal. Together, the N- and P- domains are responsible for the protein chaperone function of calreticulin. The C- and P- domains are responsible for the Ca^{2+} buffering function of calreticulin.

Calreticulin Deficiency

Calreticulin as a Ca^{2+} binding protein and a protein chaperone is critical in maintaining proper cellular function and is involved in many signaling processes and pathways. Calreticulin deficiency (*Calr*$^{-/-}$), which disrupts bradykinin receptor-mediated signaling and activation of the $InsP_3R$, is embryonic lethal in mice [62]. This is attributed to inadequate ER Ca^{2+} release through the $InsP_3R$ and insufficient activation of calcineurin during embryogenesis. Calcineurin is a Ca^{2+} and calmodulin-dependent serine-threonine phosphatase and is responsible for dephosphorylating and activating various transcription factors, a subset of which, is responsible for the expression of genes specific for cardiac development [63]. Therefore, in the absence of calreticulin, there is reduced Ca^{2+} signaling, reduced activation of calcineurin and insufficient transcription of Ca^{2+}/calcineurin-dependent genes involved in cardiogenesis, the main cause of embryonic lethality [62, 64, 65]. Cardiac specific overexpression of an activated calcineurin is sufficient to restore proper cardiac development and rescue the embryonic lethality seen in the *Calr*$^{-/-}$ mice [66]. The *Calr*$^{-/-}$ rescued mice, however, are short lived (an average lifespan of five weeks) and are presented with a number of metabolic problems. Specifically, in the absence of calreticulin, the rescued mice show stunted growth at week one and blood analysis reveal hypoglycemia and elevated levels of plasma cholesterol and triglycerides [66]. Overall the phenotype of the *Calr*$^{-/-}$ rescued mice suggested that calreticulin may play a role in modulating energy metabolism, including cholesterol metabolism.

Calreticulin deficiency in *Caenorhabditis elegans* is not embryonic lethal and *C. elegans* are therefore a useful model for characterizing the functions of calreticulin *in vivo*. The ER functions of calreticulin in *C. elegans* (designated as CRT-1, the calreticulin homologue in *C. elegans*) are

well characterized and similarly to mammalians, CRT-1 is both a protein chaperone and a Ca^{2+} binding protein. It is normally expressed in the intestine, pharynx, muscles, head neurons, coelomocytes and sperm [67]. Both CRT-1 and $InsP_3R$ are necessary for proper muscle function, a highly Ca^{2+} dependent process [68], in *C. elegans* suggesting the importance of calreticulin in regulating Ca^{2+} homeostasis [67]. CRT-1 is also involved in ER chaperone activity as illustrated by *Calr*$^{-/-}$ *C. elegans*, which are viable but exhibit temperature-dependent reproduction defects and an inability to cope with induced stress [67]. Studies also show that CRT-1 function in protein folding and quality control is important but not crucial and alternative mechanisms exist to compensate CRT-1 functions in *C. elegans* [69, 70]. These alternative mechanisms involve activation of compensatory chaperone pathways consisting of the GRP78 homologues, heat shock protein 3 and 4 and the PDI family proteins PDI-2 and PDI-3 [69]. Overall, *calr*$^{-/-}$ *C. elegans* are viable and develops a phenotype that is less severe than in mice, despite having similar roles and functions. In addition, the study of CRT-1 in *C. elegans* and its effect on lipid metabolism is a novel field and has not been investigated.

Cholesterol Homeostasis

Cholesterol is a lipid molecule that is important for cellular and physiological function. Structurally, cholesterol comprises four rings transfused together with an isooctyl hydrocarbon chain at one end and a hydroxyl group on the other end. Due to its amphiphilic nature, cholesterol, in its unesterified form (hence forth referred to as unesterified cholesterol), is able to exist in lipid bilayers and is essential for maintaining cell membrane fluidity and structure in mammals. Furthermore, cholesterol is the precursor to many physiologically important substances, including bile acids, oxysterols, steroid hormones and vitamin D [71]. Mammals

obtain cholesterol either through exogenous dietary intake or endogenous cholesterol synthesis through *de novo* pathways in the cell [72]. Furthermore, cells can package or mobilize cholesterol stored in cytosolic lipid droplets through the process of esterification and hydrolysis, respectively [72].

Cholesterol Uptake

Triglycerides and cholesterol are highly hydrophobic molecules that require protein association in order to be transported throughout the body, particularly, they are packaged into lipoproteins for transport through the blood plasma [73]. Plasma lipoprotein molecules contain a hydrophobic core with cholesterol esters and triglycerides and a surrounding phospholipid monolayer containing unesterified cholesterol and apolipoproteins [73]. Exogenous uptake of dietary lipids are bile-emulsified within the lumen of the intestine and triglycerides are hydrolyzed by pancreatic lipases into fatty acids and monoglycerides, which are then absorbed into epithelial cells that line the intestinal walls and re-esterified into triglycerides [73, 74]. The triglycerides and dietary cholesterol are then packaged with apolipoproteins into chylomicrons, the lipoproteins of the intestine [74]. The chylomicrons are then transported through the lymphatic system to the muscle and adipose tissue where the triglycerides are hydrolyzed by extracellular lipoprotein lipases into free fatty acids that are then metabolized by the myocytes and adipocytes [73]. The resulting chylomicron remnants are then delivered throughout the blood stream and taken up by the liver. Triglyceride and cholesterol are packaged into very-low-density lipoproteins (VLDL), which are delivered to muscle and adipose tissue and hydrolyzed by extracellular lipoprotein lipases to yield free fatty acids and intermediate-density lipoproteins (IDL) and eventually IDL are further hydrolyzed to form cholesterol rich low-density

lipoproteins [73]. The liver and intestine also makes high-density lipoproteins (HDL), which functions in reverse cholesterol transport through acquiring cholesterol and phospholipids from VLDL remnants, chylomicrons and cholesterol-rich extrahepatic cells and delivering the contents back to the liver [73].

For mammalian cells, the major source of exogenous cholesterol is from LDL particles, the major cholesterol carrying lipoprotein in the blood stream. It is composed mainly of cholesterol esters (40%) with a small portion of unesterified cholesterol (10%) and triglycerides (5%) all packaged in a phospholipid monolayer and organized by a single apolipoprotein B (ApoB100) molecule [75, 76]. LDL in the blood stream interacts with LDL receptors (LDLRs) presented on the cellular surface through its ApoB100 molecule and initiates receptor-mediated endocytosis to internalize the LDL particle [72, 75, 77]. Fusion of internalized LDL containing vesicles with acidic (pH<6) endosomal compartments causes the dissociation of LDLRs, which are then delivered through recycling endosomal compartments back to the plasma membrane [72]. The endosomes containing the cholesterol rich LDL particles eventually fuse with lysosomes. These are acidic hydrolytic compartments and contain acidic lipases that hydrolyze cholesterol esters to unesterified cholesterol [78]. The unesterified cholesterol are then delivered to the plasma membrane, where the majority of cellular unesterified cholesterol are distributed [79, 80]. Excess unesterified cholesterol at the plasma membrane may traffic to the ER membrane, where it can be redistributed to other parts of the cell or converted for storage [80].

Cholesterol *De Novo* Synthesis

Endogenous cholesterol biosynthesis is a complex and highly regulated pathway. The first step of cholesterol synthesis takes place in the cytosol and involves the condensation of two acetyl-

CoA molecules into acetoacetyl-CoA by the enzyme acetoacetyl-CoA thiolase 2 [71]. In the next step, 3-hydroxy-3-methylgluaryl-CoA (HMG-CoA) synthase catalyzes the condensation of acetoacetyl-CoA with another actyl-CoA to form HMG-CoA and Co-A [71]. This first part of cholesterol biosynthesis concludes with the synthesis of mevalonate from HMG-CoA. This step is a highly regulated step at the ER membrane and is catalyzed by HMG-CoA reductase, an integral membrane protein of the ER and the first committed enzyme in the pathway [71].

At the transcription level, HMG-CoA reductase expression is controlled in a sterol-dependent manner through the sterol regulatory element binding proteins (SREBPs) (discussed in more details on page 14 of chapter One) and at the post-transcriptional level, it is also controlled by sterols but involves accelerated HMG-CoA degradation mediated by insulin-induced gene (INSIG) [81, 82]. In cells where sterol levels are low HMG-CoA reductase undergoes degradation with a half-life of 12 hours. Under conditions where sterols accumulate and cholesterol biosynthesis is no longer required, the rate of HMG-CoA degradation increases and its half-life is reduced to less than 1 hour [81]. The sterols that regulate this degradation process include cholesterol but more potently lanosterol, a cholesterol precursor [83]. The accumulation of lanosterol within the ER membrane signals the cell to reduce cholesterol biosynthesis by inducing HMG-CoA reductase and INSIG interaction. The bound portion of INSIG is in complex with glycoprotein 78 (GP78), a membrane bound E3 ubiquitin ligase, which is in turn bound to ubiquitin-conjugating enzyme E2 7 (UBC7), an E2 protein that carries and supplies activated ubiquitin, and valosin-containing protein (VCP), an ATPase that is involved in ERAD [82, 83]. The lanosterol-mediated binding of HMG-CoA reductase to INSIG triggers the ubiquitination and proteosomal degradation of HMG-CoA reductase, which consequently blocks further biosynthesis of cholesterol [83].

The remaining steps of cholesterol biosynthesis involve a multistep pathway that converts mevalonate into two activated isoprenoid units, the formation of squalene from six isoprenoid units, the conversion of squalene to the four-ringed sterol lanosterol and eventually the 19 reactions that transforms lanosterol to the final sterol product cholesterol [71]. Cholesterol synthesized by the cell in the ER are then distributed to the plasma membrane or other organelles or esterified for cholesterol storage [72].

Cholesterol Storage

The accumulation of cholesterol within membranes can become cytotoxic and therefore, cells re-esterify excess membrane cholesterol for packaging and storage. Cholesterol esterification is the process whereby the carboxylate group of a long-chain fatty acid reacts and is added to the hydroxyl group of cholesterol through an ester linkage. In mammalians, this reaction is catalyzed by the ER membrane sterol O-acyltransferases (SOATs) 1 and 2, proteins of the membrane-bound *O*-acyltransferase family [84]. SOAT1 is ubiquitously expressed and preferably catalyzes the addition of oleoyl-CoA to cholesterol [85]. SOAT2 on the other hand is mostly expressed in the intestine and liver. The majority of cholesterol esters formed from SOATs partitions into lipid droplet storage within the cytoplasm. However, both SOAT1 and SOAT2 will also provide cholesterol esters for lipoprotein assembly in intestines and livers [84]. Both SOAT1 and SOAT2 are allosteric proteins activated by its sterol substrate cholesterol and therefore is able to sense levels of ER membrane cholesterol and gauge its activity accordingly [86].

Lipid droplets are classified as dynamic organelles that store triglycerides and cholesterol esters within the cell. Lipid droplets are composed of a hydrophobic lipid core surrounded by a phospholipid monolayer [87]. They are thought to originate and form from the cytosolic

membrane of the ER while lipids produced from the ER traffics to lipid droplets from these assimilated membranes [88]. Eventually the lipid droplets detach and move towards the cytoplasm as independent organelles. Mobilization of lipid droplet stores for energy metabolism and membrane synthesis occurs through lipolysis and lipophagy. Lipolysis is the process whereby lipids are broken down by cytosolic lipases and lipophagy occurs through the formation of an autophagosome, fusion with lysosome and consequently lipid degradation by lysosomal hydrolytic enzymes [89, 90].

As illustrated above, the ER membrane is the path of convergence for the exogenous uptake and trafficking, the endogenous *de novo* synthesis or for cellular storage of cholesterol. Therefore, the ER membrane is the most optimal location for the monitoring and control of cholesterol homeostasis.

The Sterol Regulatory Element-Binding Proteins

The SREBPs belong to a family of basic helix-loop-helix leucine zipper transcription factors and are synthesized as ER associated integral membrane proteins [91]. The SREBPs are thought to be the master regulators of lipid homeostasis by controlling the expression of genes involved in the uptake and biosynthesis of cholesterol and triglycerides [91].

Structure and Function

Structurally, the SREBPs are composed of three domains: an N-terminal transcription factor domain that contains a basic helix-loop-helix leucine zipper for DNA binding; two hydrophobic transmembrane regions separated by an ER luminal hydrophilic loop; and a C-terminal regulatory domain [91, 92]. The SREBPs are synthesized as inactive precursors and are ER

membrane bound with both the N- and C- terminus regions of the protein on the cytoplasmic side of the ER membrane [92]. Additionally, the C-terminus of SREBP is responsible for the interaction of SREBP with the C-terminus of another membrane protein called SREBP cleavage activating protein (SCAP) [82, 93].

There are three SREBP isoforms known as SREBP-1a, SREBP-1c and SREBP-2 [91]. SREBP-1a and -1c are synthesized from the same gene but regulated with different promoters through alternate splicing, while SREBP-2 is produced from a different gene altogether. Although structurally similar, especially at the N-terminus, all three SREBP isoforms activate target promoters with varying degrees of specificity and efficiency. These target promoters depict the genes to be regulated and contain different amounts and variations of the sterol regulatory element (SRE) nucleotide sequence (ATCACCCCAC), SRE-like nucleotide sequences and E-boxes (CANNTG) which are bound with different specificity and strength by each SREBP isoform [94]. SREBP-1a has been shown to activate genes containing SRE, SRE-like or E-box nucleotide sequences and regulates the expression of genes involved in the biosynthesis of cholesterol, fatty acids and triacylglycerols (Figure 1.2) [94, 95]. SREBP-1c activates genes containing SRE-like or E-box nucleotide sequences and is mainly responsible for the expression of genes in the biosynthetic pathway of fatty acids (Figure 1.2) [96]. Lastly, SREBP-2 activates genes containing SRE or SRE-like motifs and is mainly responsible for the expression of genes involved in cholesterol biosynthesis (Figure 1.2) [97, 98].

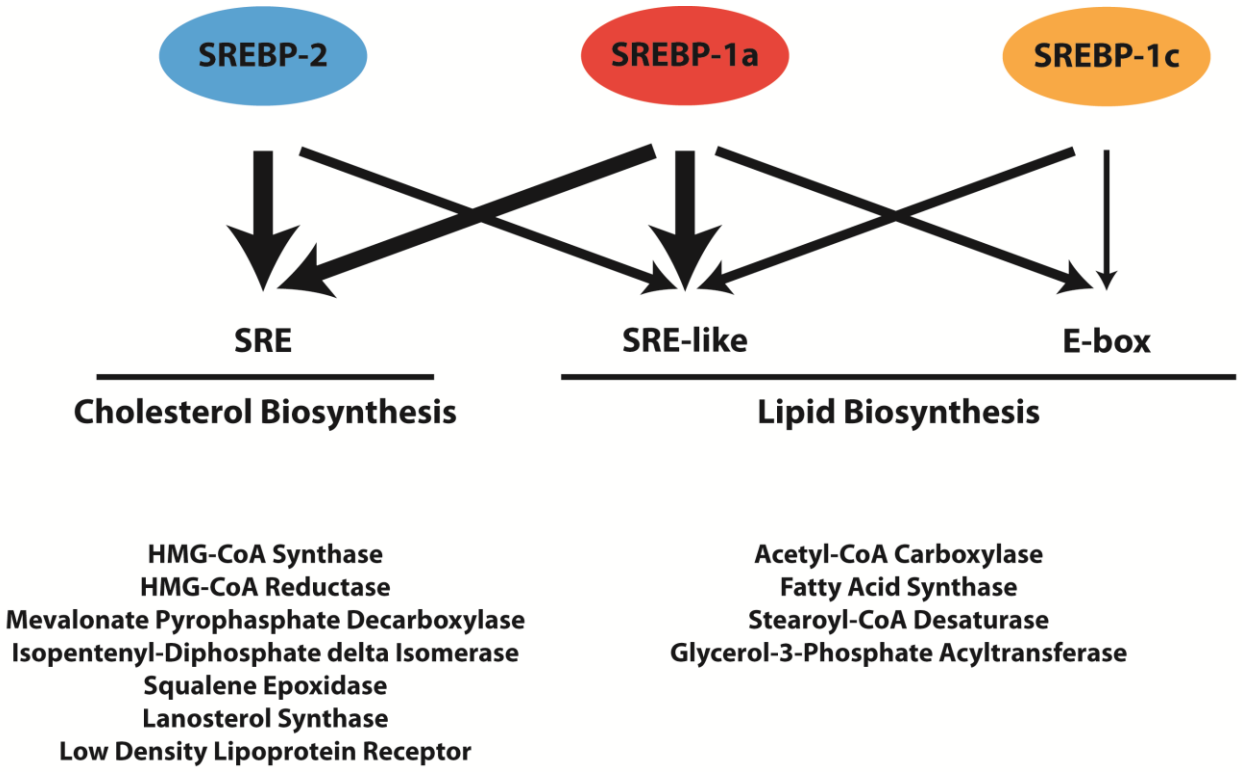

Figure 1.2 A schematic representation of the binding motifs and the main target genes of SREBPs

SREBP-2 activates genes containing the SRE or SRE-like motifs and mainly regulates genes involved in cholesterol biosynthesis. SREBP-1a activates genes containing the SRE, SRE-like or E-box motif and regulates genes involved in both cholesterol and lipid biosynthesis. SREBP-1c activates genes containing the SRE-like or E-box and mostly regulates genes involved in lipid biosynthesis. Some of the SREBP targeted enzymes involved in cholesterol and lipid biosynthesis are listed.

Regulation of SREBP Activity

As inactive precursors, the SREBPs require a proteolytic process to release the active amino-terminal transcription factor and this activation process is regulated by a molecular mechanism dependent upon the availability of ER membrane cholesterol (Figure 1.3) [99]. Although ER membrane cholesterol accounts for only ~1% of a cell's total cholesterol, it is the major site for monitoring total esterified and unesterified cholesterol [100]. The abundance of cellular cholesterol translates to an increase in ER membrane cholesterol and conversely, when there is a depletion of cellular cholesterol there is a decrease in ER membrane cholesterol. Under cholesterol abundant conditions (ER cholesterol > 5% mol of total ER lipids), ER membrane cholesterol binds to SCAP, favoring a conformation that allows binding of SCAP to INSIG, which anchors the SREBP-SCAP complex at the ER [82, 101, 102]. Under cholesterol depleted conditions (ER cholesterol < 5% mol of total ER lipids), there is a reduced interaction between INSIG and SCAP facilitated by ER membrane cholesterol and the portion of dissociated INSIG is rapidly ubiquitinated and degraded [102, 103]. Following dissociation from INSIG, SCAP is free to mediate the anterograde trafficking of the SREBP-SCAP complex to the Golgi where SREBP is processed and activated through sequential cleavage by Golgi localizing S1P and S2P [82, 104]. The proteolytic process releases the N-terminus of SREBP (nSREBP), an active transcription factor which translocates into the nucleus to activate transcription of genes involved in lipid biosynthesis. Direct termination of nSREBP activity is rapid due to its unstable nature with a half-life of 1-2 hours and degradation of nSREBP occurs through a phosphorylation-mediated ubiquitin-proteosomal pathway [105].

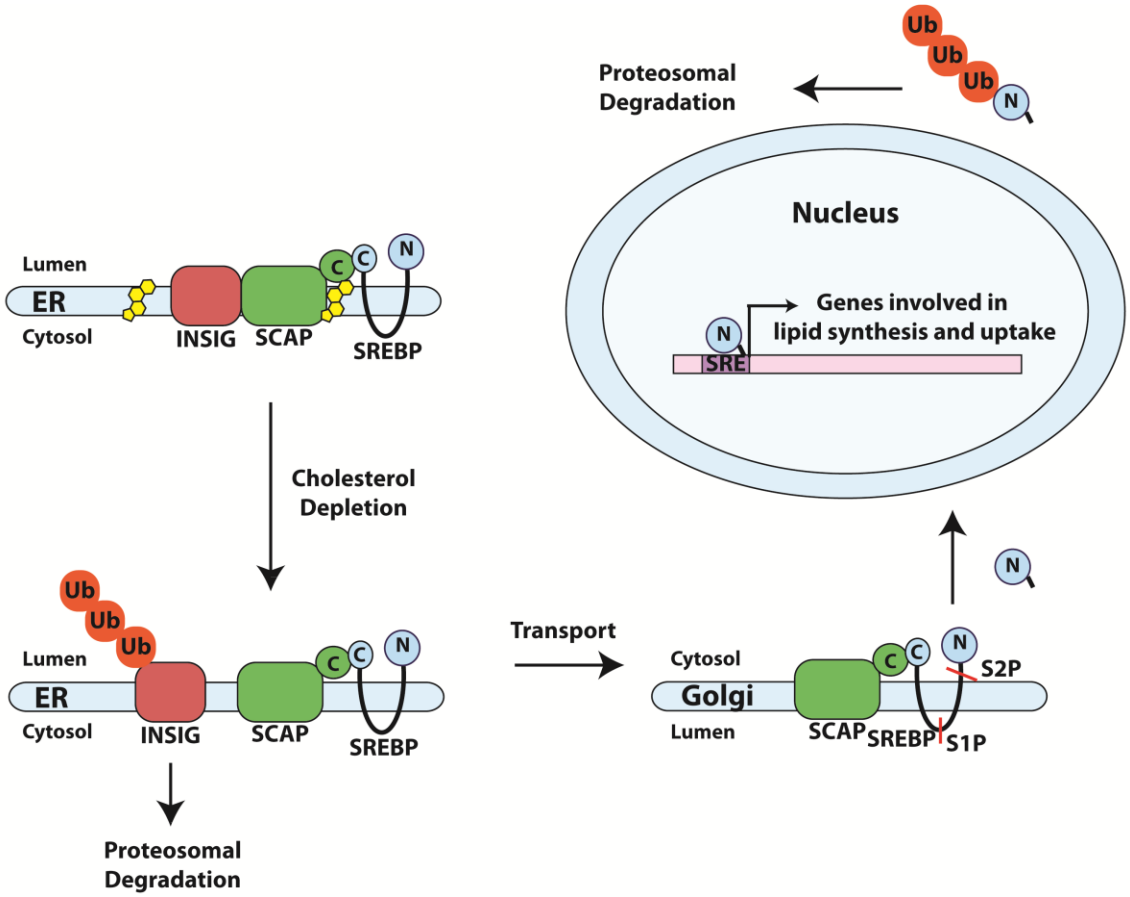

Figure 1.3 A schematic representation of the SREBP regulatory pathway

In the inactive state, the sterol regulatory element binding proteins (SREBPs) are synthesized as ER membrane precursors, complexed with SREBP cleavage activating protein (SCAP) and insulin induced gene (INSIG). Under cholesterol depleted conditions, SCAP as a membrane cholesterol sensor undergoes conformational change and dissociates from INSIG. Upon dissociation, INSIG becomes ubiquitinated and degraded. SCAP then mediates the transport of SREBP to the Golgi, where SREBP is sequentially cleaved by site-1 and site-2 proteases (S1P and S2P), releasing the active nSREBP transcription factor. The nSREBP will then translocate to the nucleus to activate transcription of genes involved in lipid biosynthesis. SREBP transcription activity is terminated upon ubiquitination and proteosomal degradation.

SREBP Activity and ER Stress

Past studies indicate that ER stress may regulate nSREBP activity regardless of sterol levels, but consensus on the underlying mechanism has not been reached [106]. It has been suggested that the increase in ERAD, through UPR activation, enhances SREBP processing and nSREBP activity due to the increase in INSIG degradation [107]. Another proposed mechanism, involve studies which show the binding of GRP78 to SREBP-1c and that overexpression of GRP78 inhibits SREBP-1c processing [108]. Therefore, GRP78 may be an inhibitory regulator of SREBP and this inhibitory effect is alleviated during ER stress, a mechanism for ER stress induced activation of SREBP. Other studies show that ER stress reduces ER to Golgi trafficking, disrupting ER intermediate Golgi compartments [109, 110]. The result is similar to that of cells treated with Brefeldin A, a molecule that inhibits anterograde trafficking and therefore prevents ER to Golgi transport. Brefeldin A treatment causes ER retention of S1P and S2P and unregulated SREBP processing [104]. Therefore, ER retention of S1P and S2P has also been suggested as a mechanism for ER stress induced SREBP activation [106].

Calreticulin Deficiency and Lipid Metabolism

The phenotypic disruption in lipid metabolism observed in the *Calr*$^{-/-}$ rescued mice may be attributed to a variety of pathways that maintain lipid homeostasis. The absence of calreticulin as a protein chaperone may have led to the disruption of lipid absorption or uptake from the blood stream. All members of the lipase gene family contain the consensus sequence Asn-X-Ser/Thr for N-linked glycosylation and are targeted for folding within the calreticulin/calnexin cycle in the ER [111]. Therefore in the absence of calreticulin the misfolding of these lipases may result in the inability for the organism to hydrolyze lipoproteins and in the accumulation of lipids in the

blood stream. The absence of calreticulin and the disruption in ER homeostasis could lead to an increase in lipoprotein assembly and secretion through the ER localizing SOAT1 and SOAT2 [84] as well as an increase in the *de novo* synthesis pathway of lipids through the ER membrane localizing SREBPs [104]. This thesis explores the effect of calreticulin deficiency and disrupted ER homeostasis on the *de novo* synthetic of lipids through the SREBP pathway.

Objectives

The objective of my PhD thesis was to investigate the molecular pathways responsible for the defect in energy metabolism observed in the *Calr*$^{-/-}$ rescued mice. Specifically I wanted to investigate the role of calreticulin and ER homeostasis in modulating cholesterol metabolism through the SREBP pathway.

Hypothesis

My hypothesis was that in the absence of calreticulin, SREBP processing and activity increases regardless of cholesterol status and therefore contributes to an increase in the biosynthesis of triglycerides and cholesterol. To test my hypothesis, I utilized wild-type and *Calr*$^{-/-}$ mouse embryonic cells and **1)** examined the effect of calreticulin deficiency on cholesterol metabolism, nSREBP activity and the SREBP processing pathway; **2)** reaffirmed the role of calreticulin deficiency in lipid metabolism *in vivo* using the *Calr*$^{-/-}$ *C. elegans* model; **3)** identified the function and domain of calreticulin responsible for modulating cholesterol metabolism; **4)** investigated the mechanism underlying the effect of calreticulin deficiency on the nSREBP activity and cholesterol metabolism.

References

[1] M.J. Berridge, M.D. Bootman, H.L. Roderick, Calcium signalling: dynamics, homeostasis and remodelling, Nature reviews. Molecular cell biology, 4 (2003) 517-529.
[2] D. Prins, M. Michalak, Organellar calcium buffers, Cold Spring Harbor perspectives in biology, 3 (2011) 197-212.
[3] J. Krebs, L.B. Agellon, M. Michalak, Ca(2+) homeostasis and endoplasmic reticulum (ER) stress: An integrated view of calcium signaling, Biochemical and biophysical research communications, 460 (2015) 114-121.
[4] H. Zhang, J. Hu, Shaping the Endoplasmic Reticulum into a Social Network, Trends in cell biology, 26 (2016) 934-943.
[5] J. Nixon-Abell, C.J. Obara, A.V. Weigel, D. Li, W.R. Legant, C.S. Xu, H.A. Pasolli, K. Harvey, H.F. Hess, E. Betzig, C. Blackstone, J. Lippincott-Schwartz, Increased spatiotemporal resolution reveals highly dynamic dense tubular matrices in the peripheral ER, Science, 354 (2016) pii: aaf3928.
[6] Y. Shibata, G.K. Voeltz, T.A. Rapoport, Rough sheets and smooth tubules, Cell, 126 (2006) 435-439.
[7] P. Georgiades, V.J. Allan, G.D. Wright, P.G. Woodman, P. Udommai, M.A. Chung, T.A. Waigh, The flexibility and dynamics of the tubules in the endoplasmic reticulum, Scientific reports, 7 (2017) 16474.
[8] D.E. Clapham, Calcium signaling, Cell, 131 (2007) 1047-1058.
[9] M.J. Berridge, Inositol trisphosphate and calcium signalling, Nature, 361 (1993) 315-325.
[10] K. Mikoshiba, M. Hattori, IP3 receptor-operated calcium entry, Science's STKE: signal transduction knowledge environment, 2000 (2000) pe1.
[11] J. Roos, P.J. DiGregorio, A.V. Yeromin, K. Ohlsen, M. Lioudyno, S. Zhang, O. Safrina, J.A. Kozak, S.L. Wagner, M.D. Cahalan, G. Velicelebi, K.A. Stauderman, STIM1, an essential and conserved component of store-operated Ca^{2+} channel function, The Journal of cell biology, 169 (2005) 435-445.
[12] J. Liou, M.L. Kim, W.D. Heo, J.T. Jones, J.W. Myers, J.E. Ferrell, Jr., T. Meyer, STIM is a Ca^{2+} sensor essential for Ca^{2+}-store-depletion-triggered Ca^{2+} influx, Current biology: CB, 15 (2005) 1235-1241.
[13] S.L. Zhang, Y. Yu, J. Roos, J.A. Kozak, T.J. Deerinck, M.H. Ellisman, K.A. Stauderman, M.D. Cahalan, STIM1 is a Ca^{2+} sensor that activates CRAC channels and migrates from the Ca^{2+} store to the plasma membrane, Nature, 437 (2005) 902-905.
[14] P.B. Stathopulos, G.Y. Li, M.J. Plevin, J.B. Ames, M. Ikura, Stored Ca^{2+} depletion-induced oligomerization of stromal interaction molecule 1 (STIM1) via the EF-SAM region: An initiation mechanism for capacitive Ca^{2+} entry, The Journal of biological chemistry, 281 (2006) 35855-35862.
[15] L. Zheng, P.B. Stathopulos, G.Y. Li, M. Ikura, Biophysical characterization of the EF-hand and SAM domain containing Ca^{2+} sensory region of STIM1 and STIM2, Biochemical and biophysical research communications, 369 (2008) 240-246.
[16] M. Fahrner, M. Muik, R. Schindl, C. Butorac, P. Stathopulos, L. Zheng, I. Jardin, M. Ikura, C. Romanin, A coiled-coil clamp controls both conformation and clustering of stromal interaction molecule 1 (STIM1), The Journal of biological chemistry, 289 (2014) 33231-33244.

[17] X. Yang, H. Jin, X. Cai, S. Li, Y. Shen, Structural and mechanistic insights into the activation of Stromal interaction molecule 1 (STIM1), Proceedings of the National Academy of Sciences of the United States of America, 109 (2012) 5657-5662.
[18] R.M. Luik, B. Wang, M. Prakriya, M.M. Wu, R.S. Lewis, Oligomerization of STIM1 couples ER calcium depletion to CRAC channel activation, Nature, 454 (2008) 538-542.
[19] Y. Baba, K. Hayashi, Y. Fujii, A. Mizushima, H. Watarai, M. Wakamori, T. Numaga, Y. Mori, M. Iino, M. Hikida, T. Kurosaki, Coupling of STIM1 to store-operated Ca^{2+} entry through its constitutive and inducible movement in the endoplasmic reticulum, Proceedings of the National Academy of Sciences of the United States of America, 103 (2006) 16704-16709.
[20] R.M. Luik, M.M. Wu, J. Buchanan, R.S. Lewis, The elementary unit of store-operated Ca^{2+} entry: local activation of CRAC channels by STIM1 at ER-plasma membrane junctions, The Journal of cell biology, 174 (2006) 815-825.
[21] S. Feske, Y. Gwack, M. Prakriya, S. Srikanth, S.H. Puppel, B. Tanasa, P.G. Hogan, R.S. Lewis, M. Daly, A. Rao, A mutation in Orai1 causes immune deficiency by abrogating CRAC channel function, Nature, 441 (2006) 179-185.
[22] C.Y. Park, P.J. Hoover, F.M. Mullins, P. Bachhawat, E.D. Covington, S. Raunser, T. Walz, K.C. Garcia, R.E. Dolmetsch, R.S. Lewis, STIM1 clusters and activates CRAC channels via direct binding of a cytosolic domain to Orai1, Cell, 136 (2009) 876-890.
[23] C. Peinelt, M. Vig, D.L. Koomoa, A. Beck, M.J. Nadler, M. Koblan-Huberson, A. Lis, A. Fleig, R. Penner, J.P. Kinet, Amplification of CRAC current by STIM1 and CRACM1 (Orai1), Nature cell biology, 8 (2006) 771-773.
[24] M. Vig, C. Peinelt, A. Beck, D.L. Koomoa, D. Rabah, M. Koblan-Huberson, S. Kraft, H. Turner, A. Fleig, R. Penner, J.P. Kinet, CRACM1 is a plasma membrane protein essential for store-operated Ca^{2+} entry, Science, 312 (2006) 1220-1223.
[25] M. Muik, I. Frischauf, I. Derler, M. Fahrner, J. Bergsmann, P. Eder, R. Schindl, C. Hesch, B. Polzinger, R. Fritsch, H. Kahr, J. Madl, H. Gruber, K. Groschner, C. Romanin, Dynamic coupling of the putative coiled-coil domain of ORAI1 with STIM1 mediates ORAI1 channel activation, The Journal of biological chemistry, 283 (2008) 8014-8022.
[26] M. Prakriya, S. Feske, Y. Gwack, S. Srikanth, A. Rao, P.G. Hogan, Orai1 is an essential pore subunit of the CRAC channel, Nature, 443 (2006) 230-233.
[27] M. Vig, A. Beck, J.M. Billingsley, A. Lis, S. Parvez, C. Peinelt, D.L. Koomoa, J. Soboloff, D.L. Gill, A. Fleig, J.P. Kinet, R. Penner, CRACM1 multimers form the ion-selective pore of the CRAC channel, Current biology: CB, 16 (2006) 2073-2079.
[28] O. Mignen, J.L. Thompson, T.J. Shuttleworth, Orai1 subunit stoichiometry of the mammalian CRAC channel pore, The Journal of physiology, 586 (2008) 419-425.
[29] A. Penna, A. Demuro, A.V. Yeromin, S.L. Zhang, O. Safrina, I. Parker, M.D. Cahalan, The CRAC channel consists of a tetramer formed by Stim-induced dimerization of Orai dimers, Nature, 456 (2008) 116-120.
[30] X. Hou, L. Pedi, M.M. Diver, S.B. Long, Crystal structure of the calcium release-activated calcium channel Orai, Science, 338 (2012) 1308-1313.
[31] I. Braakman, D.N. Hebert, Protein folding in the endoplasmic reticulum, Cold Spring Harbor perspectives in biology, 5 (2013) a013201.
[32] M. Michalak, J. Groenendyk, E. Szabo, L.I. Gold, M. Opas, Calreticulin, a multi-process calcium-buffering chaperone of the endoplasmic reticulum, The Biochemical journal, 417 (2009) 651-666.

[33] L. Lamriben, J.B. Graham, B.M. Adams, D.N. Hebert, N-Glycan-based ER Molecular Chaperone and Protein Quality Control System: The Calnexin Binding Cycle, Traffic, 17 (2016) 308-326.
[34] J. Prudent, H.M. McBride, The mitochondria-endoplasmic reticulum contact sites: a signalling platform for cell death, Current opinion in cell biology, 47 (2017) 52-63.
[35] P. Nunes-Hasler, N. Demaurex, The ER phagosome connection in the era of membrane contact sites, Biochimica et biophysica acta, 1864 (2017) 1513-1524.
[36] O. Baumann, B. Walz, Endoplasmic reticulum of animal cells and its organization into structural and functional domains, International review of cytology, 205 (2001) 149-214.
[37] J. Groenendyk, L.B. Agellon, M. Michalak, Coping with endoplasmic reticulum stress in the cardiovascular system, Annual review of physiology, 75 (2013) 49-67.
[38] C.E. Shamu, P. Walter, Oligomerization and phosphorylation of the Ire1p kinase during intracellular signaling from the endoplasmic reticulum to the nucleus, The EMBO journal, 15 (1996) 3028-3039.
[39] H.P. Harding, Y. Zhang, A. Bertolotti, H. Zeng, D. Ron, Perk is essential for translational regulation and cell survival during the unfolded protein response, Molecular cell, 5 (2000) 897-904.
[40] K. Haze, H. Yoshida, H. Yanagi, T. Yura, K. Mori, Mammalian transcription factor ATF6 is synthesized as a transmembrane protein and activated by proteolysis in response to endoplasmic reticulum stress, Molecular biology of the cell, 10 (1999) 3787-3799.
[41] C. Hetz, The unfolded protein response: controlling cell fate decisions under ER stress and beyond, Nature reviews. Molecular cell biology, 13 (2012) 89-102.
[42] A. Bertolotti, Y. Zhang, L.M. Hendershot, H.P. Harding, D. Ron, Dynamic interaction of BiP and ER stress transducers in the unfolded-protein response, Nature cell biology, 2 (2000) 326-332.
[43] K. Okamura, Y. Kimata, H. Higashio, A. Tsuru, K. Kohno, Dissociation of Kar2p/BiP from an ER sensory molecule, Ire1p, triggers the unfolded protein response in yeast, Biochemical and biophysical research communications, 279 (2000) 445-450.
[44] J. Shen, X. Chen, L. Hendershot, R. Prywes, ER stress regulation of ATF6 localization by dissociation of BiP/GRP78 binding and unmasking of Golgi localization signals, Developmental cell, 3 (2002) 99-111.
[45] S. Luo, P. Baumeister, S. Yang, S.F. Abcouwer, A.S. Lee, Induction of Grp78/BiP by translational block: activation of the Grp78 promoter by ATF4 through and upstream ATF/CRE site independent of the endoplasmic reticulum stress elements, The Journal of biological chemistry, 278 (2003) 37375-37385.
[46] D. Han, A.G. Lerner, L. Vande Walle, J.P. Upton, W. Xu, A. Hagen, B.J. Backes, S.A. Oakes, F.R. Papa, IRE1alpha kinase activation modes control alternate endoribonuclease outputs to determine divergent cell fates, Cell, 138 (2009) 562-575.
[47] C. Hetz, L.H. Glimcher, Fine-tuning of the unfolded protein response: Assembling the IRE1alpha interactome, Molecular cell, 35 (2009) 551-561.
[48] J. Hollien, J.H. Lin, H. Li, N. Stevens, P. Walter, J.S. Weissman, Regulated Ire1-dependent decay of messenger RNAs in mammalian cells, The Journal of cell biology, 186 (2009) 323-331.
[49] C. Sidrauski, P. Walter, The transmembrane kinase Ire1p is a site-specific endonuclease that initiates mRNA splicing in the unfolded protein response, Cell, 90 (1997) 1031-1039.

[50] H. Yoshida, T. Matsui, A. Yamamoto, T. Okada, K. Mori, XBP1 mRNA is induced by ATF6 and spliced by IRE1 in response to ER stress to produce a highly active transcription factor, Cell, 107 (2001) 881-891.
[51] H. Yoshida, T. Okada, K. Haze, H. Yanagi, T. Yura, M. Negishi, K. Mori, ATF6 activated by proteolysis binds in the presence of NF-Y (CBF) directly to the cis-acting element responsible for the mammalian unfolded protein response, Molecular and cellular biology, 20 (2000) 6755-6767.
[52] M. Michalak, R.E. Milner, K. Burns, M. Opas, Calreticulin, The Biochemical journal, 285 (Pt 3) (1992) 681-692.
[53] T.J. Ostwald, D.H. MacLennan, Isolation of a high affinity calcium-binding protein from sarcoplasmic reticulum, The Journal of biological chemistry, 249 (1974) 974-979.
[54] W.A. Wang, J. Groenendyk, M. Michalak, Calreticulin signaling in health and disease, The international journal of biochemistry & cell biology, 44 (2012) 842-846.
[55] K. Nakamura, A. Zuppini, S. Arnaudeau, J. Lynch, I. Ahsan, R. Krause, S. Papp, H. De Smedt, J.B. Parys, W. Muller-Esterl, D.P. Lew, K.H. Krause, N. Demaurex, M. Opas, M. Michalak, Functional specialization of calreticulin domains, The Journal of cell biology, 154 (2001) 961-972.
[56] S. Baksh, M. Michalak, Expression of calreticulin in Escherichia coli and identification of its Ca^{2+} binding domains, The Journal of biological chemistry, 266 (1991) 21458-21465.
[57] C.L. Pocanschi, G. Kozlov, U. Brockmeier, A. Brockmeier, D.B. Williams, K. Gehring, Structural and functional relationships between the lectin and arm domains of calreticulin, The Journal of biological chemistry, 286 (2011) 27266-27277.
[58] S. Arnaudeau, M. Frieden, K. Nakamura, C. Castelbou, M. Michalak, N. Demaurex, Calreticulin differentially modulates calcium uptake and release in the endoplasmic reticulum and mitochondria, The Journal of biological chemistry, 277 (2002) 46696-46705.
[59] L. Mery, N. Mesaeli, M. Michalak, M. Opas, D.P. Lew, K.H. Krause, Overexpression of calreticulin increases intracellular Ca^{2+} storage and decreases store-operated Ca^{2+} influx, The Journal of biological chemistry, 271 (1996) 9332-9339.
[60] C. Bastianutto, E. Clementi, F. Codazzi, P. Podini, F. De Giorgi, R. Rizzuto, J. Meldolesi, T. Pozzan, Overexpression of calreticulin increases the Ca^{2+} capacity of rapidly exchanging Ca^{2+} stores and reveals aspects of their lumenal microenvironment and function, The Journal of cell biology, 130 (1995) 847-855.
[61] V. Martin, J. Groenendyk, S.S. Steiner, L. Guo, M. Dabrowska, J.M. Parker, W. Muller-Esterl, M. Opas, M. Michalak, Identification by mutational analysis of amino acid residues essential in the chaperone function of calreticulin, The Journal of biological chemistry, 281 (2006) 2338-2346.
[62] N. Mesaeli, K. Nakamura, E. Zvaritch, P. Dickie, E. Dziak, K.H. Krause, M. Opas, D.H. MacLennan, M. Michalak, Calreticulin is essential for cardiac development, The Journal of cell biology, 144 (1999) 857-868.
[63] M. Michalak, J. Lynch, J. Groenendyk, L. Guo, J.M. Robert Parker, M. Opas, Calreticulin in cardiac development and pathology, Biochimica et biophysica acta, 1600 (2002) 32-37.
[64] J. Lynch, M. Michalak, Calreticulin is an upstream regulator of calcineurin, Biochemical and biophysical research communications, 311 (2003) 1173-1179.
[65] J. Groenendyk, J. Lynch, M. Michalak, Calreticulin, Ca^{2+}, and calcineurin - signaling from the endoplasmic reticulum, Molecules and cells, 17 (2004) 383-389.

[66] L. Guo, K. Nakamura, J. Lynch, M. Opas, E.N. Olson, L.B. Agellon, M. Michalak, Cardiac-specific expression of calcineurin reverses embryonic lethality in calreticulin-deficient mouse, The Journal of biological chemistry, 277 (2002) 50776-50779.
[67] B.J. Park, D.G. Lee, J.R. Yu, S.K. Jung, K. Choi, J. Lee, J. Lee, Y.S. Kim, J.I. Lee, J.Y. Kwon, J. Lee, A. Singson, W.K. Song, S.H. Eom, C.S. Park, D.H. Kim, J. Bandyopadhyay, J. Ahnn, Calreticulin, a calcium-binding molecular chaperone, is required for stress response and fertility in Caenorhabditis elegans, Molecular biology of the cell, 12 (2001) 2835-2845.
[68] S. Gao, M. Zhen, Action potentials drive body wall muscle contractions in Caenorhabditis elegans, Proceedings of the National Academy of Sciences of the United States of America, 108 (2011) 2557-2562.
[69] W. Lee, K.R. Kim, G. Singaravelu, B.J. Park, D.H. Kim, J. Ahnn, Y.J. Yoo, Alternative chaperone machinery may compensate for calreticulin/calnexin deficiency in Caenorhabditis elegans, Proteomics, 6 (2006) 1329-1339.
[70] D. Lee, G. Singaravelu, B.J. Park, J. Ahnn, Differential requirement of unfolded protein response pathway for calreticulin expression in Caenorhabditis elegans, Journal of molecular biology, 372 (2007) 331-340.
[71] N.M. Cerqueira, E.F. Oliveira, D.S. Gesto, D. Santos-Martins, C. Moreira, H.N. Moorthy, M.J. Ramos, P.A. Fernandes, Cholesterol Biosynthesis: A Mechanistic Overview, Biochemistry, 55 (2016) 5483-5506.
[72] T.Y. Chang, C.C. Chang, N. Ohgami, Y. Yamauchi, Cholesterol sensing, trafficking, and esterification, Annual review of cell and developmental biology, 22 (2006) 129-157.
[73] K.R. Feingold, C. Grunfeld, Introduction to Lipids and Lipoproteins, in: L.J. De Groot, G. Chrousos, K. Dungan, K.R. Feingold, A. Grossman, J.M. Hershman, C. Koch, M. Korbonits, R. McLachlan, M. New, J. Purnell, R. Rebar, F. Singer, A. Vinik (Eds.) Endotext, South Dartmouth (MA), 2000.
[74] K.J. Williams, Molecular processes that handle -- and mishandle -- dietary lipids, The Journal of clinical investigation, 118 (2008) 3247-3259.
[75] M.S. Brown, S.E. Dana, J.L. Goldstein, Receptor-dependent hydrolysis of cholesteryl esters contained in plasma low density lipoprotein, Proceedings of the National Academy of Sciences of the United States of America, 72 (1975) 2925-2929.
[76] T. Hevonoja, M.O. Pentikainen, M.T. Hyvonen, P.T. Kovanen, M. Ala-Korpela, Structure of low density lipoprotein (LDL) particles: basis for understanding molecular changes in modified LDL, Biochimica et biophysica acta, 1488 (2000) 189-210.
[77] M.S. Brown, J.L. Goldstein, A receptor-mediated pathway for cholesterol homeostasis, Science, 232 (1986) 34-47.
[78] S. Sugii, P.C. Reid, N. Ohgami, H. Du, T.Y. Chang, Distinct endosomal compartments in early trafficking of low density lipoprotein-derived cholesterol, The Journal of biological chemistry, 278 (2003) 27180-27189.
[79] E.B. Neufeld, A.M. Cooney, J. Pitha, E.A. Dawidowicz, N.K. Dwyer, P.G. Pentchev, E.J. Blanchette-Mackie, Intracellular trafficking of cholesterol monitored with a cyclodextrin, The Journal of biological chemistry, 271 (1996) 21604-21613.
[80] R.E. Infante, A. Radhakrishnan, Continuous transport of a small fraction of plasma membrane cholesterol to endoplasmic reticulum regulates total cellular cholesterol, eLife, 6 (2017) pii: e25466.

[81] N. Sever, T. Yang, M.S. Brown, J.L. Goldstein, R.A. DeBose-Boyd, Accelerated degradation of HMG CoA reductase mediated by binding of insig-1 to its sterol-sensing domain, Molecular cell, 11 (2003) 25-33.
[82] J.L. Goldstein, R.A. DeBose-Boyd, M.S. Brown, Protein sensors for membrane sterols, Cell, 124 (2006) 35-46.
[83] B.L. Song, N.B. Javitt, R.A. DeBose-Boyd, Insig-mediated degradation of HMG CoA reductase stimulated by lanosterol, an intermediate in the synthesis of cholesterol, Cell metabolism, 1 (2005) 179-189.
[84] M.A. Rogers, J. Liu, B.L. Song, B.L. Li, C.C. Chang, T.Y. Chang, Acyl-CoA:cholesterol acyltransferases (ACATs/SOATs): Enzymes with multiple sterols as substrates and as activators, The Journal of steroid biochemistry and molecular biology, 151 (2015) 102-107.
[85] C.C. Chang, A. Miyazaki, R. Dong, A. Kheirollah, C. Yu, Y. Geng, H.N. Higgs, T.Y. Chang, Purification of recombinant acyl-coenzyme A:cholesterol acyltransferase 1 (ACAT1) from H293 cells and binding studies between the enzyme and substrates using difference intrinsic fluorescence spectroscopy, Biochemistry, 49 (2010) 9957-9963.
[86] Y. Zhang, C. Yu, J. Liu, T.A. Spencer, C.C. Chang, T.Y. Chang, Cholesterol is superior to 7-ketocholesterol or 7 alpha-hydroxycholesterol as an allosteric activator for acyl-coenzyme A:cholesterol acyltransferase 1, The Journal of biological chemistry, 278 (2003) 11642-11647.
[87] K. Tauchi-Sato, S. Ozeki, T. Houjou, R. Taguchi, T. Fujimoto, The surface of lipid droplets is a phospholipid monolayer with a unique Fatty Acid composition, The Journal of biological chemistry, 277 (2002) 44507-44512.
[88] Y. Ohsaki, K. Soltysik, T. Fujimoto, The Lipid Droplet and the Endoplasmic Reticulum, Advances in experimental medicine and biology, 997 (2017) 111-120.
[89] M. Suzuki, Regulation of lipid metabolism via a connection between the endoplasmic reticulum and lipid droplets, Anatomical science international, 92 (2017) 50-54.
[90] A.R. Thiam, R.V. Farese, Jr., T.C. Walther, The biophysics and cell biology of lipid droplets, Nature reviews. Molecular cell biology, 14 (2013) 775-786.
[91] H. Shimano, Sterol regulatory element-binding protein family as global regulators of lipid synthetic genes in energy metabolism, Vitamins and hormones, 65 (2002) 167-194.
[92] J. Sakai, A. Nohturfft, D. Cheng, Y.K. Ho, M.S. Brown, J.L. Goldstein, Identification of complexes between the COOH-terminal domains of sterol regulatory element-binding proteins (SREBPs) and SREBP cleavage-activating protein, The Journal of biological chemistry, 272 (1997) 20213-20221.
[93] M. Matsuda, B.S. Korn, R.E. Hammer, Y.A. Moon, R. Komuro, J.D. Horton, J.L. Goldstein, M.S. Brown, I. Shimomura, SREBP cleavage-activating protein (SCAP) is required for increased lipid synthesis in liver induced by cholesterol deprivation and insulin elevation, Genes & development, 15 (2001) 1206-1216.
[94] M. Amemiya-Kudo, H. Shimano, A.H. Hasty, N. Yahagi, T. Yoshikawa, T. Matsuzaka, H. Okazaki, Y. Tamura, Y. Iizuka, K. Ohashi, J. Osuga, K. Harada, T. Gotoda, R. Sato, S. Kimura, S. Ishibashi, N. Yamada, Transcriptional activities of nuclear SREBP-1a, -1c, and -2 to different target promoters of lipogenic and cholesterogenic genes, Journal of lipid research, 43 (2002) 1220-1235.
[95] H. Shimano, J.D. Horton, R.E. Hammer, I. Shimomura, M.S. Brown, J.L. Goldstein, Overproduction of cholesterol and fatty acids causes massive liver enlargement in transgenic mice expressing truncated SREBP-1a, The Journal of clinical investigation, 98 (1996) 1575-1584.

[96] H. Shimano, J.D. Horton, I. Shimomura, R.E. Hammer, M.S. Brown, J.L. Goldstein, Isoform 1c of sterol regulatory element binding protein is less active than isoform 1a in livers of transgenic mice and in cultured cells, The Journal of clinical investigation, 99 (1997) 846-854.
[97] J.D. Horton, I. Shimomura, M.S. Brown, R.E. Hammer, J.L. Goldstein, H. Shimano, Activation of cholesterol synthesis in preference to fatty acid synthesis in liver and adipose tissue of transgenic mice overproducing sterol regulatory element-binding protein-2, The Journal of clinical investigation, 101 (1998) 2331-2339.
[98] J.D. Horton, J.L. Goldstein, M.S. Brown, SREBPs: activators of the complete program of cholesterol and fatty acid synthesis in the liver, The Journal of clinical investigation, 109 (2002) 1125-1131.
[99] A. Nohturfft, R.A. DeBose-Boyd, S. Scheek, J.L. Goldstein, M.S. Brown, Sterols regulate cycling of SREBP cleavage-activating protein (SCAP) between endoplasmic reticulum and Golgi, Proceedings of the National Academy of Sciences of the United States of America, 96 (1999) 11235-11240.
[100] A. Das, M.S. Brown, D.D. Anderson, J.L. Goldstein, A. Radhakrishnan, Three pools of plasma membrane cholesterol and their relation to cholesterol homeostasis, eLife, 3 (2014) e02882.
[101] L.P. Sun, L. Li, J.L. Goldstein, M.S. Brown, Insig required for sterol-mediated inhibition of Scap/SREBP binding to COPII proteins in vitro, The Journal of biological chemistry, 280 (2005) 26483-26490.
[102] A. Radhakrishnan, J.L. Goldstein, J.G. McDonald, M.S. Brown, Switch-like control of SREBP-2 transport triggered by small changes in ER cholesterol: a delicate balance, Cell metabolism, 8 (2008) 512-521.
[103] T. Yang, P.J. Espenshade, M.E. Wright, D. Yabe, Y. Gong, R. Aebersold, J.L. Goldstein, M.S. Brown, Crucial step in cholesterol homeostasis: sterols promote binding of SCAP to INSIG-1, a membrane protein that facilitates retention of SREBPs in ER, Cell, 110 (2002) 489-500.
[104] R.A. DeBose-Boyd, M.S. Brown, W.P. Li, A. Nohturfft, J.L. Goldstein, P.J. Espenshade, Transport-dependent proteolysis of SREBP: relocation of site-1 protease from Golgi to ER obviates the need for SREBP transport to Golgi, Cell, 99 (1999) 703-712.
[105] A. Sundqvist, M.T. Bengoechea-Alonso, X. Ye, V. Lukiyanchuk, J. Jin, J.W. Harper, J. Ericsson, Control of lipid metabolism by phosphorylation-dependent degradation of the SREBP family of transcription factors by SCF(Fbw7), Cell metabolism, 1 (2005) 379-391.
[106] S.M. Colgan, D. Tang, G.H. Werstuck, R.C. Austin, Endoplasmic reticulum stress causes the activation of sterol regulatory element binding protein-2, The international journal of biochemistry & cell biology, 39 (2007) 1843-1851.
[107] J.N. Lee, J. Ye, Proteolytic activation of sterol regulatory element-binding protein induced by cellular stress through depletion of Insig-1, The Journal of biological chemistry, 279 (2004) 45257-45265.
[108] H.L. Kammoun, H. Chabanon, I. Hainault, S. Luquet, C. Magnan, T. Koike, P. Ferre, F. Foufelle, GRP78 expression inhibits insulin and ER stress-induced SREBP-1c activation and reduces hepatic steatosis in mice, The Journal of clinical investigation, 119 (2009) 1201-1215.
[109] T.H. Lee, A.D. Linstedt, Osmotically induced cell volume changes alter anterograde and retrograde transport, Golgi structure, and COPI dissociation, Molecular biology of the cell, 10 (1999) 1445-1462.

[110] G. Amodio, M. Renna, S. Paladino, C. Venturi, C. Tacchetti, O. Moltedo, S. Franceschelli, M. Mallardo, S. Bonatti, P. Remondelli, Endoplasmic reticulum stress reduces the export from the ER and alters the architecture of post-ER compartments, The international journal of biochemistry & cell biology, 41 (2009) 2511-2521.
[111] M.H. Doolittle, M. Peterfy, Mechanisms of lipase maturation, Clinical lipidology, 5 (2010) 71-85.

Chapter Two: Calreticulin Deficiency and SREBP Processing and Activity

A version of this chapter has been previously published in:

W.A. Wang, W.X. Liu, S. Durnaoglu, S.K. Lee, J. Lian, R. Lehner, J. Ahnn, L.B. Agellon and M. Michalak, "Loss of Calreticulin Uncovers a Critical Role for Calcium in Regulating Cellular Lipid Homeostasis," *Scientific Reports*, vol. 7, issue 1, 5941-5955.

Author contributions:

The laboratory of Sun-Kyung Lee at the Research Institute of Natural Science in Hanyang University, Seoul, performed the experiments and analyzed the data presented in Figure 2.3 Neutral lipid levels in the absence of calreticulin and Figure 2.9 nSREBP expression in *C. elegans* in the absence of calreticulin.

Introduction

Calreticulin is a Ca^{2+} binding protein chaperone that resides in the ER lumen and is important for maintaining ER functions and homeostasis [1]. Calreticulin deficiency is embryonic lethal in mice but cardiac-specific expression of constitutively active calcineurin enables *Calr*$^{-/-}$ mice to overcome lethality and survive to term [2]. The blood plasma of *Calr*$^{-/-}$ rescued mice contain a higher than normal concentration of lipids, indicating a disruption in lipid metabolism [2]. The underlying cause of this may be due to a disruption in lipid uptake, lipid storage or lipid biosynthesis. Here we investigated the effect of calreticulin deficiency on lipid biosynthesis through the SREBPs, known regulators of genes involved in lipid biosynthesis [3]. First we established the effect of calreticulin deficiency, seen in the *Calr*$^{-/-}$ rescued mice, in *Calr*$^{-/-}$ *C. elegans*, which is not lethal [4], and *Calr*$^{-/-}$ mouse embryonic fibroblasts [5]. We then measured nSREBP activity and examined the SREBP processing pathway in the absence of calreticulin. This study shows that in the absence of calreticulin there is an increase in SREBP processing and activity, however this was not due to disruptions to the components of the SREBP processing pathway.

Materials and Methods

C. elegans Analysis

For Sudan Black B staining, larvae and young adults were fixed in a buffer containing 80 mM KCl, 20 mM NaCl, 7 mM Na_2 Ethylene-bis(oxyethylenenitrilo)tetraacetic acid (EGTA), 15 mM piperazine-N,N'-bis(2-ethanesulfonic acid) (PIPES) pH 7.4, 0.5 mM spermidine, 0.2 mM spermine, 0.1% β-mercaptoethanol, 2% paraformaldehyde, followed by three freeze-thaw cycles. Worms were washed with 70% ethanol and stained in a saturated solution of Sudan Black B in 70% ethanol. Differential interference contrast (DIC) images were captured using Zeiss Axio Imager microscope.

CE548 worms expressing *epEx141*[*sbp-1*::*GFP*::*SBP-1*] in *sbp-1*(*ep79)* background was crossed with *crt-1* (*jh101*) to visualize nuclear localization of GFP:SBP-1 [6, 7]. Fluorescent images were captured and the ratio of fluorescence intensity in the nucleus and the cytoplasm immediately outside of the nucleus was analyzed using ImageJ.

Cell Culture, Transfection and Treatment

Wild-type and *Calr*$^{-/-}$ mouse embryonic fibroblasts (referred to as wild-type and *Calr*$^{-/-}$ cells, respectively) were previously described [5]. Cells were cultured in Dulbecco's Modified Eagle's Medium (DMEM) (Sigma-Aldrich) with 10% fetal bovine serum (FBS) (Sigma-Aldrich). In certain experiments we used lipid-free media, which is DMEM supplemented with 10% lipoprotein deficient FBS (Sigma-Aldrich #S5394).

For luciferase activity measurements, cells were transfected with reporter plasmids (0.25 μg) using DharmaFECT Duo transfection reagent (Thermo Fisher Scientific) into 48-well plates for

24-48 hours. Reporter activity (luciferase) was measured using a Dual-Luciferase® Reporter Assay System (Promega), which measures Firefly luciferase activity under the control of a test promoter normalized to Renilla luciferase activity under the control of the reference cytomegalovirus (CMV) promoter. The SRE luciferase reporter vector contains the human SREBP-2 promoter, which has a canonical and functional SRE nucleotide sequence, upstream of the Firefly luciferase gene sequence [8, 9]. This plasmid was a kind gift from Dr. Zlokovic's lab [10]. To confirm the functionality of the SRE in the human SREBP-2 gene promoter, the SRE sequence (5'-ATCACCCCAC-3') was mutated to 5'-ATTACCACGC-3' to create a mutated SRE luciferase reporter plasmid (referred to as mutSRE luciferase reporter). The following DNA primers were used:

The forward primer – 5'-CGATGACGCGCCATTACCACGC-3';

the reverse primer – 5'-CGAAGCGGTGCGCGTGGTAATGGCGCGTCATCG-3'.

To assess nSREBP activity, cells were co-transfected with the SRE luciferase reporter vector or the negative control mutSRE luciferase reporter vector with the pGL4.75 CMV control plasmid at a 40:1 ratio. The XBP1 splicing luciferase reporter plasmid was previously described [11]. To assess XBP1 splicing, cells were transfected with the XBP1 splicing luciferase reporter vector alone, as the plasmid contains an internal Renilla luciferase control. The cholesterol biosynthesis (SREBP) Pathway biomarkers were from SwitchGear Genomics. Following transfection and treatment, cells were harvested with Passive Lysis Buffer (50% glycerol, 2.5% trans-1,2-diaminocyclohexane-N,N,N, 'N'-tetraacetic acid monohydrate and 0.5% N,N-Bis(3-D-gluconamideopropyl) cholamide) (Promega) and the bioluminescence of Firefly and Renilla luciferase were measured using AutoLumat Plus LB 953 luminometer (Berthold Technologies).

For assessment of sterol sensitivity, cells were transfected with the appropriate luciferase reporter plasmids and cultured in normal media or lipid-free media supplemented without or with differing concentrations of methyl-β-cyclodextrin (MβCD) encapsulated cholesterol (Sigma-Aldrich #C4951). For assessment of S1P and S2P ER retention, cells were transfected with the appropriate luciferase reporter plasmids and treated with 1 μg/mL Brefeldin A (Sigma-Aldrich) in normal media for 16 hours. For S1P or calreticulin silencing, cells were co-transfected with scrambled siRNA or siRNA specific for S1P or calreticulin (Santa Cruz Biotechnology) with the appropriate luciferase reporter plasmids. For induction of ER stress, cells were transfected with the appropriate luciferase reporter plasmids and treated with 1 μM thapsigargin (TG) in normal media.

For induction of ER stress and ATF6 processing, cells were treated with 5 ng/mL tunicamycin (TUN) (Sigma-Aldrich) for 24 hours, followed by immunoblot analysis. For nSREBP-2 degradation, cells were treated with 400 μg/mL of cycloheximide in normal media for 0, 20, 40, 60, 90, 120, 150 or 180 min, followed by immunoblot analysis.

Lipid Staining and Imaging

Cells were cultured on 25 mm cover slips and the indicated treatments were applied. For neutral lipid staining, cells were washed 3 times with phosphate-buffered saline (PBS), fixed with 3.7% formaldehyde (in PBS) for 30 min, washed 3 times with PBS and incubated for at 37°C with stain solution, prepared by diluting the BODIPY 505/515 stock (1 mg/mL in 100% ethanol) 1/1000 in PBS. The cover slips were washed 3 times with PBS before visualization. BODIPY 505/515 staining was visualized using the Argon laser, with excitation at 488 nm and emission

from 505 – 515 nm. Staining was visualized and imaged using a Leica TCS SP5 confocal microscope.

For BODIPY FL-labelled LDL uptake, cells were serum starved for 24 hours, followed by incubation with 10 μg/mL of BODIPY FL-labelled LDL in serum free media for 0, 10, 15, 30 or 60 min. Cells were washed 3 times with PBS, fixed with 3.7% formaldehyde (in PBS) for 1 hour and washed 3 times with PBS before visualization. BODIPY FL-LDL was visualized using the Argon laser, with excitation at 514 nm and emission from 520 – 580 nm. Staining was visualized and imaged using a Leica TCS SP5 confocal microscope.

Lipid Biosynthesis and Measurement

Cells were treated with normal or lipid-free media in 6 cm dishes for 24 hours. Cells were then washed once with warm serum free media and incubated with 2 mL of serum free media containing 50 μM acetate and 10 μCi [^{3}H] acetate (specific activity 18.5 GBq/mmol). Following the incubation, cells were washed 2 times with PBS, harvested in 2 mL PBS and lysed by sonication. For normalization, 500 μL of each lysate were taken for DNA concentration determination. Total lipids from 1 mL of lysate were extracted using the Folch method (chloroform:methanol, 2:1), dried under nitrogen, solubilized in 100 μL of chloroform and separated by thin-layered chromatography (TLC) using heptane/isopropyl ether/acetic acid (60/40/4 by volume) as the mobile phase. TLC plates were exposed to iodine vapor for visualization of lipid classes and then the lipid bands were scraped from the TLC plate and the radioactivity associated with each lipid class was determined by liquid scintillation spectrometry. The sample radioactivity was normalized to the DNA concentration of the starting sample.

For the measurement of total cellular triacylglycerols, cholesterol esters and unesterified cholesterol, cells were homogenized in PBS and passed through an 18 micron clearance ball bearing homogenizer 25 times. Extraction of lipids from the homogenate was performed using the Folch method as previously described [12] and the lipid classes were analyzed using high-performance liquid chromatography (Lipodomics, University of Alberta). The concentration of total triacylglycerols, total cholesterol esters and total unesterified cholesterol in cell homogenates was measured using commercially available colorimetric assays (Stanbio Laboratory, Boerne, TX).

Quantitative Polymerase Chain Reaction Analysis

Total RNA was isolated from cells using RNeasy Mini Kit (QIAGEN) and first strand cDNA synthesis was performed with iScript Reverse Transcription Supermix for reverse transcriptase quantitative polymerase chain reaction (RT-qPCR) (BIO-RAD). For the qPCR reaction, we used PerfeCTa SYBR Green FastMix (Quanta BioSciences) and quantification was performed on Rotor-Gene Q (QIAGEN).

The following primers were used:

SREBP-1 forward – 5′-GCGGCTGTTGTCTACCATAA-3′;

SREBP-1 reverse – 5′-CTGGGCTAGATTCCACCTTTC-3′;

SREBP-2 forward – 5′-GAGGCGGACAACACACAATA-3′;

SREBP-2 reverse – 5′-CGGCTCAGAGTCAATGGAATA-3′;

LDLR forward – 5 ′-TGCATTTTCCGTCTCTACACT-3′;

LDLR reverse – 5′-CAACGCAGAAGCTAAGGATGA-3′;

HMG-CoA reductase forward – 5′-ACTGACATGCAGCCGAAG-3′;

HMG-CoA reductase reverse – 5′-CACATTCACTCTTGACGCTCT-3′;

SQLE forward – 5′-GCTCCTGTTAATGTCGTTTCTG-3′;

SQLE reverse – 5′-TCTCTGCTTTGCCTCTTATTGG-3′;

LSS forward – 5′-GCAGAGAGATGTGTGATATGTGA-3′;

LSS reverse – 5′-AGGCTGAGGATGGACACT-3′;

IDI1 forward – 5′-CATCAGATTGGGCCTTGTAGT-3′;

IDI1 reverse – 5′-ATTGGTGTGAAGCGAGCA-3′;

REPIN1 forward – 5′-CTGTTCCAGCATCGGTTCT-3′;

REPIN1 reverse – 5′-GCAGTTGTGAACTCGAACCT-3′;

18S forward – 5’-AACCCGTTGAACCCCATT-3’;

18S reverse – 5’-CCATCCAATCGGTAGTAGCG-3’.

Immunoprecipitation and Immunoblot Analysis

For SCAP and INSIG co-immunoprecipitation, cells plated in 10 cm plates were harvested at 80-90% confluency with 500 μL Lysis Buffer (50 mM 4-(2-hydroxyethyl)-1-piperazineethanesulfonic acid (Hepes), pH 7.4, 200 mM NaCl, 2% 3-[(3-cholamidopropyl)dimethylammonio]-1-propanesulfonate (CHAPS)) with protease inhibitors (0.5 mM phenylmethylsulfonyl fluoride, 0.5 mM benzamidine, 0.05 μg/mL Na-tosyl-Lys-chloromethylketone, (N-f3dcarbamoyl) oxirane-2-carboxylic acid (E-64), 0.025 μg/mL leupeptin and 0.01 μg/mL pepstatin) for 30 min on ice. Cell lysates were pelleted by centrifugation at 11,200 × g for 15 min. The supernatant was diluted with the addition of 2/3 volume of Lysis Buffer and precleared with 1/15th volume of 10% Protein A Sepharose CL-4B bead (GE Healthcare Life Sciences) suspended in HBS (50 mM Hepes, pH 7.4, 200 mM NaCl) for 30 min

at 4°C, then pelleted for 10 sec. The supernatant was collected and incubated overnight at 4°C with 2-3 μL of specific antibodies. The sample was incubated with 100 μL of 10% Protein A beads for 4 hours at 4°C, then washed 5 times with HBS in the presence of 1% CHAPS, 2 times with HBS alone, and re-suspended in 30 μL sodium dodecyl sulfate polyacrylamide gel electrophoresis (SDS-PAGE) sample buffer (60 mM tris(hydroxymethyl)aminomethane (Tris-HCl), pH 6.8, 1% SDS, 10% glycerol and 3% β-mercaptoethanol and 0.01% bromophenol blue) followed by immunoblot analysis.

For protein analysis cells plated in 10 cm plates were harvested at 80-90% confluency with 500 μL Radioimmunoprecipitation (RIPA) buffer (50 mM Tris-HCl, pH 7.5, 150 mM NaCl, 1 mM ethylenediaminetetraacetic acid (EDTA), 1 mM EGTA, 1% Triton X-100, 0.1% SDS, 0.5% sodium deoxycholate (NaDOC)) with protease inhibitors for 30 min on ice. Cell lysates were pelleted by centrifugation at 16,100 × g for 10 min. Protein concentration of the supernatant soluble protein sample was measured with the Bradford Protein Assay (BIO-RAD). Protein samples were made with the appropriate amount of protein concentration and 3X SDS-PAGE sample buffer followed by immunoblot analysis.

Immunoblot analysis was carried out as previously described [11]. Antibodies used were mouse anti-SREBP-1 (1:200; Santa Cruz Biotechnology sc-13551), rabbit anti-SREBP-2 (1:500; Abcam ab30682), rabbit anti-INSIG1 (1:500; Cedarlane 22115-1-AP), rabbit anti-SCAP (1:500; Cedarlane 12266-1-AP), goat anti-calreticulin (1:500; previously generated in the lab), rabbit anti-calnexin (1:2000; Stressgen Bioreagents ADI-SPA-860), rabbit anit-GRP78 (1:2000, Abcam ab21695), mouse anti-ATF6 (1:500; IMGENEX IMG-273) and mouse anti-γ-tubulin (1:1000; Thermo Fisher Scientific MA1-850). Secondary antibodies used were horseradish peroxidase

(HRP) conjugated: rabbit anti-mouse, goat anti-rabbit or rabbit anti-goat (1:2000; Jackson ImmunoResearch). Immunoblot images were scanned and quantified by densitometry using Image Studio Lite Ver 5.0 (Li-Cor).

Statistical Analysis

All statistical analyses were performed using the GraphPad Software. Means were compared using the Student's t-test or analysis of variance (ANOVA) where appropriate. Significant differences were attributed to p-values<0.05.

Results

Calreticulin Deficiency Disrupts Lipid Homeostasis

The blood plasma collected from the *Calr*$^{-/-}$ rescued mice appeared opaque and white due to higher lipid concentrations than the wild-type mice (Figure 2.1) [2]. To ensure that the blood plasma lipid accumulation in the absence of calreticulin was not due to a disruption in lipid uptake, we evaluated the effect of calreticulin deficiency on LDL uptake. We measured uptake of fluorescently labelled LDL in wild-type and *Calr*$^{-/-}$ fibroblast cell lines obtained from the embryo of the wild-type and *Calr*$^{-/-}$ mice (cell lines used consistently within this thesis and will be referred to as wild-type and *Calr*$^{-/-}$ cells) [5] and observed no differences in the ability for LDL uptake (Figure 2.2). Next, we verified the phenotype of the *Calr*$^{-/-}$ rescued mice in a different organism; we examined calreticulin deficiency in *C. elegans*. Unlike in mice, calreticulin deficiency is not lethal in *C. elegans* and therefore, provides a more direct observation [4]. The worms deficient in calreticulin (*crt-1*) revealed a more intense Sudan black staining as compared to wild-type (*N2*), indicating an accumulation of neutral lipids in the absence of calreticulin (Figure 2.3). We also investigated the effect of calreticulin deficiency on lipid content within the wild-type and *Calr*$^{-/-}$ cells. We observed a higher BODIPY 505/515 staining in the *Calr*$^{-/-}$ cells than the wild-type cells (Figure 2.4), which was consistent with the greater concentration of neutral lipids seen in the *Calr*$^{-/-}$ rescued mice [2] and the *Calr*$^{-/-}$ *C. elegans*. Further biochemical analysis of wild-type and *Calr*$^{-/-}$ cells revealed increased cellular concentration of triacylglycerols and cholesterol esters but not unesterified cholesterol in *Calr*$^{-/-}$ cells (Figure 2.5). Therefore, the impact of the absence of calreticulin on neutral lipid concentration was consistent

among three different experimental models and verifies the effect of calreticulin deficiency on lipid homeostasis.

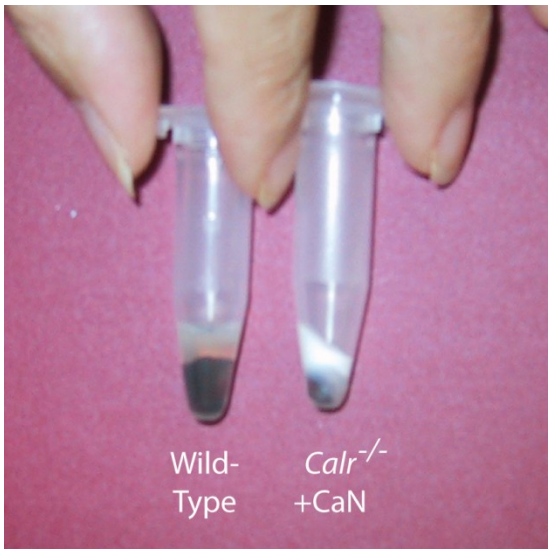

Figure 2.1 Blood sample from wild-type and *Calr*$^{-/-}$ rescued mice

Serum from wild-type (*wt*) and calreticulin-deficient (*Calr*$^{-/-}$) mouse rescued by cardiac-specific expression of the constitutively activated calcineurin (*Calr*$^{-/-}$+CaN) [2].

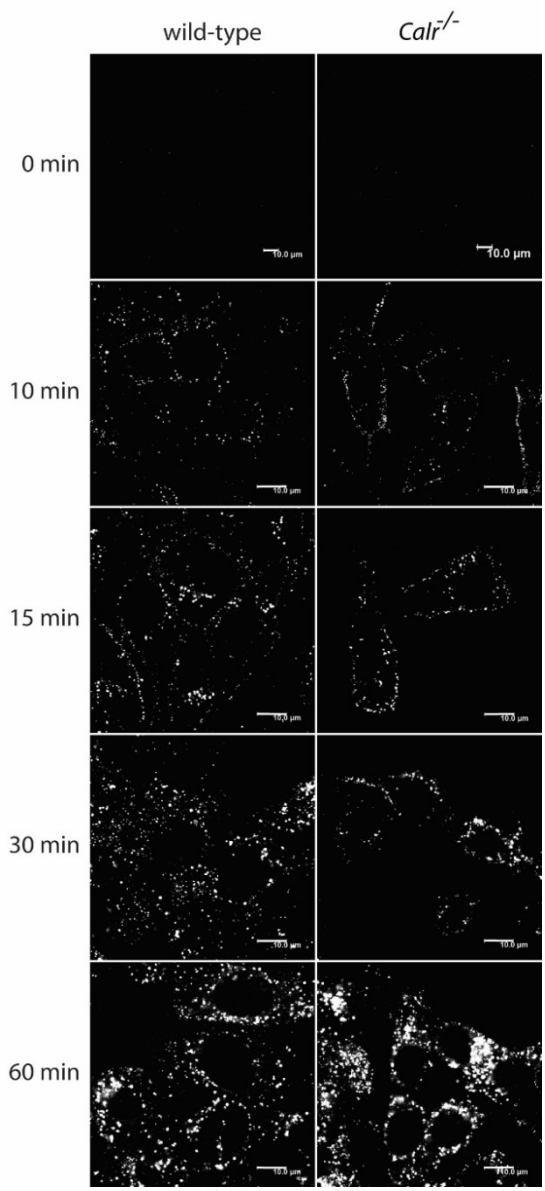

Figure 2.2 Uptake of LDL in wild-type and *Calr*$^{-/-}$ cells

Uptake of LDL complexed with fluorescent BODIPY and incubated with wild-type and *Calr*$^{-/-}$ mouse embryonic fibroblast cells for 0, 10, 15, 30 and 60 min as indicated in the figure. Representative of 3 biological experiments; at least 15 replicate images per treatment within each experiment.

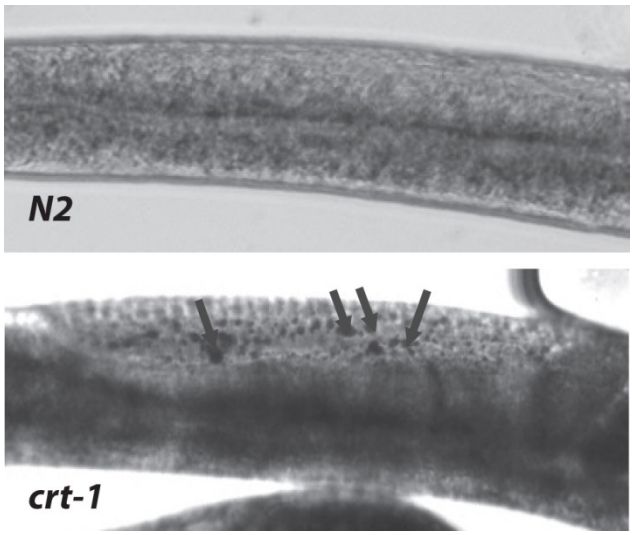

Figure 2.3 Neutral lipid levels in the absence of calreticulin

Sudan black staining of neutral lipids in wild-type (*N2*) and calreticulin deficient (*crt-1*) *C. elegans*. Lipid droplets are indicated by the arrows.

This experiment was performed by Sung-Kyung Lee et al. from Hanyang University, Seoul, South Korea.

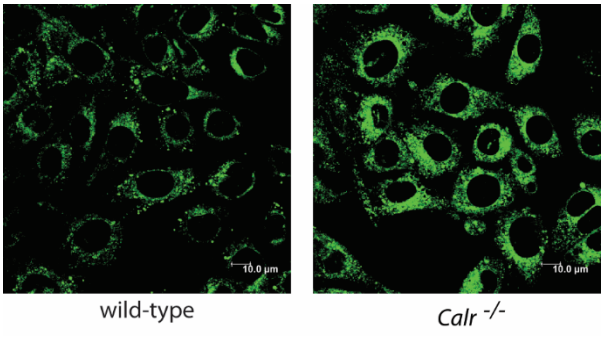

Figure 2.4 Neutral lipid levels in the absence of calreticulin

BODIPY 505/515 staining of neutral lipids in wild-type and *Calr*$^{-/-}$ mouse embryonic fibroblast cells. Representative of 3 biological experiments; at least 15 replicate images per treatment within each experiment.

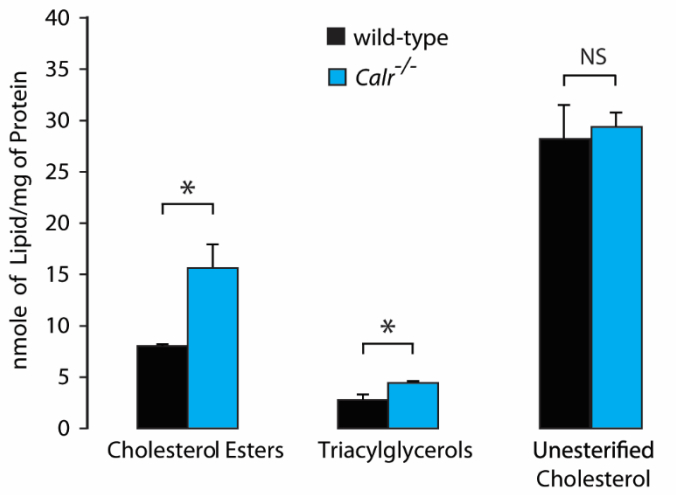

Figure 2.5 Lipid levels in wild-type and *Calr*$^{-/-}$ cells

Cholesterol ester, triacylglycerols and unesterified cholesterol levels in wild-type and *Calr*$^{-/-}$ mouse embryonic fibroblast cells. *Indicates statistically significant differences: cholesterol esters, *p*-value=0.0374; triacylglycerols, *p*-value=0.0451. NS, not significant. Representative of 3 biological experiments; 1 replicate per experiment (Student's t-test).

Since SREBPs are known regulators of genes involved in lipid homeostasis, we hypothesized that the increase in neutral lipid concentration caused by the lack of calreticulin was attributable to enhanced neutral lipid synthesis, potentially due to increased activity of SREBPs. To investigate, we used a cholesterol biosynthesis pathway screening assay system to assess the overall stimulation of SREBP responsive genes in wild-type and *Calr*$^{-/-}$ cells. This analysis revealed that luciferase activity driven by promoters from genes encoding fatty acid synthase (FASN), isopentyl-diphosphate delta isomerase 1 (IDI1), INSIG-1, lanosterol synthase (LSS), mevalonate pyrophosphate decarboxylase (MVD), LDLR and squalene epoxidase (SQLE) were all enhanced in the absence of calreticulin (Figure 2.6A). We then examined whether the increase in promoter activity of SREBP targeted genes, in the absence of calreticulin, translated to the increase in mRNA abundance. Additional reverse transcriptase quantitative polymerase chain reaction (RT-qPCR) analysis showed increases in SQLE, IDI1, LSS, LDLR, and HMG-CoA reductase mRNA in *Calr*$^{-/-}$ cells as compared to wild-type (Figure 2.6B). Lastly, we wanted to see if the upregulation of SREBP targeted genes in the absence of calreticulin equated to an increase in the rate of lipid biosynthesis. We measured *de novo* synthesis of cholesterol and triacylglycerols from acetate and showed that there was a higher rate of synthesis in *Calr*$^{-/-}$ cells as compared to wild-type (Figure 2.7). Taken together these findings demonstrated that the elimination of the calreticulin gene increased lipid biosynthesis through the increase in the expression of SREBP targeted genes.

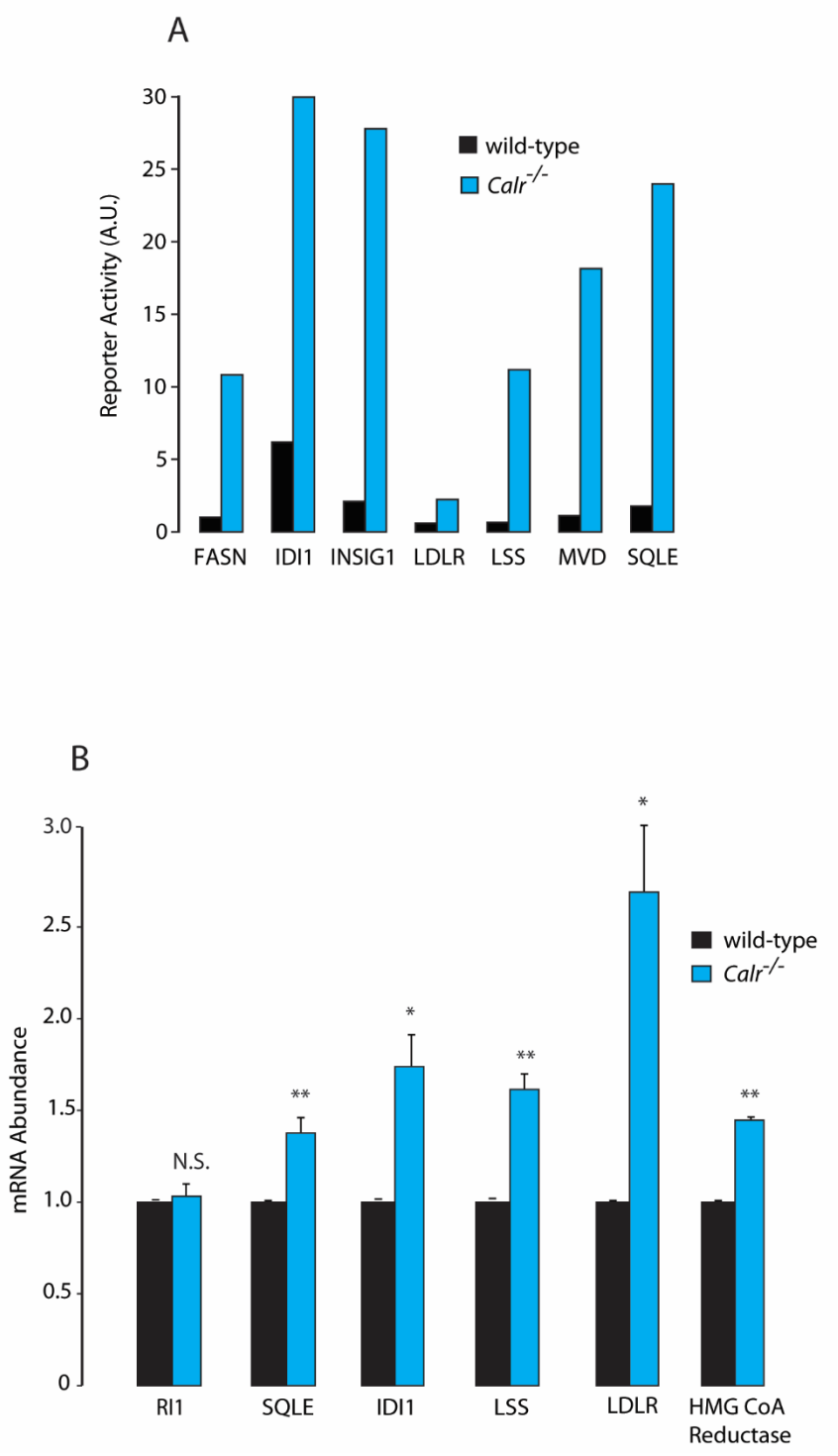
A
Reporter Activity (A.U.)
30
25
20
15
10
5
0
wild-type
Calr-/-
FASN
IDI1
INSIG1
LDLR
LSS
MVD
SQLE
B
mRNA Abundance
3.0
2.5
2.0
1.5
1.0
0.5
0
N.S.
**
*
**
*
**
wild-type
Calr-/-
RI1
SQLE
IDI1
LSS
LDLR
HMG CoA Reductase

Figure 2.6 SREBP target gene expression in wild-type and *Calr*$^{-/-}$ cells

A. SwitchGear Cholesterol Biosynthesis Pathway Assay for SREBP target genes in wild-type and *Calr*$^{-/-}$ mouse embryonic fibroblast cells; fatty acid synthase (FASN), isopentyl-diphosphate delta isomerase 1 (IDI1), insulin induced gene-1 (INSIG-1), lanosterol synthase (LSS), mevalonate pyrophosphate decarboxylase (MVD), the LDL receptor (LDLR) and squalene epoxidase (SQLE). Representative of 2 biological experiments; 2 replicates per experiment.

B. qPCR analysis of replication initiator 1 (RI1), SQLE, IDI1, LSS, LDLR and 3-hydroxy-3-methyl-glutaryl-CoA (HMG-CoA) reductase mRNA level in wild-type and *Calr*$^{-/-}$ mouse embryonic fibroblast cells. Results were normalized to 18S rRNA (internal control). **Indicates statistically significant differences: SQLE in wild-type vs. *Calr*$^{-/-}$ cells, *p*-value=0.0041; LSS in wild-type vs. *Calr*$^{-/-}$ cells, *p*-value=0.001; HMG-CoA reductase in wild-type vs. *Calr*$^{-/-}$ cells, *p*-value=0.0001. *Indicates statistically significant differences: IDI1 in wild-type vs. *Calr*$^{-/-}$ cells, *p*-value=0.0133; LDLR in wild-type vs. *Calr*$^{-/-}$ cells, *p*-value=0.0112. Representative of 4 biological experiments; 2 replicates per experiment. NS. Not significant (Student's t-test).

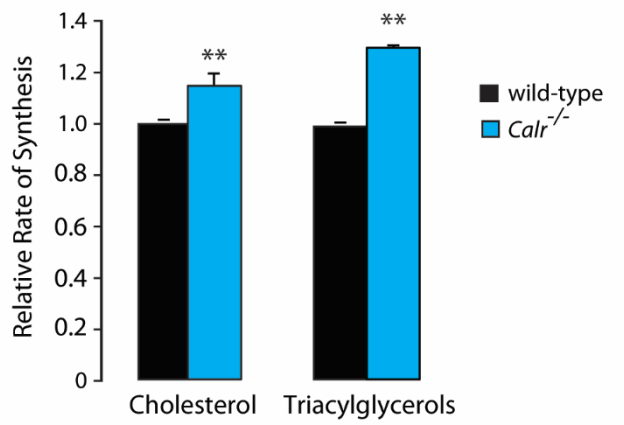

Figure 2.7 Rate of lipid synthesis in wild-type and *Calr*$^{-/-}$ cells

Analysis of rates of lipid synthesis through the measurement of radioactivity of cholesterol and triacylglycerols in wild-type and *Calr*$^{-/-}$ mouse embryonic fibroblast cells following incubation with Ci [^{3}H] acetate. ** Indicates statistically significant differences: cholesterol, *p*-value=0.0012; triacylglycerols, *p*-value=0.0006 (Student's t-test). Representative of 3 biological experiments; 3 replicates per experiment.

Calreticulin Deficiency Increases SREBP Processing and Activity

To determine the basis for increased expression of SREBP targeted genes and rate of lipid biosynthesis, we examined SREBP abundance and activity. We measured the abundance of SREBP-1 and SREBP-2 mRNA and protein. qPCR analysis showed no differences in the abundance of SREBP-1 or SREBP-2 mRNA between wild-type and *Calr*$^{-/-}$ cells (Figure 2.8A). Protein analysis on the other hand, showed increased precursor and nuclear forms of SREBP-1 and SREBP-2 (nSREBP1 and nSREBP2) in *Calr*$^{-/-}$ cells as compared to wild-type (Figure 2.8B). There was also an increase in the ratio of the nuclear to total (nuclear and precursor forms) abundance of SREBP-1 (Figure 2.8C) and SREBP-2 (Figure 2.8D) protein expression in *Calr*$^{-/-}$ cells as compared to wild-type. Next, we wanted to determine if the same effect was evident in *Calr*$^{-/-}$ *C. elegans*. Importantly, *C. elegans* are not capable of cholesterol biosynthesis and they only have one sterol regulatory transcription factor, *sbp-1*, the homologue of mammalian SREBP-1c [13]. We created a GFP-tagged *sbp-1* and showed a higher GFP-SBP-1 nuclear distribution in the *Calr*$^{-/-}$ *C. elegans* (*crt-1*) as compared to wild-type (*N2*) (Figure 2.9). These findings suggest that there is an increase in SREBP processing in the absence of calreticulin.

We assessed the activity of nSREBP using a SRE-luciferase reporter. First, we validated the SRE-luciferase reporter by mutating the SRE within the promoter and assessing the difference in the level of response to cholesterol between the SRE- and mutated SRE- luciferase reporters. HeLa cells expressing the SRE-luciferase reporter had an increase in nSREBP activity in lipid-free media and this increase was abolished when the cells were treated with 0.25 μg/mL of cholesterol in lipid-free media (Figure 2.10). When HeLa cells were transfected with the mutated SRE-luciferase reporter, there was no longer a change in nSREBP activity as a response to the

presence or absence of cholesterol (Figure 2.10), indicating that the SRE-luciferase reporter correctly measures nSREBP activity and respond accordingly to cholesterol status.

We then used the SRE-luciferase reporter to measure nSREBP activity in wild-type and *Calr*$^{-/-}$ cells. Consistent with the increase in SREBP processing, there was also an increase in nSREBP activity in the *Calr*$^{-/-}$ cells as compared to wild-type (Figure 2.11A). Importantly, ectopic expression of calreticulin in *Calr*$^{-/-}$ cells decreased nSREBP activity to a level comparable to that of wild-type cells (Figure 2.11A). Conversely, calreticulin-specific siRNA-mediated silencing of calreticulin in HEK293T cells increased nSREBP activity, reproducing the effect seen in *Calr*$^{-/-}$ cells (Figure 2.11B). We also validated our observations using the mutated SRE-luciferase construct. The increase in nSREBP activity in the *Calr*$^{-/-}$ cells expressing the SRE-luciferase reporter was abolished in the *Calr*$^{-/-}$ cells expressing the mutated SRE-luciferase reporter (Figure 2.12), indicating that the observed increase in luciferase activity is specific to nSREBP activity on the SRE motif. Therefore, the increase in SRE-luciferase activity in *Calr*$^{-/-}$ cells indicates an increase in nSREBP activity regardless of cholesterol status. Taken together, the elimination or attenuation of calreticulin gene expression consistently led to an increase in nSREBP activity.

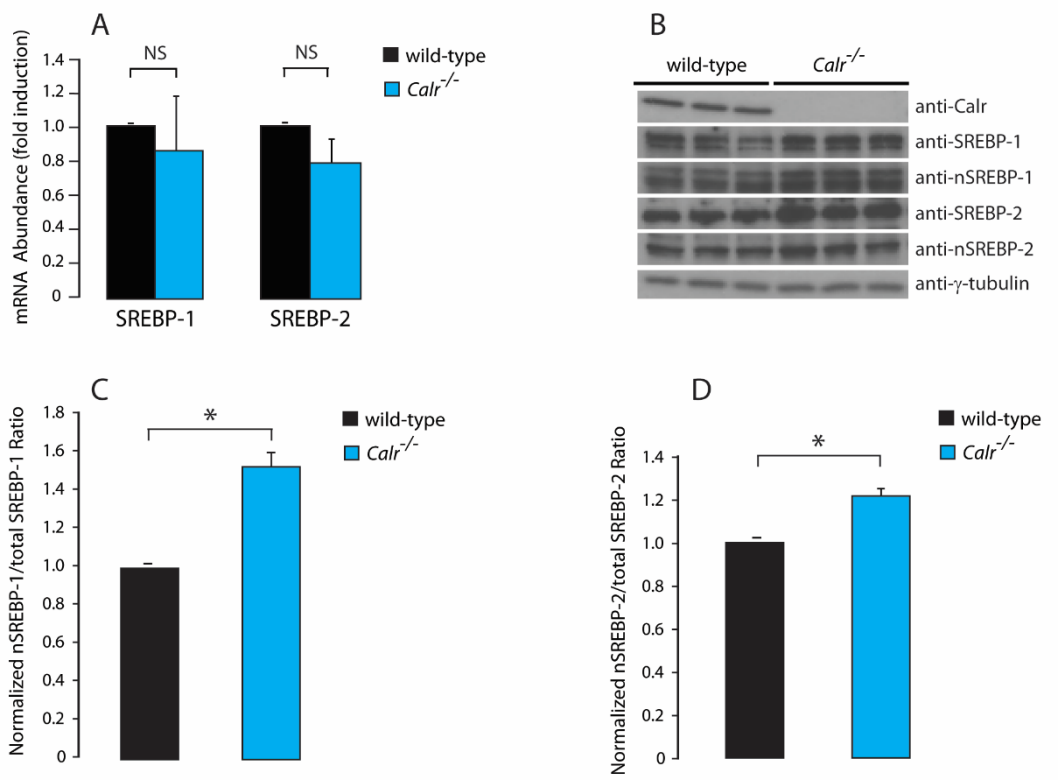

Figure 2.8 SREBP expression in the absence of calreticulin

A. qPCR analysis of total SREBP-1 and SREBP-2 mRNA abundance in wild-type and *Calr*$^{-/-}$ mouse embryonic fibroblast cells. Results were normalized to 18S rRNA (internal control). NS, not significant. Representative of 5 biological experiments; 2 replicates per experiment (Student's t-test).

B. Immunoblot of wild-type and *Calr*$^{-/-}$ mouse embryonic fibroblast cells probed with anti-SREBP-1, anti-nSREBP-1, anti-SREBP-2 and anti-nSREBP-2 antibodies. Anti-γ-tubulin antibodies were used as a loading control. Representative of 3 biological experiments; 1 replicate per experiment.

C,D. Quantitative analysis of immunoblots showing the ratio of nuclear to total (precursor and nuclear forms) **(C)** SREBP-1 and **(D)** SREBP-2 in wild-type and *Calr*$^{-/-}$ mouse embryonic fibroblast cells. *Indicates statistically significant differences: SREBP-1, *p*-value=0.0017;

SREBP-2, *p*-value=0.0218. Representative of 3 biological experiments; 1 replicate per experiment (Student's t-test).

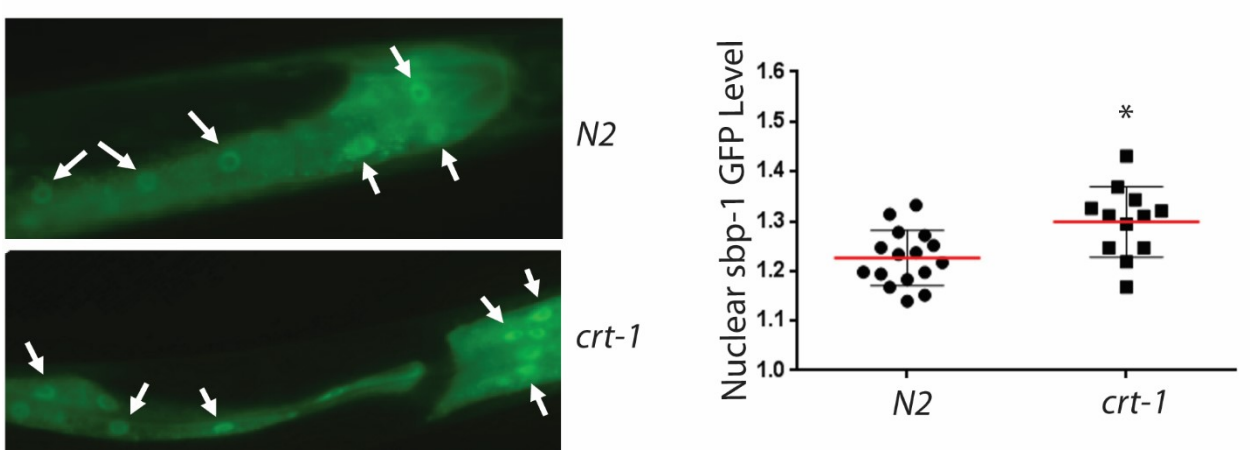

Figure 2.9 nSREBP expression in *C. elegans* in the absence of calreticulin

GFP:SBP-1 accumulation in the intestinal nucleus (as indicated by the arrows) in wild-type (*N2*) and calreticulin deficient (*crt-1*) *C. elegans*. Worms expressing GFP:SBP-1 driven by the *sbp-1* promoter are shown (*left panel*). The average ratio of fluorescence in the nucleus and cytoplasm was calculated in each worm and presented as a scatter-plot (*right-panel*). *Indicates statistically significant differences: p-value<0.01. Representative of 3 biological replicates (Student's t-test). This experiment was performed by Sung-Kyung Lee et al. from Hanyang University, Seoul, South Korea.

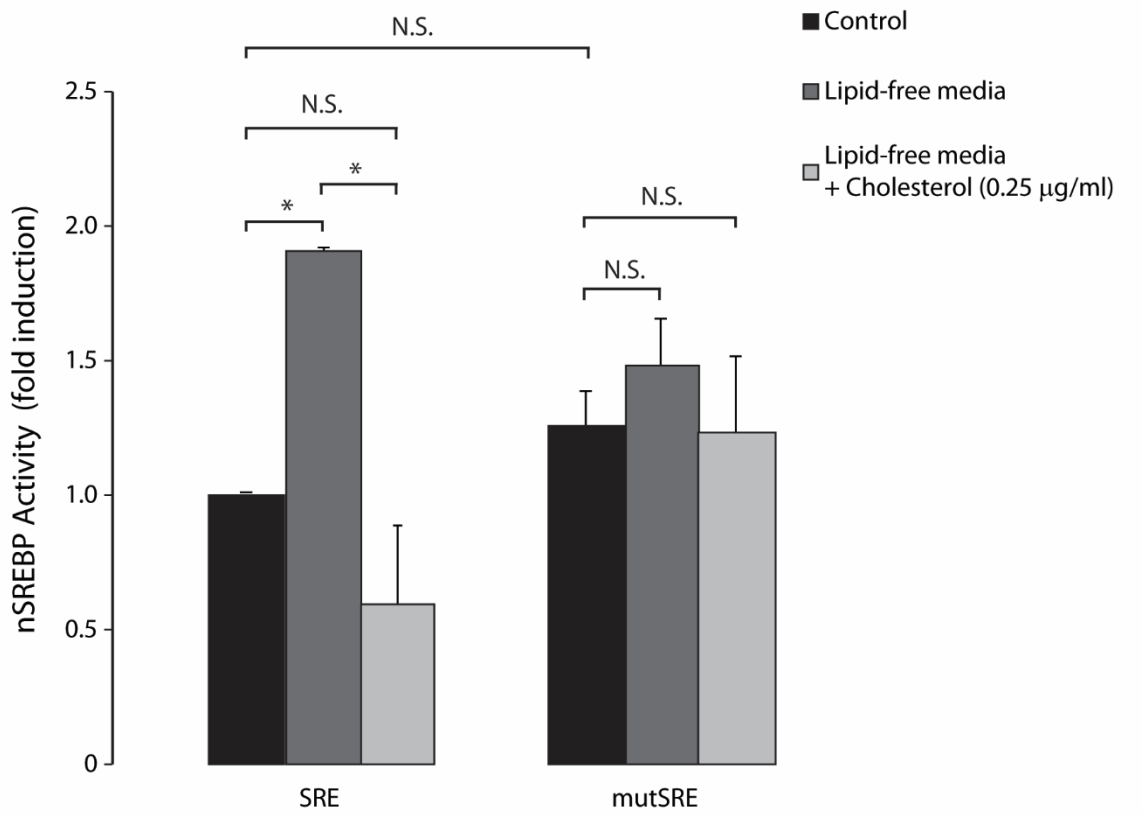

Figure 2.10 Mutational analysis of the SRE luciferase reporter SRE element in HeLa cells

nSREBP activity in HeLa cells transfected with the SRE luciferase reporter plasmid or the mutated SRE (mutSRE) luciferase reporter plasmid treated with control media, lipid-free media and lipid-free media plus cholesterol (0.25 μg/ml). SRE nucleotide sequence was mutated from ATCACCCCAC to ATTACCACGC. *Indicates statistically significant differences: HeLa cells with the SRE luciferase reporter in control vs. lipid-free media, p-value<0.05; HeLa cells with the SRE luciferase reporter in lipid-free media vs. lipid-free media plus cholesterol (0.25 μg/ml), p-value<0.05. NS, not significant. Representative of 3 trials with 3 experiments; 3 replicates per experiment (ANOVA).

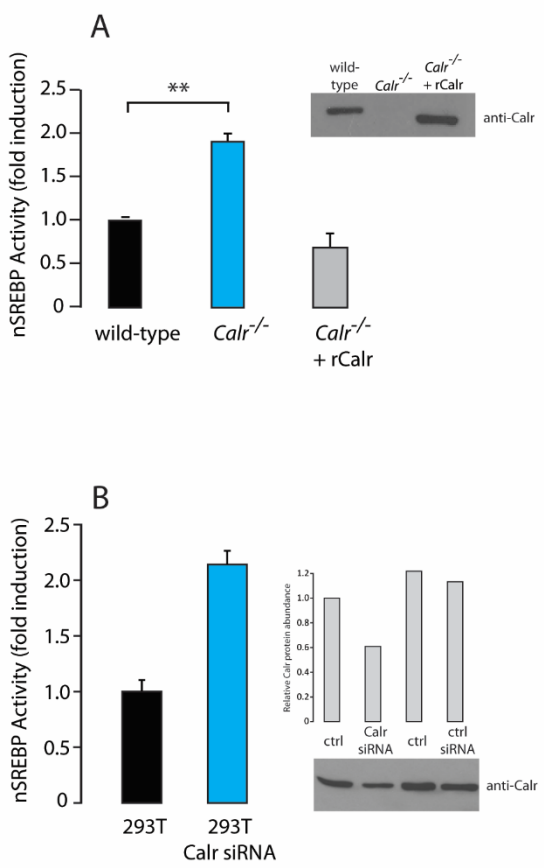

Figure 2.11 nSREBP activity in the absence of calreticulin

A. Wild-type, *Calr*$^{-/-}$ mouse embryonic fibroblast cells and *Calr*$^{-/-}$ mouse embryonic fibroblast cells transfected with a calreticulin expression vector (*Calr*$^{-/-}$+rCalr) were transfected with the SRE luciferase reporter plasmids followed by luciferase assay. **Indicates statistically significant differences: *p*-value=0.0006. Representative of 3 biological experiments; 3 replicates per experiment (Student's t-test). rCalr, recombinant calreticulin. Inset: immunoblot with anti-calreticulin antibodies.

B. HEK293T cells were co-transfected with scrambled or calreticulin specific siRNA and the SRE luciferase reporter plasmids. Representative of 3 biological experiments; 3 replicates per experiment. Inset: immunoblot with anti-calreticulin antibodies. Calr, calreticulin. Ctrl, control.

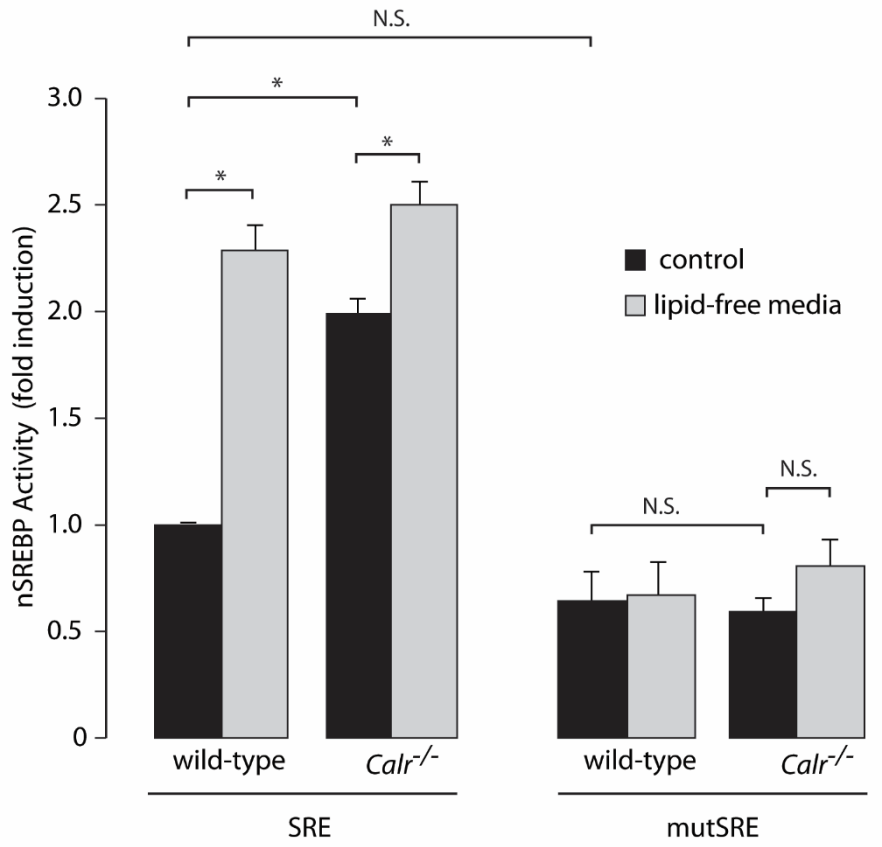

Figure 2.12 Mutational analysis of the SRE luciferase reporter SRE element in wild-type and *Calr*$^{-/-}$ cells

nSREBP activity in wild-type and *Calr*$^{-/-}$ mouse embryonic fibroblast cells transfected with the SRE luciferase reporter plasmid or the mutated SRE (mutSRE) luciferase reporter plasmid treated with normal media and lipid-free media. *Indicates statistically significant differences: wild-type cells with the SRE luciferase reporter in control vs. lipid-free media, p-value<0.05; *Calr*$^{-/-}$ cells with the SRE luciferase reporter in control vs. lipid-free media, p-value<0.05; wild-type and *Calr*$^{-/-}$cells with the SRE luciferase reporter in control media, p-value<0.05. NS, not significant. Representative of 3 trials with 3 experiments; 3 replicates per experiment (ANOVA).

Processing Pathway of SREBP is not altered in the Absence of Calreticulin

The loss of calreticulin consistently led to an increase in SREBP processing and nSREBP activity in the absence of any change to the intracellular concentration of unesterified cholesterol (Figure 2.5). Therefore, we assessed the functionality of the SREBP processing pathway. SREBP processing is sensitive to the availability of ER membrane cholesterol [14] and this is mediated through SCAP, an ER membrane sterol sensor complexed with SREBP [15, 16]. SCAP is an ER protein that requires glucose-mediated *N*-glycosylation at N263, N590 and N641 for proper folding and functionality [17]. Thus, in the absence of calreticulin, a protein chaperone responsible for folding of *N*-glycosylated proteins [1], SCAP folding and functional quality may be compromised, resulting in the increased nSREBP activity seen in *Calr*$^{-/-}$ cells. To assess the function of SCAP as a cholesterol sensor, we incubated wild-type and *Calr*$^{-/-}$ cells with lipid-free media supplemented with increasing concentrations of cholesterol (0, 0.5, 0.75 and 1.0 μg/mL) and then measured nSREBP activity. The nSREBP activity was increased in both wild-type and *Calr*$^{-/-}$ cells grown in lipid-free media and there was a corresponding decrease in nSREBP activity with increasing concentrations of cholesterol for both cell lines (Figure 2.13). Furthermore, in *Calr*$^{-/-}$ cells there was a corresponding increase in *de novo* cholesterol synthesis from acetate following removal of cholesterol source in the growth media (Figure 2.14). These results demonstrated that the loss of calreticulin did not abolish the functionality of SCAP and the SREBP pathway at the level of sterol sensing and response.

Calreticulin deficiency leads to accelerated folding machinery and increase in protein export from the ER [18]. This may lead to a decrease in quality control and folding efficiency and an increase in ER associated degradation. Therefore, we measured protein levels of SCAP and

INSIG, important components of the SREBP processing pathway. Immunoblot analysis showed no difference in the abundance of SCAP or INSIG proteins between wild-type and *Calr*$^{-/-}$ cells (Figure 2.15A). Another structural function of SCAP that we investigated was its ability to bind INSIG, the ER membrane protein that anchors the SREBP-SCAP complex to the ER under cholesterol abundant conditions [19]. SCAP was co-immunoprecipitated with INSIG in both wild-type and *Calr*$^{-/-}$ cells (Figure 2.15B,C), indicating that the INSIG-SCAP interaction was not affected by the absence of calreticulin under cholesterol abundant conditions.

A critical step in SREBP processing is the translocation of SREBPs to the Golgi where it is proteolytically cleaved by S1P and S2P, respectively. S1P and S2P are both N-glycosylated proteins [20, 21] and therefore calreticulin may play a role in regulating folding of both proteases. Therefore, we asked whether the increased nSREBP activity seen in the absence of calreticulin is attributable to changes in proteolytic processing due to ER retention of S1P and S2P. In accordance to what was previously reported [22], Brefeldin A treatment of wild-type cells led to proteolytic processing of SREBP in the absence of lipid depletion (Figure 2.16A). Similarly, there was an increase in SREBP processing in Brefeldin A treated *Calr*$^{-/-}$ cells (Figure 2.16A), thus indicating that the increased abundance of nSREBP in *Calr*$^{-/-}$ cells was not attributable to ER retention of S1P and S2P.

We further assessed SREBP proteolytic processing by silencing S1P expression and measuring nSREBP activity. The disruption of SREBP cleavage by S1P should prevent any nSREBP activity and show that the effect of calreticulin deficiency on SREBP processing occurs before proteolysis within the Golgi. Silencing of S1P reduced nSREBP activity in *Calr*$^{-/-}$ cells to a level comparable to the wild-type cells (Figure 2.16B), indicating that the cause of increased nSREBP activity in the absence of calreticulin lies upstream of proteolytic processing.

To ensure that the SREBP processing pathway is functional, we assessed nSREBP degradation. The increase in nSREBP activity in the absence of calreticulin may be due to an altered decrease in the rate of nSREBP proteosomal degradation. To test this, cells were treated with cycloheximide, an inhibitor of protein synthesis, followed by immunoblot analysis of nSREBP-2 levels. We found that there was no difference in the rate of degradation of nSREBP-2, ~2-3 hours, between wild-type and *Calr*$^{-/-}$ cells (Figure 2.17). Taken together, these observations indicate that these critical steps in the SREBP processing pathway are all functional in the absence of calreticulin.

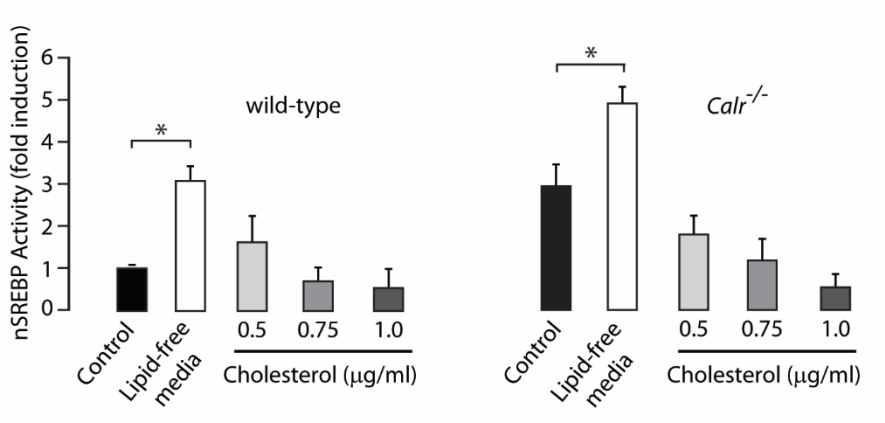

Figure 2.13 nSREBP activity in response to cholesterol status

nSREBP activity in wild-type (*left panel*) and *Calr*$^{-/-}$ (*right panel*) mouse embryonic fibroblast cells with control media, lipid-free media and lipid-free media plus 0.5, 0.75 and 1.0 mg/mL of cholesterol. *Indicates statistically significant differences: wild-type cells with control vs. lipid-free media, p-value<0.05; *Calr*$^{-/-}$ cells with control vs. lipid-free media, p-value<0.05. Representative of 3 biological experiments; 3 replicates per experiment (ANOVA).

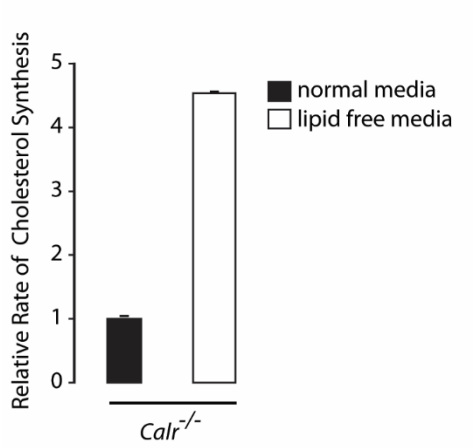

Figure 2.14 Rate of cholesterol synthesis in *Calr*$^{-/-}$ cells cultured with normal and lipid-free media

De novo rate of cholesterol synthesis through the measurement of radioactivity of cholesterol in *Calr*$^{-/-}$ mouse embryonic fibroblast cells treated with normal or lipid-free media containing Ci [^{3}H] acetate. Representative of 3 biological experiments; 3 replicates per experiment.

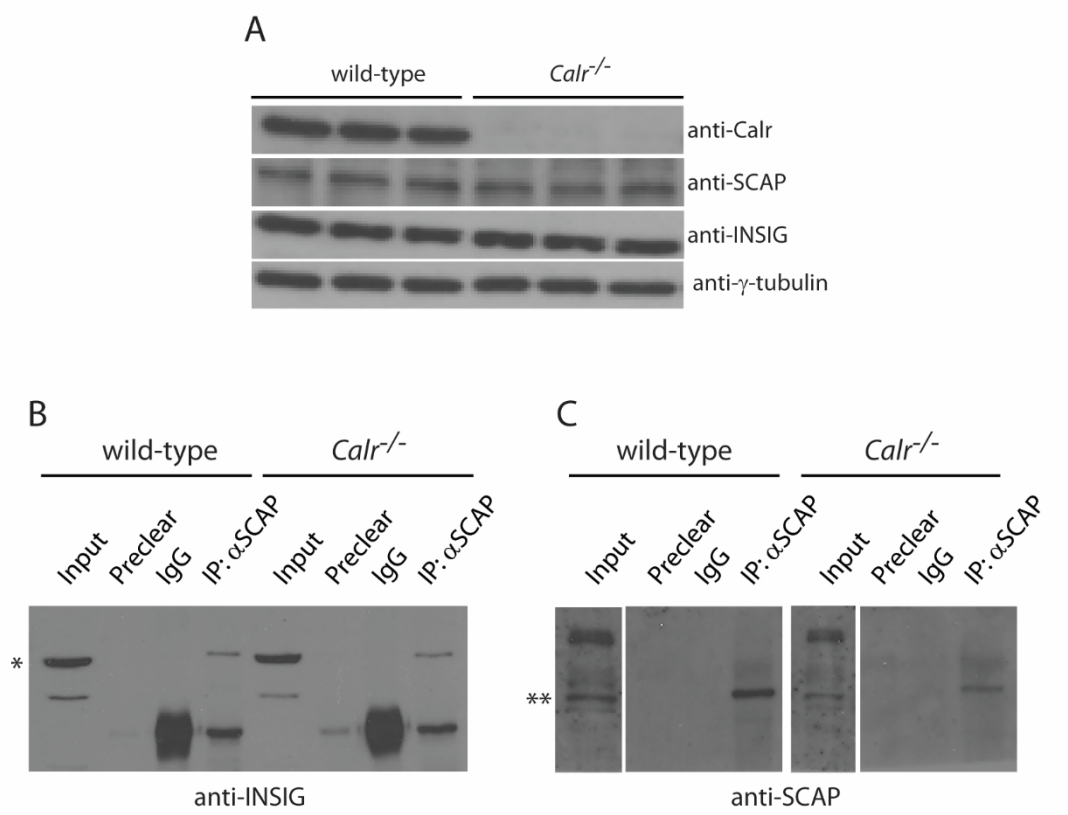

Figure 2.15 SCAP and INSIG expression and interaction

A. Immunoblot of wild-type and *Calr*$^{-/-}$ mouse embryonic fibroblast cells probed with anti-Calr, anti-SCAP and anti-INSIG antibodies. Anti-γ-tubulin antibodies were used as a loading control. Representative of 3 biological experiments; 3 replicates per experiment.

B,C. Immunoprecipitation (*IP*) assay was carried out on wild-type and *Calr*$^{-/-}$ mouse embryonic fibroblast cell lysates with anti-SCAP antibodies. Immunoblot of wild-type and *Calr*$^{-/-}$ anti-SCAP IP was carried out with (**B)** anti-INSIG and **(C)** anti-SCAP antibodies. *Indicates the INSIG protein band. **Indicates the SCAP protein band. Representative of 3 biological experiments; 1 replicate per experiment.

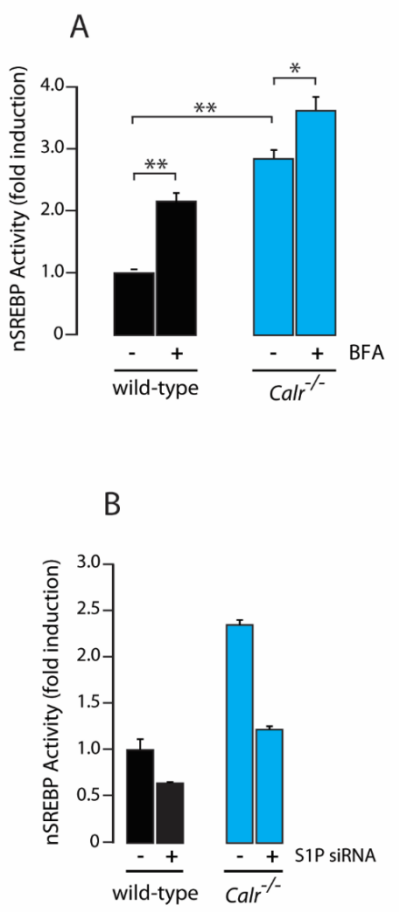

Figure 2.16 ER to Golgi translocation and activity of proteases

A. nSREBP activity in wild-type and *Calr*$^{-/-}$ mouse embryonic fibroblast cells treated with 1 μg/mL Brefeldin A (BFA). **Indicates statistically significant differences: wild-type cells in control vs. BFA treatment, *p*-value=0.0004; wild-type and *Calr*$^{-/-}$ cells in control conditions, *p*-value=0.0001. *Indicates statistically significant differences: *Calr*$^{-/-}$ cells in control vs. BFA treatment, *p*-value=0.0331. Representative of 3 biological experiments; 3 replicates per experiment (Student's t-test).

B. nSREBP activity in wild-type and *Calr*$^{-/-}$ mouse embryonic fibroblast cells transfected with scrambled or S1P specific siRNA. Representative of 2 biological experiments; 3 replicates per experiment.

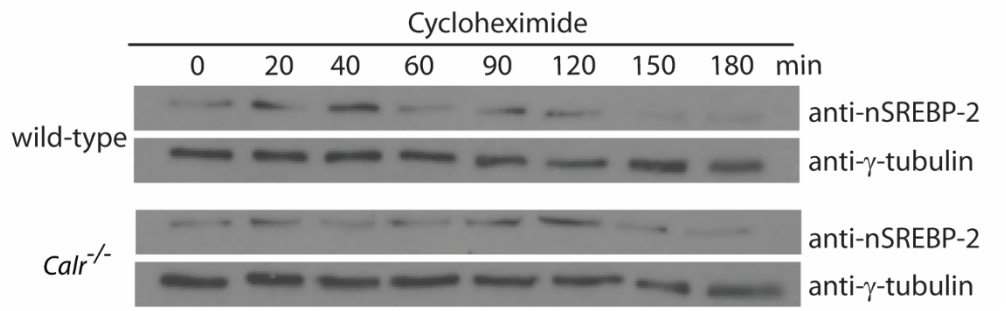

Figure 2.17 nSREBP-2 degradation

Immunoblot of wild-type and *Calr*$^{-/-}$ mouse embryonic fibroblast cells, treated with 400 μg/mL of cycloheximide for 0, 20, 40, 60, 90, 120, 150 and 180 min, probed with anti-nSREBP-2 antibodies. Anti-γ-tubulin antibodies were used as a loading control. Representative of 3 biological experiments; 1 replicate per experiment.

ER Stress and the Unfolded Protein Response is not Involved

SREBP processing and activity can be induced by the activation of UPR, an ER stress coping mechanism [23-25]. To see if *Calr*$^{-/-}$ cells were undergoing ER stress and inducing UPR, the mechanism behind nSREBP activation, we measured activing transcription factor 6 (ATF6) processing and XBP1 mRNA splicing (Figure 2.18). We found that the ratio of nuclear ATF6 (nATF6) to total (precursor and nuclear forms) ATF6 and XBP1 mRNA splicing were not affected by the absence of calreticulin (Figure 2.18). Therefore, there was no activation of UPR in *Calr*$^{-/-}$ cells. Importantly, induction of UPR with tunicamycin, an inhibitor of *N*-glycosylation, or thapsigargin, a SERCA inhibitor, increased both ATF6 processing and XBP1 splicing in both wild-type and *Calr*$^{-/-}$ cells (Figure 2.18). We therefore conclude that the UPR was fully functional in the absence of calreticulin and that the increased activity of nSREBP seen in *Calr*$^{-/-}$ cells was not due to UPR activity.

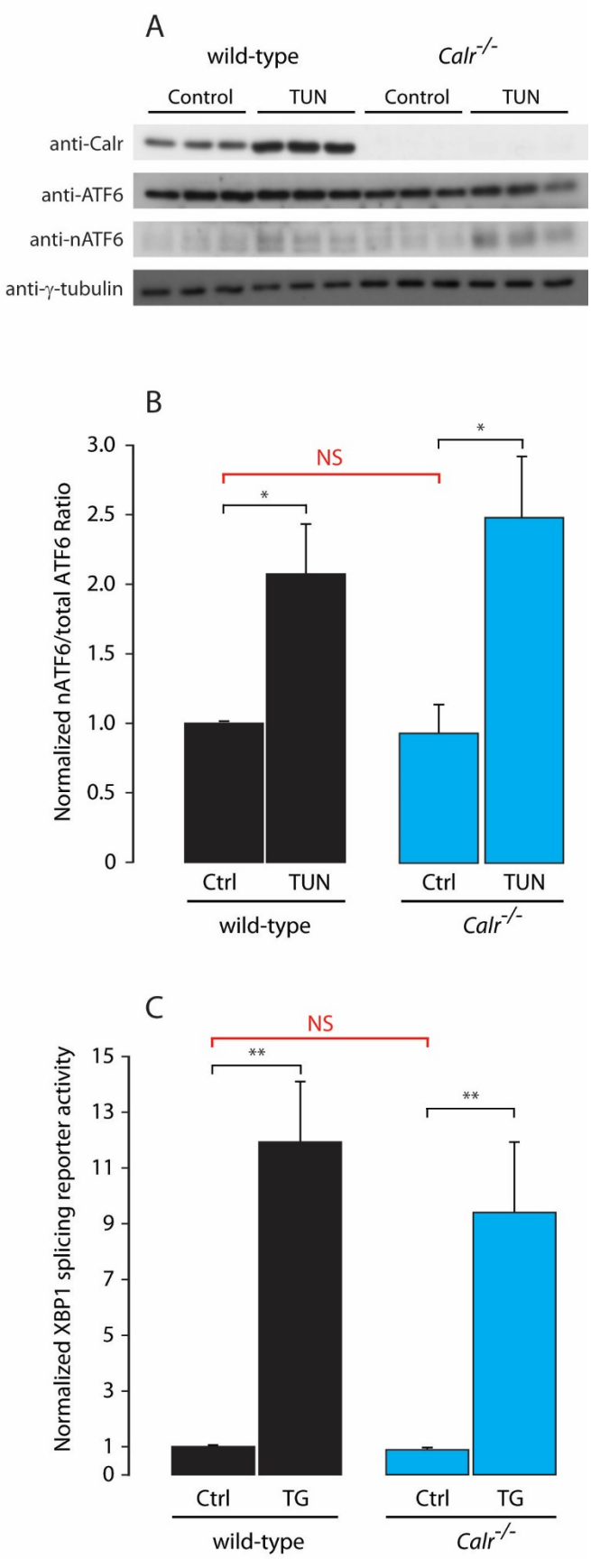
A
wild-type
Calr-/-
Control
TUN
Control
TUN
anti-Calr
anti-ATF6
anti-nATF6
anti-γ-tubulin
B
Normalized nATF6/total ATF6 Ratio
3.0
2.5
2.0
1.5
1.0
0.5
0
NS
*
*
Ctrl
TUN
Ctrl
TUN
wild-type
Calr-/-
C
Normalized XBP1 splicing reporter activity
15
13
11
9
7
5
3
1
0
NS
**
**
Ctrl
TG
Ctrl
TG
wild-type
Calr-/-

Figure 2.18 Unfolded protein response (UPR) in the absence of calreticulin

A. Immunoblot of wild-type and *Calr*$^{-/-}$ mouse embryonic fibroblast cells treated with control or 5 ng/mL of tunicamycin (TUN), probed with anti-Calr, anti ATF6, anti-nuclear ATF6 (nATF6) antibodies. Anti-g-tubulin antibodies were used as loading control. Representative of 3 biological experiments; 3 replicates per experiment.

B. Quantitative analysis of immunoblots showing the ratio of nuclear to total (precursor and nuclear forms) ATF6 in wild-type and *Calr*$^{-/-}$ mouse embryonic fibroblast cells treated with control (ctrl) or 5 ng/mL of TUN. *Indicates statistically significant differences: wild-type cells treated with ctrl vs. TUN, *p*-value=0.0393; *Calr*$^{-/-}$ cells treated with ctrl vs. TUN, *p*-value=0.0265. NS, not significant. Representative of 3 biological experiments; 3 replicates per experiment (Student's t-test).

C. XBP1 luciferase activity in wild-type and *Calr*$^{-/-}$ mouse embryonic fibroblast cells treated with ctrl or 1 μM thapsigargin (TG). **Indicates statistically significant differences: wild-type cells treated with ctrl vs. TG, *p*-value=0.0005; *Calr*$^{-/-}$ cells treated with ctrl vs. TG, *p*-value=0.0051. NS, not significant. Representative of 6 biological experiments; 2 replicates per experiment (Student's t-test).

Discussion

The mechanism controlling cellular cholesterol homeostasis was elucidated by the Brown and Goldstein laboratory [3, 26, 27]. This elegant machinery comprises several cellular components that enable the cell to sense the concentration of intracellular cholesterol and maintain its concentration within a narrow physiological range [28]. This sensing mechanism occurs at the ER where ~1% of a cell's total cholesterol resides in the unesterified form [29]. This small portion of ER membrane cholesterol controls the processing of ER membrane SREBP to its active form as a transcription factor that is responsible for the expression of genes involved in lipid uptake and biosynthesis [3, 30]. The SREBP-SCAP complex is retained at the ER under cholesterol abundant conditions and thereby preventing the processing of the SREBP precursor by the Golgi residing S1P and S2P [3]. This ER cholesterol store is supplied by two of the three distinct plasma membrane cholesterol pools. The larger of these two pools is easily accessible by the bacterial protein Perfringolysin O (PFO) variant, which binds unesterified cholesterol in membranes [29]. The smaller of these two pools becomes PFO accessible only after treatment of the plasma membrane with sphingomyelinase, which releases sphingomyelin sequestered cholesterol [29]. The remaining pool is termed the "essential" plasma membrane cholesterol since depletion of this pool causes cell death [29]. The cellular components responsible for the transport of cholesterol from the plasma membrane to the ER and vice versa, as well as the itinerary of the transport mechanism are not well determined, although it is well accepted that the concentration of cholesterol that ends up in the ER is what controls the fate of the SREBP-SCAP complex.

In this study, we provide evidence illustrating that the absence of calreticulin, an ER protein important in maintaining ER homeostasis, disrupts lipid homeostasis of eukaryotic cells. We showed that there is an accumulation of neutral lipids in the absence of calreticulin in mice, *C. elegans* and mouse embryonic fibroblasts. This accumulation is in part due to the continual increase in nSREBP activity in the absence of calreticulin. Importantly, the components of the SREBP processing pathway, many of which are likely candidates of the chaperone activity of calreticulin, are not affected by the absence of calreticulin. Firstly, we showed that the cholesterol sensing mechanism of the SREBP-SCAP complex remained fully functional. We also showed that the effect of calreticulin deficiency on increased nSREBP activity was not dependent on the concentration of intracellular unesterified cholesterol, induction of the UPR nor was it due to uncontrolled processing through unfolding of SCAP, INSIG or S1P and S2P. Furthermore, the processing pathway of ATF6 mirrors that of SREBP, as both undergo processing by Golgi localizing S1P and S2P [31]. Therefore, by showing that the ATF6 pathway was unaffected by the absence of calreticulin, we not only rule out the possibility of UPR induction, we also showed that the effect of calreticulin deficiency on nSREBP activity was specific to SREBP. Overall, this study establishes the connection between calreticulin and lipid synthesis through the SREPB pathway and showed that the mechanism underlying this connection is unlikely due to the chaperone activity of calreticulin.

References

[1] M. Michalak, J. Groenendyk, E. Szabo, L.I. Gold, M. Opas, Calreticulin, a multi-process calcium-buffering chaperone of the endoplasmic reticulum, The Biochemical journal, 417 (2009) 651-666.

[2] L. Guo, K. Nakamura, J. Lynch, M. Opas, E.N. Olson, L.B. Agellon, M. Michalak, Cardiac-specific expression of calcineurin reverses embryonic lethality in calreticulin-deficient mouse, The Journal of biological chemistry, 277 (2002) 50776-50779.

[3] M.S. Brown, J.L. Goldstein, The SREBP pathway: regulation of cholesterol metabolism by proteolysis of a membrane-bound transcription factor, Cell, 89 (1997) 331-340.

[4] B.J. Park, D.G. Lee, J.R. Yu, S.K. Jung, K. Choi, J. Lee, J. Lee, Y.S. Kim, J.I. Lee, J.Y. Kwon, J. Lee, A. Singson, W.K. Song, S.H. Eom, C.S. Park, D.H. Kim, J. Bandyopadhyay, J. Ahnn, Calreticulin, a calcium-binding molecular chaperone, is required for stress response and fertility in *Caenorhabditis elegans*, Molecular biology of the cell, 12 (2001) 2835-2845.

[5] K. Nakamura, A. Zuppini, S. Arnaudeau, J. Lynch, I. Ahsan, R. Krause, S. Papp, H. De Smedt, J.B. Parys, W. Muller-Esterl, D.P. Lew, K.H. Krause, N. Demaurex, M. Opas, M. Michalak, Functional specialization of calreticulin domains, The Journal of cell biology, 154 (2001) 961-972.

[6] A.K. Walker, F. Yang, K. Jiang, J.Y. Ji, J.L. Watts, A. Purushotham, O. Boss, M.L. Hirsch, S. Ribich, J.J. Smith, K. Israelian, C.H. Westphal, J.T. Rodgers, T. Shioda, S.L. Elson, P. Mulligan, H. Najafi-Shoushtari, J.C. Black, J.K. Thakur, L.C. Kadyk, J.R. Whetstine, R. Mostoslavsky, P. Puigserver, X. Li, N.J. Dyson, A.C. Hart, A.M. Naar, Conserved role of SIRT1 orthologs in fasting-dependent inhibition of the lipid/cholesterol regulator SREBP, Genes & development, 24 (2010) 1403-1417.

[7] A.K. Walker, R.L. Jacobs, J.L. Watts, V. Rottiers, K. Jiang, D.M. Finnegan, T. Shioda, M. Hansen, F. Yang, L.J. Niebergall, D.E. Vance, M. Tzoneva, A.C. Hart, A.M. Naar, A conserved SREBP-1/phosphatidylcholine feedback circuit regulates lipogenesis in metazoans, Cell, 147 (2011) 840-852.

[8] X. Hua, J. Wu, J.L. Goldstein, M.S. Brown, H.H. Hobbs, Structure of the human gene encoding sterol regulatory element binding protein-1 (SREBF1) and localization of SREBF1 and SREBF2 to chromosomes 17p11.2 and 22q13, Genomics, 25 (1995) 667-673.

[9] R. Sato, J. Inoue, Y. Kawabe, T. Kodama, T. Takano, M. Maeda, Sterol-dependent transcriptional regulation of sterol regulatory element-binding protein-2, The Journal of biological chemistry, 271 (1996) 26461-26464.

[10] R.D. Bell, R. Deane, N. Chow, X. Long, A. Sagare, I. Singh, J.W. Streb, H. Guo, A. Rubio, W. Van Nostrand, J.M. Miano, B.V. Zlokovic, SRF and myocardin regulate LRP-mediated amyloid-beta clearance in brain vascular cells, Nature cell biology, 11 (2009) 143-153.

[11] S.H. Back, K. Lee, E. Vink, R.J. Kaufman, Cytoplasmic IRE1alpha-mediated XBP1 mRNA splicing in the absence of nuclear processing and endoplasmic reticulum stress, The Journal of biological chemistry, 281 (2006) 18691-18706.

[12] J. Folch, M. Lees, G.H. Sloane Stanley, A simple method for the isolation and purification of total lipids from animal tissues, The Journal of biological chemistry, 226 (1957) 497-509.

[13] B.C. Mullaney, K. Ashrafi, C. elegans fat storage and metabolic regulation, Biochimica et biophysica acta, 1791 (2009) 474-478.

[14] A. Sokolov, A. Radhakrishnan, Accessibility of cholesterol in endoplasmic reticulum membranes and activation of SREBP-2 switch abruptly at a common cholesterol threshold, The Journal of biological chemistry, 285 (2010) 29480-29490.
[15] J.L. Goldstein, R.A. DeBose-Boyd, M.S. Brown, Protein sensors for membrane sterols, Cell, 124 (2006) 35-46.
[16] M. Matsuda, B.S. Korn, R.E. Hammer, Y.A. Moon, R. Komuro, J.D. Horton, J.L. Goldstein, M.S. Brown, I. Shimomura, SREBP cleavage-activating protein (SCAP) is required for increased lipid synthesis in liver induced by cholesterol deprivation and insulin elevation, Genes & development, 15 (2001) 1206-1216.
[17] C. Cheng, P. Ru, F. Geng, J. Liu, J.Y. Yoo, X. Wu, X. Cheng, V. Euthine, P. Hu, J.Y. Guo, E. Lefai, B. Kaur, A. Nohturfft, J. Ma, A. Chakravarti, D. Guo, Glucose-Mediated N-glycosylation of SCAP Is Essential for SREBP-1 Activation and Tumor Growth, Cancer cell, 28 (2015) 569-581.
[18] M. Molinari, K.K. Eriksson, V. Calanca, C. Galli, P. Cresswell, M. Michalak, A. Helenius, Contrasting functions of calreticulin and calnexin in glycoprotein folding and ER quality control, Molecular cell, 13 (2004) 125-135.
[19] T. Yang, P.J. Espenshade, M.E. Wright, D. Yabe, Y. Gong, R. Aebersold, J.L. Goldstein, M.S. Brown, Crucial step in cholesterol homeostasis: sterols promote binding of SCAP to INSIG-1, a membrane protein that facilitates retention of SREBPs in ER, Cell, 110 (2002) 489-500.
[20] D. Cheng, P.J. Espenshade, C.A. Slaughter, J.C. Jaen, M.S. Brown, J.L. Goldstein, Secreted site-1 protease cleaves peptides corresponding to luminal loop of sterol regulatory element-binding proteins, The Journal of biological chemistry, 274 (1999) 22805-22812.
[21] N.G. Zelenski, R.B. Rawson, M.S. Brown, J.L. Goldstein, Membrane topology of S2P, a protein required for intramembranous cleavage of sterol regulatory element-binding proteins, The Journal of biological chemistry, 274 (1999) 21973-21980.
[22] R.A. DeBose-Boyd, M.S. Brown, W.P. Li, A. Nohturfft, J.L. Goldstein, P.J. Espenshade, Transport-dependent proteolysis of SREBP: relocation of site-1 protease from Golgi to ER obviates the need for SREBP transport to Golgi, Cell, 99 (1999) 703-712.
[23] S.M. Colgan, D. Tang, G.H. Werstuck, R.C. Austin, Endoplasmic reticulum stress causes the activation of sterol regulatory element binding protein-2, The international journal of biochemistry & cell biology, 39 (2007) 1843-1851.
[24] H.L. Kammoun, H. Chabanon, I. Hainault, S. Luquet, C. Magnan, T. Koike, P. Ferre, F. Foufelle, GRP78 expression inhibits insulin and ER stress-induced SREBP-1c activation and reduces hepatic steatosis in mice, The Journal of clinical investigation, 119 (2009) 1201-1215.
[25] J.N. Lee, J. Ye, Proteolytic activation of sterol regulatory element-binding protein induced by cellular stress through depletion of Insig-1, The Journal of biological chemistry, 279 (2004) 45257-45265.
[26] J.D. Horton, J.L. Goldstein, M.S. Brown, SREBPs: activators of the complete program of cholesterol and fatty acid synthesis in the liver, The Journal of clinical investigation, 109 (2002) 1125-1131.
[27] M.S. Brown, J.L. Goldstein, A receptor-mediated pathway for cholesterol homeostasis, Science, 232 (1986) 34-47.
[28] R.G. Anderson, Joe Goldstein and Mike Brown: from cholesterol homeostasis to new paradigms in membrane biology, Trends in cell biology, 13 (2003) 534-539.

[29] A. Das, M.S. Brown, D.D. Anderson, J.L. Goldstein, A. Radhakrishnan, Three pools of plasma membrane cholesterol and their relation to cholesterol homeostasis, eLife, 3 (2014) e02882.
[30] A. Radhakrishnan, J.L. Goldstein, J.G. McDonald, M.S. Brown, Switch-like control of SREBP-2 transport triggered by small changes in ER cholesterol: a delicate balance, Cell metabolism, 8 (2008) 512-521.
[31] J. Ye, R.B. Rawson, R. Komuro, X. Chen, U.P. Dave, R. Prywes, M.S. Brown, J.L. Goldstein, ER stress induces cleavage of membrane-bound ATF6 by the same proteases that process SREBPs, Molecular cell, 6 (2000) 1355-1364.

Chapter Three: Calreticulin Calcium Binding and SREBP Activity

A version of this chapter has been previously published in:

W.A. Wang, W.X. Liu, S. Durnaoglu, S.K. Lee, J. Lian, R. Lehner, J. Ahnn, L.B. Agellon and M. Michalak, "Loss of Calreticulin Uncovers a Critical Role for Calcium in Regulating Cellular Lipid Homeostasis," *Scientific Reports*, vol. 7, issue 1, 5941-5955.

Introduction

The ER is a major Ca^{2+} storage organelle and Ca^{2+} concentrations within the ER is tightly regulated, with total Ca^{2+} in excess of 2 mM and free Ca^{2+} in the range of 50-250 μM [1-3]. Within the lumen of the ER, Ca^{2+} concentration is maintained by Ca^{2+} binding chaperones and folding enzymes, including calreticulin, GRP78 and PDIs [4]. In turn, ER luminal Ca^{2+} ensure the proper function of these protein folding chaperones and enzymes [5]. Additionally the Ca^{2+} within the ER is necessary for the many functions of the ER, including protein synthesis and posttranslational modifications, protein folding, lipid synthesis and interchaperone interactions [1, 6]. Consequently, any disruption in ER Ca^{2+} homeostasis may result in impaired ER function and homeostasis cumulating in pathology. Calreticulin is both a protein chaperone and a Ca^{2+} binding protein within the ER and these two functions are performed by distinct domains of calreticulin [7]. In the absence of calreticulin, cells have reduced ER Ca^{2+} store (by 50%) and impaired folding of the bradykinin receptor and the bradykinin-induced ER Ca^{2+} release from the $InsP_3R$ [8]. The N and P domain function as the chaperone unit of calreticulin and when *Calr*$^{-/-}$ cells are stably expressing the NP-domain of calreticulin, ER Ca^{2+} release induced by bradykinin is restored [8]. The C and P domain, on the other hand, function as the Ca^{2+} buffering regions of calreticulin and when *Calr*$^{-/-}$ cells are stably expressing the PC-domain of calreticulin, ER Ca^{2+} store capacity is restored but bradykinin-induced ER Ca^{2+} release is still impaired [8]. In this study, we identified the function of calreticulin responsible for modulating nSREBP activity using *Calr*$^{-/-}$ cells that stably express the NP- or PC- domains. Furthermore, we investigated the conundrum in which there is an increased nSREBP activity in the absence of calreticulin without

any changes to the level of unesterified cholesterol. We do this by observing overall cellular distribution of unesterified cholesterol in wild-type and *Calr*$^{-/-}$ cells.

Materials and Methods

Cell Culture and Treatments

Wild-type and *Calr*$^{-/-}$ cells and culturing conditions were previously described in chapter two [8]. *Calr*$^{-/-}$ cells stably expressing full-length calreticulin, the chaperone region (NP-domain) of calreticulin or the Ca^{2+} binding region (PC-domain) of calreticulin were previously described [8]. For luciferase measurements, SRE-luciferase [9] and XBP1 splicing luciferase [10] experiments were previously described in chapter two.

To assess the effect of Ca^{2+}, cells were transfected with the appropriated luciferase reporter plasmids and subjected to different Ca^{2+} manipulating methods. To deplete ER Ca^{2+}, cells were treated with 0.5 μM thapsigargin for 24 hours. To deplete extracellular Ca^{2+}, cells were treated with EGTA in the culture media for 24 hours. The EGTA concentration required was obtained with the EGTA calculator MaxChelator (maxchelator.stanford.edu). Total free Ca^{2+} in growth media was determined to be 2.17 mM (1.8 mM from DMEM and 0.37 mM from FBS). To achieve the following extracellular Ca^{2+} concentrations: 500 μM, 300 μM, 150 μM, and 100 μM, the following EGTA concentrations were used: 1.67 mM, 1.87 mM, 2.02 mM, and 2.08 mM, respectively.

For measurement of SREBP-1 and SREBP-2 precursor and nuclear protein level measurements, cells were treated with normal or lipid-free media or normal media with 2.02 mM EGTA (final Ca^{2+} concentration of 150 μM) for 24 hours and harvested for immunoblot analysis.

Immunoblot Analysis

Sample preparations and immunoblot analysis were previously described in chapter two [10].

Fura-2AM Calcium Measurements

For Ca^{2+} measurements, wild-type cells, *Calr*$^{-/-}$ cells and *Calr*$^{-/-}$ cells stably expressing full-length, the NP-domain and the PC-domain of calreticulin were loaded with Fura-2 AM and fluorescence was measured as previously described [11]. Measurement of ER Ca^{2+} was obtained through induction of Ca^{2+} release from ER stores by treatment with 1 μM thapsigargin.

Lipid Staining and Imaging

Cell preparation was previously described in chapter two.

For ER and SREBP-2 co-localization, cells were transfected with an ER-targeted red fluorescent protein (ER-RFP) expressing plasmid (10 μg), using the NEON transfection system (Thermo Fisher Scientific) for 24 hours. Cells were then washed 3 times with PBS, fixed with 3.7% formaldehyde (in PBS) for 1 hour, washed 3 times with PBS and permeabilized with 0.3 M glycine in PBS with 0.1% Tween. Cells were then washed 3 times with PBS, incubated with rabbit anti-SREBP-2 antibody (1 μg/mL) overnight at 4°C, washed 3 times with PBS, incubated with goat anti-rabbit Alexa Fluor® 305 (1:1000 dilution in PBS) for 2 hours and washed 3 times with PBS before visualization. ER-RFP was visualized with the Red HeNe laser, with excitation at 514 nm and emission peak at 584 nm. Alexa Fluor® 305 was visualized with the UV laser, with excitation at 405 nm and emission peak at 430 nm. Staining was visualized and imaged using a Leica TCS SP5 confocal microscope.

For ER and unesterified cholesterol co-localization, cells were transfected with the ER-RFP plasmid (10 μg), using the NEON transfection system (Thermo Fisher Scientific) for 24 hours followed by filipin staining. Cells were then washed 3 times with PBS, fixed with 3.7%

formaldehyde (in PBS) for 1 hour, washed 3 times with PBS, incubated with 1.5 mg/mL of glycine in PBS for 10 min at room temperature, stained with 0.05 mg/mL of filipin in PBS with 10% FBS for 2 hours at room temperature in the dark. Cells were then washed 3 times with PBS before visualization. ER-RFP was visualized with the Red HeNe laser, with excitation at 514 nm and emission peak at 584 nm. Filipin staining was visualized with the UV laser, with excitation at 405 nm and emission peak at 430 nm. Staining was visualized and imaged using a Leica TCS SP5 confocal microscope.

Overlap of filipin and ER-RFP signals was analyzed using ImageJ. A straight line was drawn across the middle of each cell and identified as the region of interest (ROI). The signal intensity of each channel (blue for filipin and red for ER-RFP) for each cell was obtained using the corresponding ROI and the values were plotted along the same X axis coordinates to identify regions of overlap.

Subcellular Fractionation and Lipid Analysis

Wild-type and *Calr*$^{-/-}$ cells were grown in 150 mm dishes to 90% confluency. Three dishes were used per gradient separation. Gradients were prepared on day one, a day prior to cell harvest. Optiprep (60% iodixanol in water) (Sigma-Aldrich) was used and diluted to a working solution of 50% iodixanol in diluent buffer (0.25 M sucrose and 60 mM Tris, pH 7.4). 6%, 9%, 12%, 15%, 18%, 21%, 24% and 27% dilutions of iodixanol was prepared with working solution in homogenization buffer (0.25 M sucrose and 10 mM Tris, pH 7.4) and 500 μL of each dilution was sequentially layered in polyallomer (13×51 mm) centrifuge tubes. The formed gradients were stored overnight at 4°C. On day two, cells were harvested. Cells were washed 2 times with PBS and scraped into 800 μL of homogenization buffer. The homogenate was passed through an

18 micron clearance ball bearing homogenizer 30 times and centrifuged at 800×g for 10 minutes at 4°C. One hundred μL of homogenate was kept for total protein analysis and 800 μL of the homogenate was layered on top of the previously prepared iodixanol gradient. The gradients were centrifuged using the Optima™ Ultracentrifuge (Beckman Coulter) at 144,203 × g for 6 hours at 4°C and twelve fractions (400 μL per fraction) were collected from the top of gradients into 1.5 mL Eppendorf tubes. 100 μL of each fraction were taken for protein analysis and the remaining of each fraction were taken for lipid extraction and gas chromatography analysis.

Proteins were precipitated by addition of 300 μL (3×sample volume) of 100% acetone to each total and fraction samples and incubated overnight at 4°C. The samples were then centrifuged at 16,100 × g for 10 minutes at 4°C. The pellets were washed with 100% ethanol and then re-centrifuged at 16,100 × g for 10 min at 4°C. The resulting pellets were dissolved in 100 μL 1X SDS-PAGE sample buffer and processed for immunoblot analysis.

For lipid extraction, individual fractions were mixed with 2 mL of solution containing 17.5 mM Tris, pH 7.3, 10 mM $CaCl_2$, 2 units of phospholipase C from *Clostridium welchii* (Sigma-Aldrich) and 2 mL diethyl ether. The samples were mixed and incubated for 2 hours at 30°C with constant mixing. 1 mL of tridecanoin (2 μg/mL in chloroform) and 6 mL of chloroform:methanol (2:1) was added followed by centrifugation at 600 × g for 10 minutes. The lower phase was removed and passed through a Pasteur pipette containing anhydrous Na_2SO_4 into a smaller glass tube. The resulting mixture was dried under nitrogen and the remaining residue was dissolved in 100 μL Sylon BFT (Supelco), incubated for 1 hour at room temperature and analyzed by gas chromatography (Agilent Technologies, 6890 Series equipped with a flame ionization detector; Palo Alto, CA). Samples were injected onto an Agilent high performance capillary column (HP-

5, 15 m×0.32 mm×0.25 μm). The oven temperature was raised from 170 to 290°C at 20°C/minute and then to 340°C at 10°C/minute with helium as a carrier gas (87 cm/s) with a constant flow rate of 4.5 mL/minute [12].

Results

ER Calcium affects SREBP Activity

Calreticulin deficiency in cells leads to a ~50% reduction of total ER luminal Ca^{2+} content and this can be rescued with re-expression of the full-length or the PC-domain but not the NP-domain of calreticulin [8]. To confirm this we measured ER Ca^{2+} content, using the SERCA inhibitor thapsigargin (for thapsigargin releasable Ca^{2+}) [13]. In agreement to what was previously published [8], compared to wild-type cells, *Calr*$^{-/-}$ cells had a reduction in total ER luminal Ca^{2+} content and this was normalized by the stable expression of full-length recombinant calreticulin, or its Ca^{2+} binding PC-domain, but not with its chaperone NP-domain (Figure 3.1). Next we used these *Calr*$^{-/-}$ cells stably expressing the full length, the Ca^{2+} binding domain or the chaperone domain of calreticulin to identify the domain or function of calreticulin responsible for the changes seen in nSREBP activity. When we measured nSREBP activity, only the *Calr*$^{-/-}$ cells expressing full-length, or the Ca^{2+} binding PC-domain of calreticulin exhibited nSREBP activity to a level seen in the wild-type cells (Figure 3.2). Therefore, it is the lack of the Ca^{2+} binding function of calreticulin, or consequently the reduction of ER Ca^{2+}, that is responsible for the increased nSREBP activity seen in *Calr*$^{-/-}$ cells.

Next, we examined if reduction of total ER Ca^{2+} stores had a direct effect on nSREBP activity in wild-type cells and whether we could reproduce the enhanced nSREBP activity observed in the absence of calreticulin. We evaluated the nSREBP activity in wild-type cells under reduced Ca^{2+} conditions by gradually chelating extracellular Ca^{2+} concentration, a method that has been previously reported to reduce total ER Ca^{2+} [14]. Decreasing extracellular Ca^{2+} concentration

from 500 μM to 100 μM progressively and concomitantly increased nSREBP activity in wild-type cells (Figure 3.3), whereas the same treatment didn't have effect on *Calr*$^{-/-}$ cells (Figure 3.4). At 150 μM extracellular Ca^{2+} concentration, nSREBP activity in wild-type cells were no longer different from the nSREBP activity in *Calr*$^{-/-}$ cells (Figure 3.3). To confirm that the treatment of cells with 150 μM Ca^{2+} increased SREBP processing, we treated wild-type cells with reduced Ca^{2+} concentration (150 μM) and measured protein levels of SREBP-1 and SREBP-2 (Figure 3.5A). In agreement with the increase in nSREBP activity seen in *Calr*$^{-/-}$ cells and wild-type cells with reduced Ca^{2+} concentrations, there was an increase in ratio of nuclear to total (precursor and nuclear forms) SREBP-1 and SREBP-2 protein in wild-type cells exposed to 150 μM extracellular Ca^{2+} (Figure 3.5B,C). To ensure that the lowering of extracellular Ca^{2+} was not affecting nSREBP activity through the induction of ER stress and UPR activity, we measured XBP1 splicing luciferase activity under each Ca^{2+} concentrations. Lowering extracellular Ca^{2+} concentrations from 500 μM to 150 μM in both wild-type and *Calr*$^{-/-}$ cells did not induce XBP1 splicing (Figure 3.6). Thapsigargin treatment to deplete total ER Ca^{2+} stores completely, expectedly increased XBP1 splicing in both wild-type and *Calr*$^{-/-}$ cells (Figure 3.6). This demonstrated that lowering Ca^{2+} concentration in wild-type cells, without changing cholesterol levels, was sufficient to reproduce the increased nSREBP activity seen in the absence of calreticulin. Altogether, these results showed that the reduction of total ER luminal Ca^{2+} content is responsible for the increased level of nSREBP activity in *Calr*$^{-/-}$ cells.

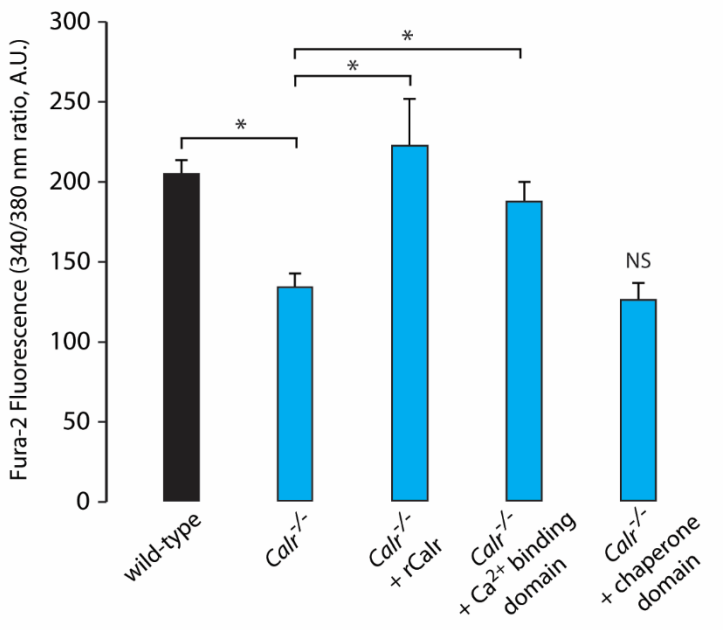

Figure 3.1 Calreticulin functional domains and ER Ca^{2+}

Total ER luminal Ca^{2+} (thapsigargin releasable pool of total Ca^{2+}) in wild-type, *Calr*$^{-/-}$ mouse embryonic fibroblast cells and *Calr*$^{-/-}$ mouse embryonic fibroblast cells stably expressing full-length recombinant calreticulin (*Calr*$^{-/-}$+rCalr), the PC-domain of calreticulin (*Calr*$^{-/-}$+Ca^{2+} binding domain) or the NP-domain of calreticulin (*Calr*$^{-/-}$+chaperone domain). *Indicates statistically significant differences: wild-type vs. *Calr*$^{-/-}$ cells, p-value<0.05; *Calr*$^{-/-}$ vs. *Calr*$^{-/-}$ +rCalr, p-value<0.05; *Calr*$^{-/-}$ vs. *Calr*$^{-/-}$+Ca^{2+} binding domain, p-value<0.05. NS, not significant. Representative of 3 biological experiments; 2 replicates per experiment (ANOVA).

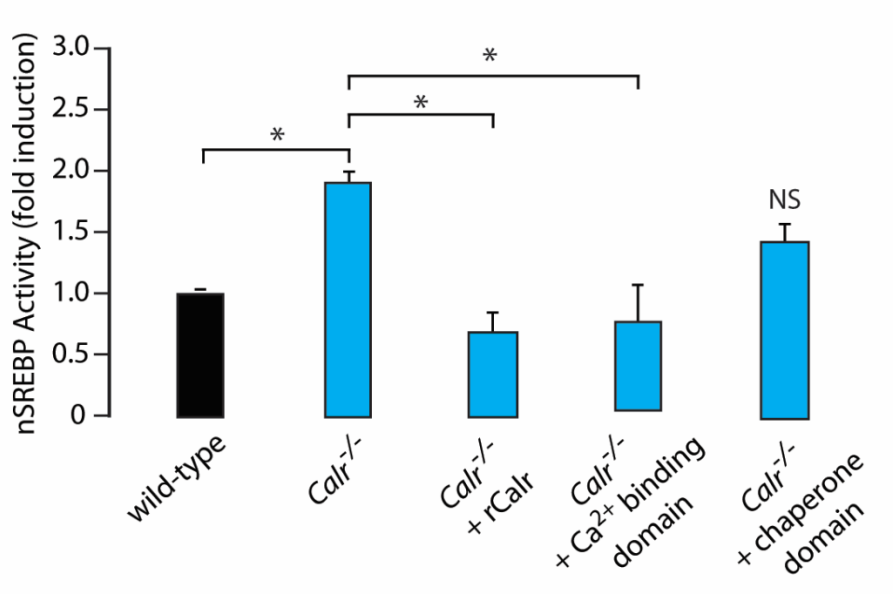

Figure 3.2 Calreticulin functional domains and nSREBP activity

nSREBP activity in wild-type, *Calr*$^{-/-}$ mouse embryonic fibroblast cells, *Calr*$^{-/-}$+rCalr, *Calr*$^{-/-}$ +Ca^{2+} binding domain or *Calr*$^{-/-}$+chaperone domain. *Indicates statistically significant differences: wild-type vs. *Calr*$^{-/-}$ cells, p-value<0.05; *Calr*$^{-/-}$ vs. *Calr*$^{-/-}$+rCalr, p-value<0.05; *Calr*$^{-/-}$ vs. *Calr*$^{-/-}$+Ca^{2+} binding domain, p-value<0.05. NS, not significant. Representative of 3 biological experiments; 2 replicates per experiment (ANOVA).

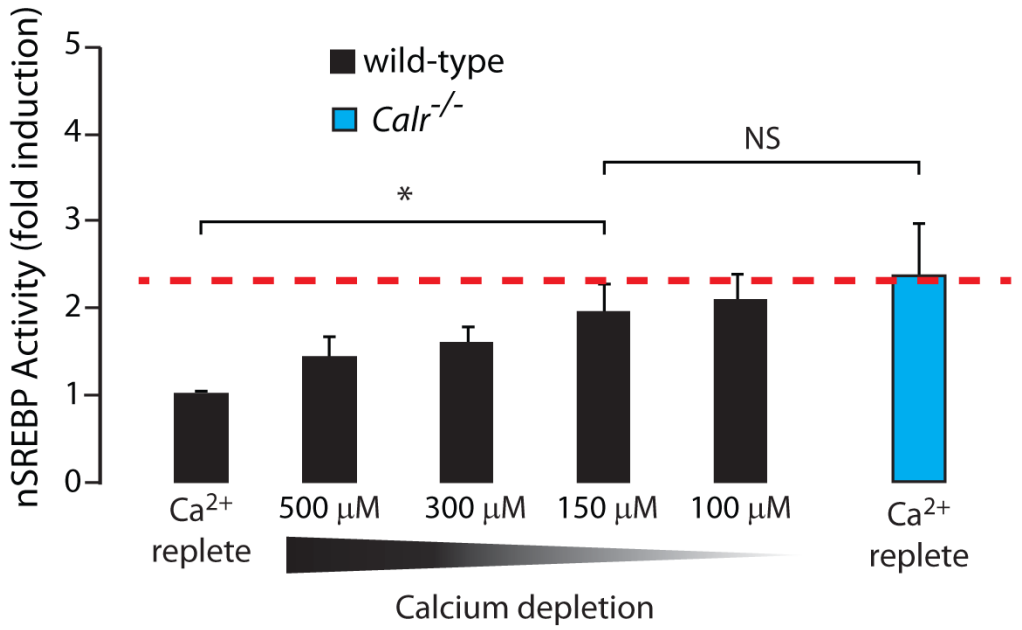

Figure 3.3 Reducing extracellular Ca^{2+} and nSREBP activity in wild-type cells

nSREBP activity in wild-type mouse embryonic fibroblast cells exposed to Ca^{2+} replete (2.17 mM) conditions and EGTA treatment to decrease extracellular Ca^{2+} concentrations (500 μM, 300 μM, 150 μM and 100 μM) to deplete total ER Ca^{2+} stores and *Calr*$^{-/-}$ mouse embryonic fibroblast cells exposed to Ca^{2+} replete (2.17 mM) conditions. *Indicates statistically significant differences: wild-type vs. *Calr*$^{-/-}$ cells in Ca^{2+} replete conditions, p-value<0.05; wild-type cells in Ca^{2+} replete conditions vs. 150 μM Ca^{2+}, p-value<0.05. NS, not significant. Representative of 7 biological experiments; 2 replicates per experiment (ANOVA).

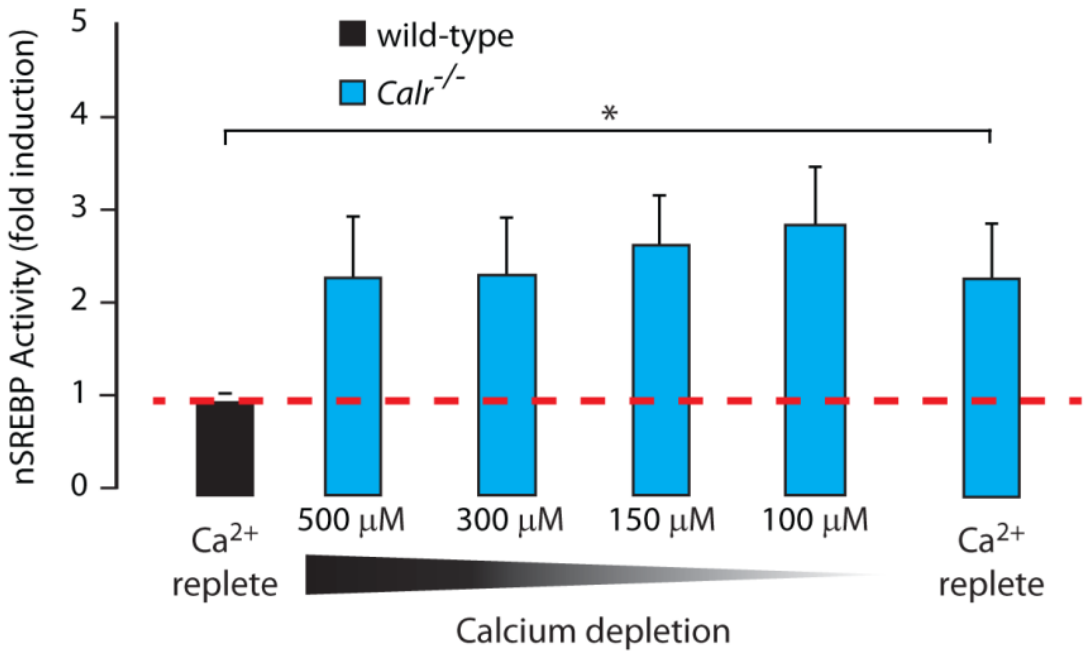

Figure 3.4 Reducing extracellular Ca^{2+} and nSREBP activity in *Calr*$^{-/-}$ cells

nSREBP activity in *Calr*$^{-/-}$ mouse embryonic fibroblast cells exposed to Ca^{2+} replete (2.17 mM) conditions and EGTA treatment to decrease extracellular Ca^{2+} concentrations (500 µM, 300 µM, 150 µM and 100 µM) to deplete total ER Ca^{2+} stores and wild-type exposed to Ca^{2+} replete (2.17 mM) conditions. *Indicates statistically significant differences: *Calr*$^{-/-}$ vs. wild-type cells in Ca^{2+} replete conditions, p-value<0.05. NS, not significant. Representative of 7 biological experiments; 2 replicates per experiment (ANOVA).

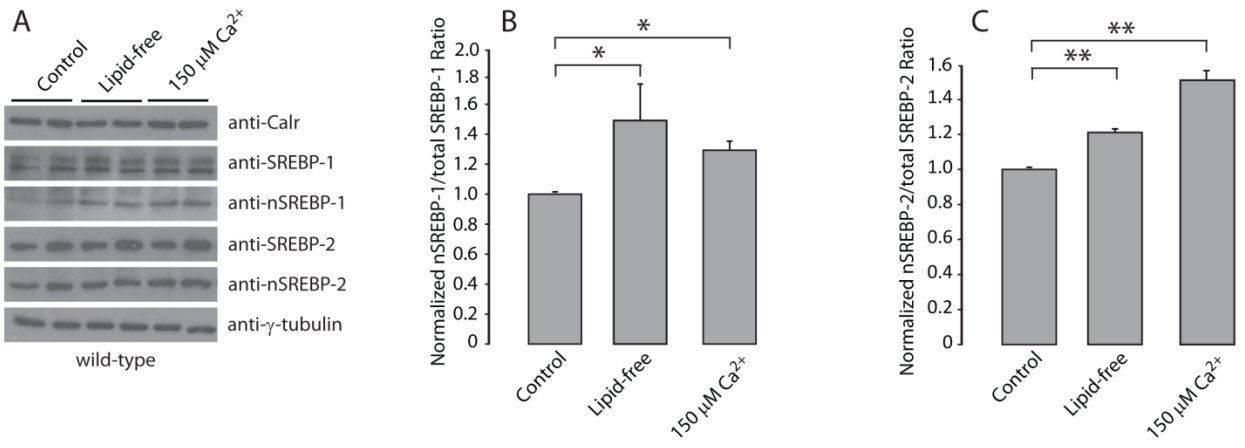

Figure 3.5 Reducing extracellular Ca^{2+} and SREBP protein expression

A. Immunoblot of wild-type mouse embryonic fibroblast cells grown in control media, lipid-free media and control media with EGTA for a final extracellular Ca^{2+} concentration of 150 μM, probed with anti-calreticulin, anti-SREBP-1, anti-nSREBP-1, anti-SREBP-2 and anti-nSREBP-2 antibodies. Anti-γ-tubulin antibodies were used as a loading control. Representative of 3 biological experiments; 1 replicate per experiment.

B,C. Quantitative analysis of immunoblots showing the ratio of nuclear to total (precursor and nuclear forms) **(B)** SREBP-1 and **(C)** SREBP-2 in wild-type mouse embryonic fibroblast cells grown in control media, lipid-free media and control media with 150 μM Ca^{2+}. *Indicates statistically significant differences: for **(B)** SREBP-1 control vs. lipid-free media, *p*-value=0.0432; SREBP-1 control vs. control media with 150 μM Ca^{2+}, *p*-value=0.0146. **Indicates statistically significant differences: for **(C)** SREBP-2 control vs. lipid-free media, *p*-value=0.0012; SREBP-2 control vs. control media with 150 μM Ca^{2+}, *p*-value=0.0013. Representative of 3 biological experiments; 1 replicate per experiment (Student's t-test).

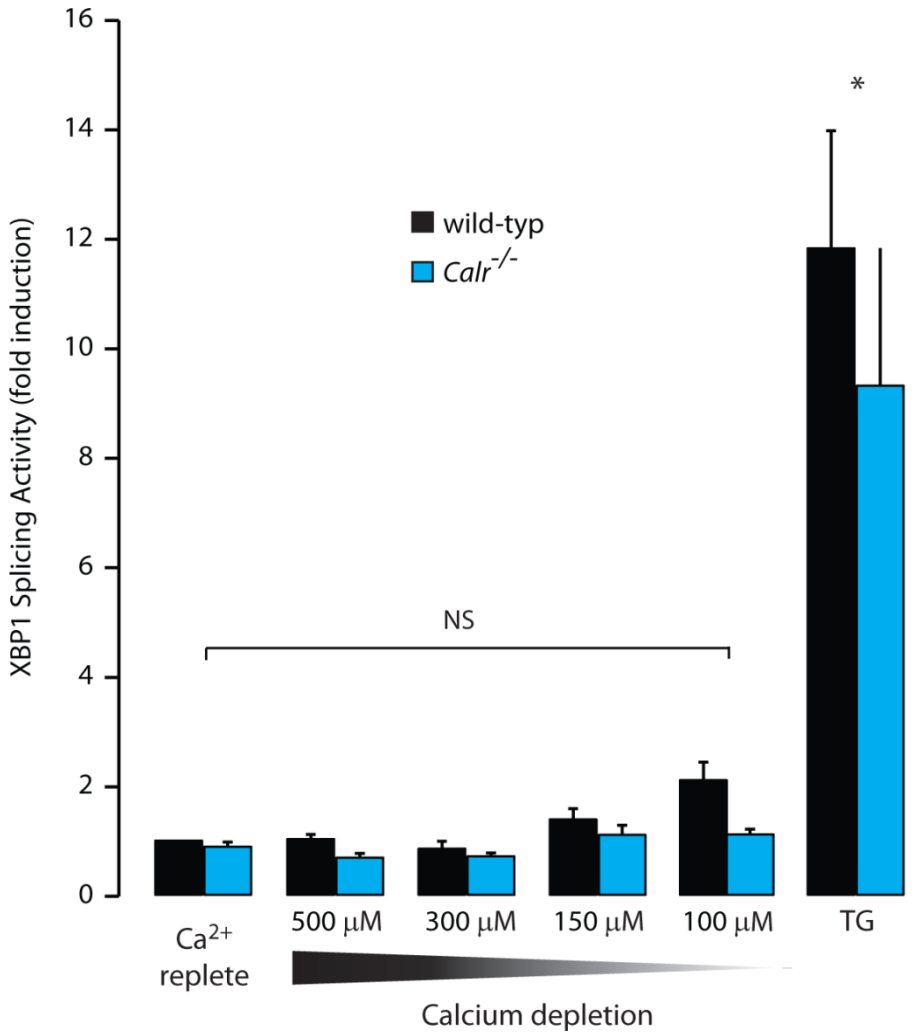

Figure 3.6 Reducing extracellular Ca^{2+} and ER stress

XBP1 luciferase activity in wild-type and *Calr*$^{-/-}$ mouse embryonic fibroblast cells exposed to Ca^{2+} replete (2.17 mM) conditions, treated with EGTA to decrease extracellular Ca^{2+} concentrations (500 µM, 300 µM, 150 µM and 100 µM) to deplete total ER Ca^{2+} stores and treated with 0.5 µM thapsigargin (TG) for ER Ca^{2+} depleted conditions. *Indicates statistically significant differences: wild-type and *Calr*$^{-/-}$ cells treated with Ca^{2+} replete vs. TG, p-value<0.05. NS, not significant. Representative of 6 biological experiments; 2 replicates per experiment (ANOVA).

ER Calcium Affects Intracellular Cholesterol Distribution

In the absence of calreticulin or with reduced total ER Ca^{2+}, nSREBP activity is enhanced even under abundant total cholesterol conditions. Furthermore, the level of intracellular unesterified cholesterol is unchanged between wild-type and *Calr*$^{-/-}$ cells. Therefore, the underlying cause of increased nSREBP acitivity in the absence of calreticulin or under reduced total ER Ca^{2+} is still unknown. To address this we examined the intracellular distribution of unesterified cholesterol. First we stained wild-type and *Calr*$^{-/-}$ cells expressing ER targeted red fluorescent protein (ER-RFP) with anti-SREBP-2 antibodies and found that SREBP-2 overlaps with the ER in both cell types (Pearson's Coefficient=0.231±0.035 and Pearson's Coefficient=0.291±0.038, respectively) (Figure 3.7). Next we used filipin, a fluorescent polyene antibiotic that binds unesterified cholesterol within cells [15, 16]. In wild-type cells, filipin staining co-localized with the ER-RFP marker (Pearson's Coefficient=0.212±0.013), and analysis of the filipin and ER-RFP fluorescent signals revealed excellent overlap, indicating a significant proportion of unesterified cholesterol co-localized with the ER (Figure 3.8A). In contrast, there was substantially less co-localization between filipin and ER-RFP (Pearson's Coefficient=0.116±0.026) in *Calr*$^{-/-}$ cells and analysis of signal overlap was much reduced (Figure 3.8B). We also cultured wild-type cells with reduced extracellular Ca^{2+} concentration (150 μM) to reduce ER Ca^{2+} stores [14], a condition that increased nSREBP activity. In wild-type cells exposed to 150 μM Ca^{2+}, the co-localization between filipin and ER-RFP was also reduced (Pearson's Coefficient=0.118±0.025) and analysis of signal overlap was also reduced (Figure 3.8C), reminiscent of the pattern exhibited by *Calr*$^{-/-}$ cells cultured under normal conditions (Figure 3.8B). Together, this was the first indication that in the absence of calreticulin or under reduced total ER Ca^{2+}, there is an altered distribution of

unesterified cholesterol away from the ER as marked by ER-RFP and SREBP-2. In addition, under all of these conditions, ER-RFP fluorescence indicate that ER morphology is not changed between wild-type, *Calr*$^{-/-}$ and wild-type cells treated with 150 μM Ca^{2+} (Figure 3.8).

To confirm the difference in the distribution of unesterified cholesterol seen with filipin staining, we conducted subcellular fractionation of wild-type and *Calr*$^{-/-}$ cells over an iodixanol gradient and measured levels of unesterified cholesterol within each fraction. Immunoblot of wild-type and *Calr*$^{-/-}$ fractions indicate the separation of ER (fractions 6 to10) marked by anti-calnexin antibodies and cytosol (fractions 3 to 5) marked by anti-glyceraldehyde 3-phosphate dehydrogenase (GAPDH) antibodies (Figure 3.9A). In agreement with the distribution of unesterified cholesterol revealed by filipin staining, the distribution of unesterified cholesterol detected in the subcellular fractions of wild-type and *Calr*$^{-/-}$ cells were distinctly different (Figure 3.9B). The distribution of unesterified cholesterol in wild-type cells, revealed a peak within calnexin positive fractions (ie. ER fractions) in fraction 6 (Figure 3.9B). In contrast, the distribution of unesterified cholesterol in *Calr*$^{-/-}$ cells had a peak in fraction 7 and 8 (Figure 3.9B). These results demonstrated that the ER distribution of unesterified cholesterol, which regulated the processing and activity of nSREBP, was altered in the absence of calreticulin and more importantly, by the reduction in ER Ca^{2+}.

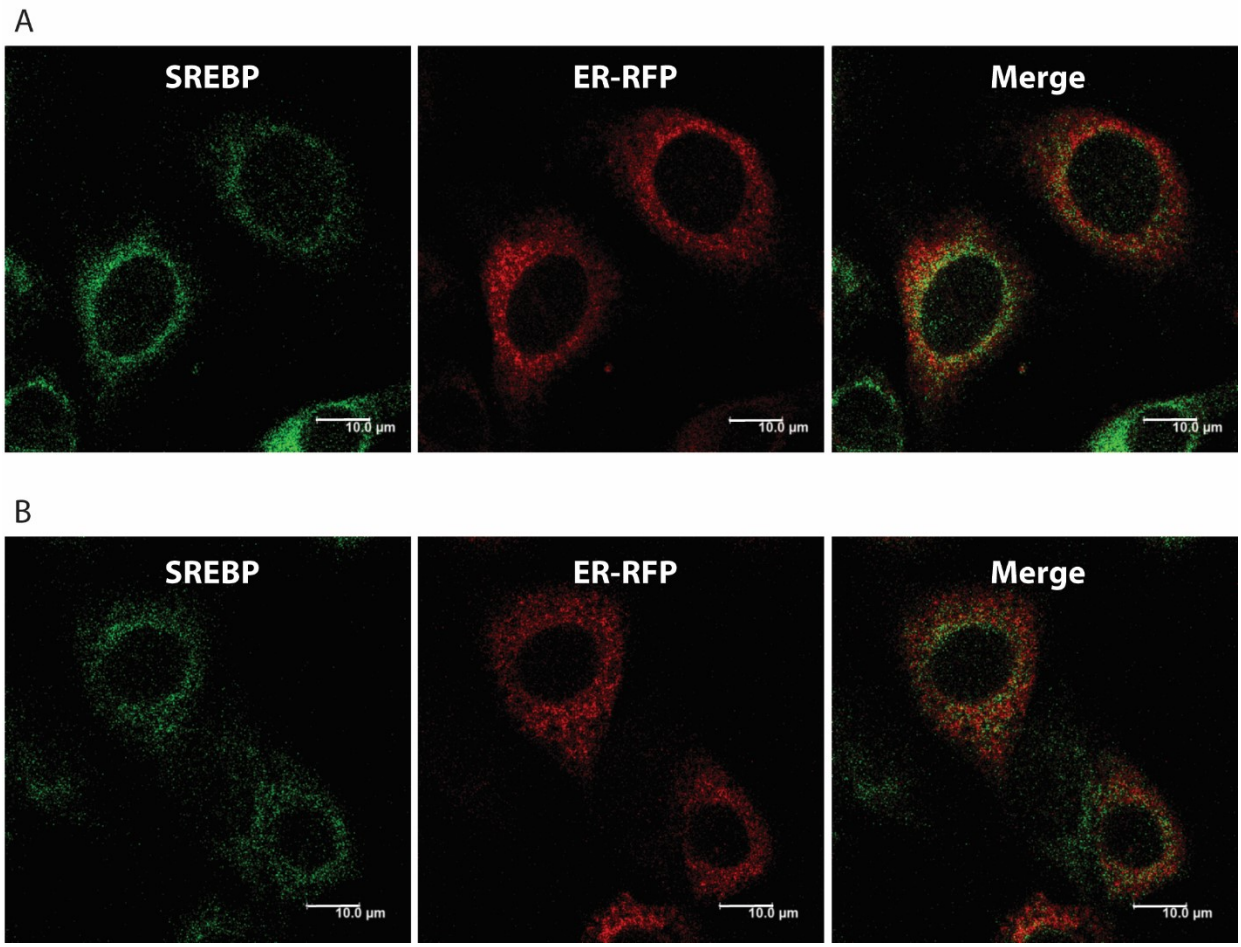

Figure 3.7 Cellular distribution of SREBP-2 in wild-type and *Calr*$^{-/-}$ cells

(A) Wild-type and **(B)** *Calr*$^{-/-}$ mouse embryonic fibroblast cells expressing ER-targeted red fluorescent protein (ER-RFP) were stained with anti-SREBP-2 antibodies. Wild-type cells Pearson's coefficient=0.231±0.035 (n=15); *Calr*$^{-/-}$ cells Pearson's coefficient=0.291±0.038 (n=15).

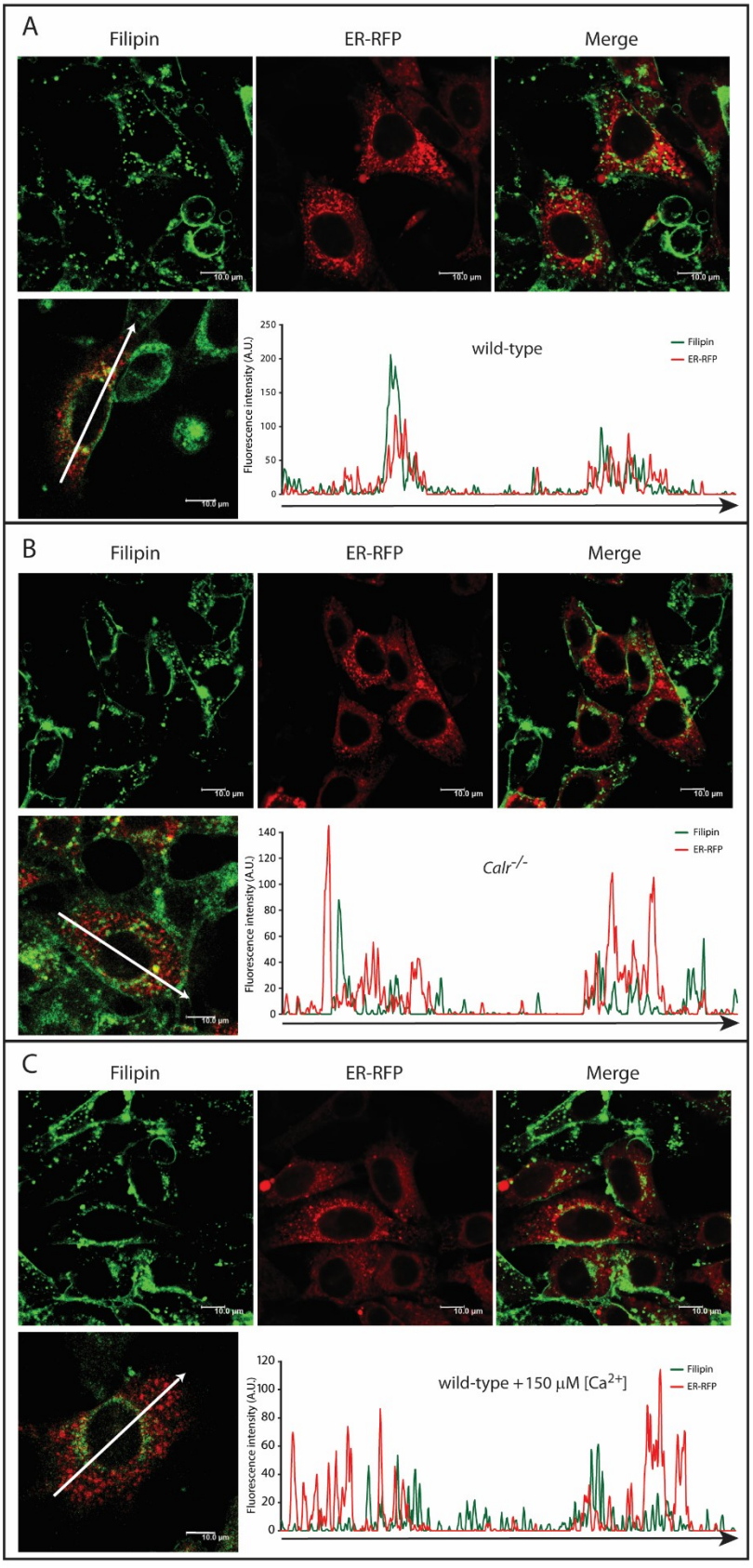
A
Filipin
ER-RFP
Merge
10.0 µm
wild-type
Filipin
ER-RFP
Fluorescence intensity (A.U.)
250
200
150
100
50
0
B
Filipin
ER-RFP
Merge
10.0 µm
Calr-/-
Filipin
ER-RFP
Fluorescence intensity (A.U.)
140
120
100
80
60
40
20
0
C
Filipin
ER-RFP
Merge
10.0 µm
wild-type +150 µM [Ca2+]
Filipin
ER-RFP
Fluorescence intensity (A.U.)
120
100
80
60
40
20
0

Figure 3.8 Intracellular distribution of cholesterol in wild-type cells, *Calr*$^{-/-}$ cells and wild-type cells with reduced extracellular Ca^{2+}

(A) Wild-type, **(B)** *Calr*$^{-/-}$ mouse embryonic fibroblast cells and **(C)** wild-type mouse embryonic fibroblast cells treated with 150 μM Ca^{2+} expressing ER-targeted red fluorescent protein (ER-RFP) were stained with filipin. A representative of 3 independent analyses is presented. Wild-type cells Pearson's coefficient=0.212±0.013 (n=15), *Calr*$^{-/-}$ cells Pearson's coefficient=0.116±0.026 (n=15) and wild-type cells treated with 150 μM Ca^{2+} Pearson's coefficient=0.118±0.025 (n=15). Graphic representation of overlap of filipin and ER-RFP signals is presented in the figure. The arrows indicate the direction of the scan represented in the graph.

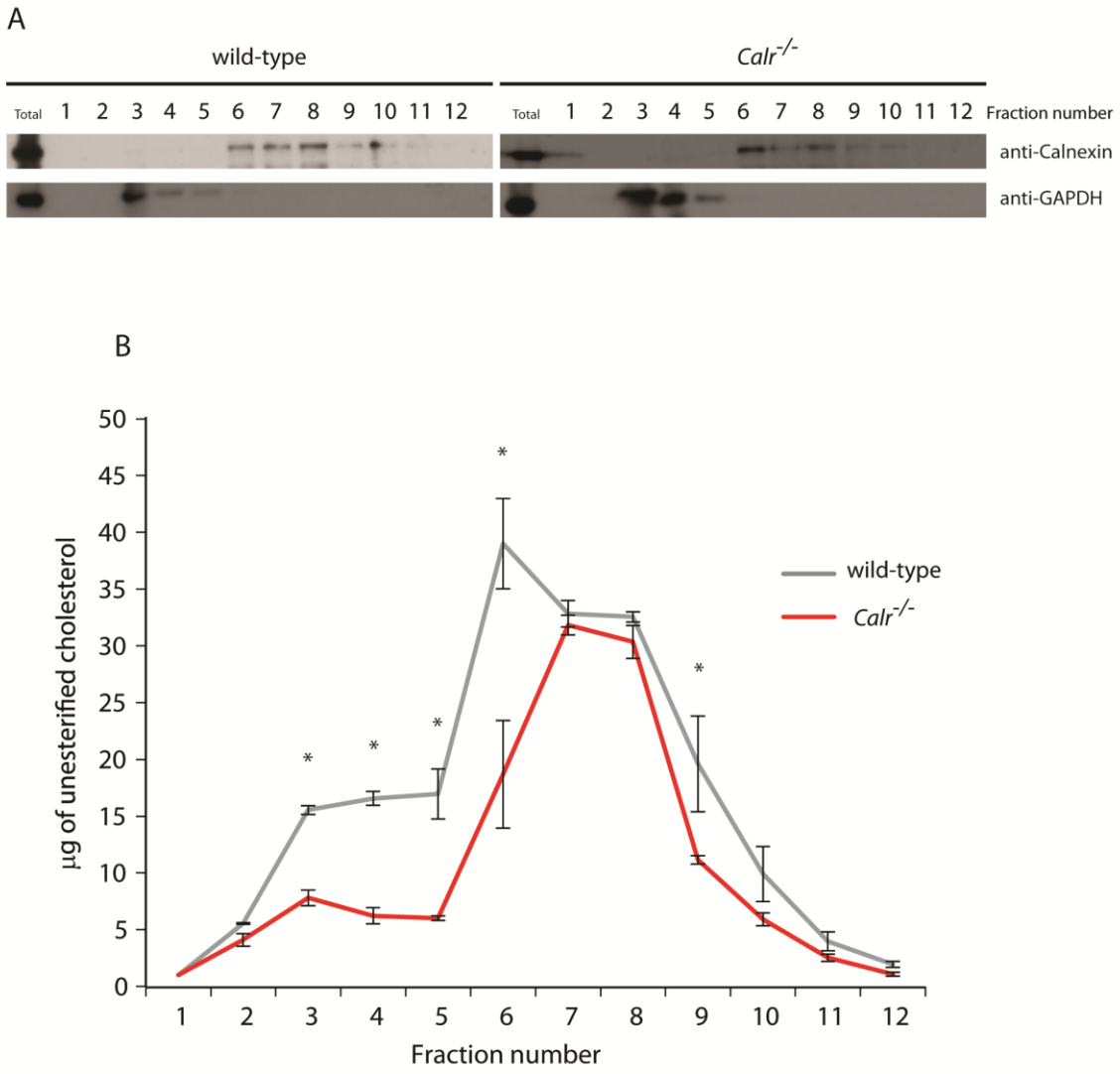

Figure 3.9 Distribution of unesterified cholesterol in wild-type and *Calr*$^{-/-}$ cells

A. Immunoblot of wild-type and *Calr*$^{-/-}$ mouse embryonic fibroblast subcellular fractions probed with anti-calnexin (representing ER fractions) and anti-GAPDH (representing cytosol fractions) antibodies. Representative of 3 biological experiments; 1 replicate per experiment.

B. Distribution of unesterified cholesterol in the subcellular fractions of wild-type and *Calr*$^{-/-}$ mouse embryonic fibroblast cells. *Indicates statistically significant differences: wild-type vs. *Calr*$^{-/-}$ cell fractions, p-value<0.05. Representative of 3 biological experiments; 1 replicate per experiment (ANOVA).

Discussion

The study of calreticulin as a multifunctional protein that maintains ER homeostasis has uncovered a multitude of pathways involved in a variety of physiological processes and disorders [7]. In this study investigating the link between calreticulin deficiency and energy metabolism, we uncovered a critical role for ER Ca^{2+} in maintaining cholesterol homeostasis in eukaryotic cells. We showed that the enhanced nSREBP activity in the absence of calreticulin, which have reduced ER Ca^{2+} [8], can be normalized to a level comparable to that in wild-type cells simply by expressing the Ca^{2+} binding domain of calreticulin. Conversely, we showed that depletion of ER Ca^{2+} in wild-type cells, independently of calreticulin, caused the enhancement of nSREBP activity in a concentration-dependent manner. Reduced ER Ca^{2+} lead to an enhanced nSREBP activity regardless of cholesterol levels and occurred independently of ER stress or UPR activation. Evidently, through direct staining and subcellular fractionation, we found that reduced ER Ca^{2+}, which does not impact on total levels of unesterified cholesterol, does impact on the intracellular distribution of unesterified cholesterol. We propose that the reduction in ER Ca^{2+} shifts the intracellular distribution of unesterified cholesterol within the ER to a pool that is not directly accessible to the compartments of the cholesterol sensing mechanism inherent to the SREBP-SCAP complex (Figure 3.10). Therefore, ER Ca^{2+} status may be a previously unrecognized determinant of the basal sensitivity of the sterol sensing mechanism of the SREBP pathway, a master regulator of lipid homeostasis.

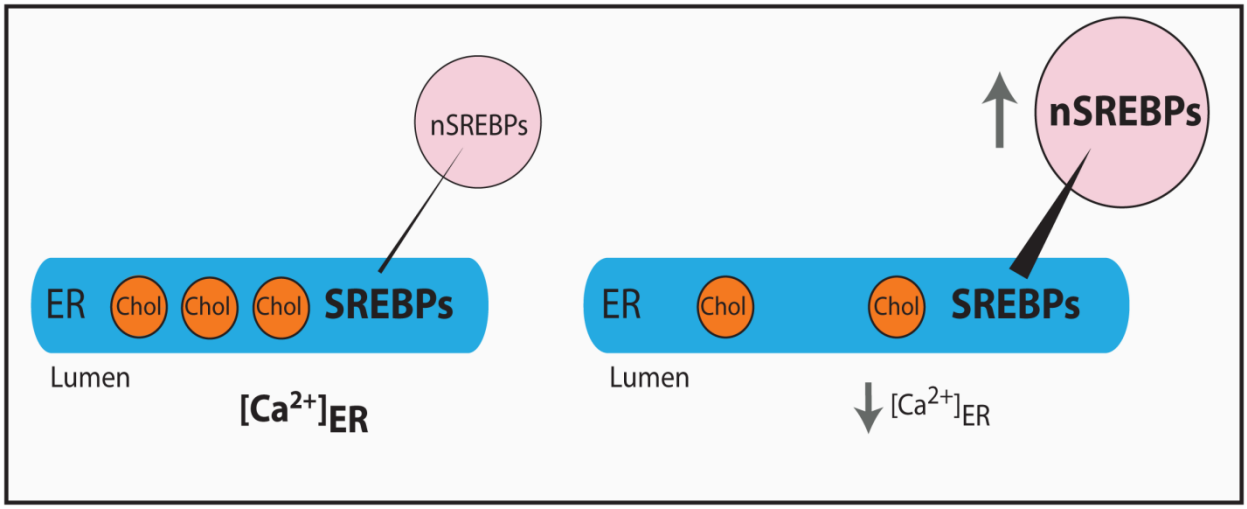

Figure 3.10 A schematic representation depicting the role of ER Ca^{2+} on cholesterol homeostasis

The model shows cross talk between ER Ca^{2+} and intracellular cholesterol distribution. The small amount of unesterified cholesterol (*chol*) found at the ER regulates the processing and activity of SREBP. Under cholesterol abundant conditions (*left*), SREBP processing is limited. Reducing total ER luminal Ca^{2+} (*right*) shifts the distribution of unesterified cholesterol away from the pool that regulates SREBP processing and activity. The decrease in this pool of ER membrane cholesterol enhances SREBP processing and increases nuclear SREBP (nSREBP) abundance and activity.

References

[1] E.F. Corbett, M. Michalak, Calcium, a signaling molecule in the endoplasmic reticulum?, Trends in biochemical sciences, 25 (2000) 307-311.
[2] R. Yu, P.M. Hinkle, Rapid turnover of calcium in the endoplasmic reticulum during signaling. Studies with cameleon calcium indicators, The Journal of biological chemistry, 275 (2000) 23648-23653.
[3] N. Solovyova, N. Veselovsky, E.C. Toescu, A. Verkhratsky, Ca(2+) dynamics in the lumen of the endoplasmic reticulum in sensory neurons: direct visualization of Ca(2+)-induced Ca(2+) release triggered by physiological Ca(2+) entry, The EMBO journal, 21 (2002) 622-630.
[4] D. Prins, M. Michalak, Organellar calcium buffers, Cold Spring Harbor perspectives in biology, 3 (2011) a004069.
[5] E.F. Corbett, K.M. Michalak, K. Oikawa, S. Johnson, I.D. Campbell, P. Eggleton, C. Kay, M. Michalak, The conformation of calreticulin is influenced by the endoplasmic reticulum luminal environment, The Journal of biological chemistry, 275 (2000) 27177-27185.
[6] J.F. Sambrook, The involvement of calcium in transport of secretory proteins from the endoplasmic reticulum, Cell, 61 (1990) 197-199.
[7] M. Michalak, J. Groenendyk, E. Szabo, L.I. Gold, M. Opas, Calreticulin, a multi-process calcium-buffering chaperone of the endoplasmic reticulum, The Biochemical journal, 417 (2009) 651-666.
[8] K. Nakamura, A. Zuppini, S. Arnaudeau, J. Lynch, I. Ahsan, R. Krause, S. Papp, H. De Smedt, J.B. Parys, W. Muller-Esterl, D.P. Lew, K.H. Krause, N. Demaurex, M. Opas, M. Michalak, Functional specialization of calreticulin domains, The Journal of cell biology, 154 (2001) 961-972.
[9] R.D. Bell, R. Deane, N. Chow, X. Long, A. Sagare, I. Singh, J.W. Streb, H. Guo, A. Rubio, W. Van Nostrand, J.M. Miano, B.V. Zlokovic, SRF and myocardin regulate LRP-mediated amyloid-beta clearance in brain vascular cells, Nature cell biology, 11 (2009) 143-153.
[10] S.H. Back, K. Lee, E. Vink, R.J. Kaufman, Cytoplasmic IRE1alpha-mediated XBP1 mRNA splicing in the absence of nuclear processing and endoplasmic reticulum stress, The Journal of biological chemistry, 281 (2006) 18691-18706.
[11] L. Mery, N. Mesaeli, M. Michalak, M. Opas, D.P. Lew, K.H. Krause, Overexpression of calreticulin increases intracellular Ca^{2+} storage and decreases store-operated Ca^{2+} influx, The Journal of biological chemistry, 271 (1996) 9332-9339.
[12] D. Sahoo, T.C. Trischuk, T. Chan, V.A. Drover, S. Ho, G. Chimini, L.B. Agellon, R. Agnihotri, G.A. Francis, R. Lehner, ABCA1-dependent lipid efflux to apolipoprotein A-I mediates HDL particle formation and decreases VLDL secretion from murine hepatocytes, Journal of lipid research, 45 (2004) 1122-1131.
[13] M. Treiman, C. Caspersen, S.B. Christensen, A tool coming of age: thapsigargin as an inhibitor of sarco-endoplasmic reticulum Ca(2+)-ATPases, Trends in pharmacological sciences, 19 (1998) 131-135.
[14] P. Pinton, D. Ferrari, E. Rapizzi, F. Di Virgilio, T. Pozzan, R. Rizzuto, The Ca^{2+} concentration of the endoplasmic reticulum is a key determinant of ceramide-induced apoptosis: significance for the molecular mechanism of Bcl-2 action, The EMBO journal, 20 (2001) 2690-2701.

[15] S. Mukherjee, X. Zha, I. Tabas, F.R. Maxfield, Cholesterol distribution in living cells: fluorescence imaging using dehydroergosterol as a fluorescent cholesterol analog, Biophysical journal, 75 (1998) 1915-1925.
[16] P.C. Reid, N. Sakashita, S. Sugii, Y. Ohno-Iwashita, Y. Shimada, W.F. Hickey, T.Y. Chang, A novel cholesterol stain reveals early neuronal cholesterol accumulation in the Niemann-Pick type C1 mouse brain, Journal of lipid research, 45 (2004) 582-591.

Chapter Four: Store Operated Calcium Entry and SREBP

Introduction

ER as a major Ca^{2+} store plays an important role in maintaining general cellular Ca^{2+} homeostasis. To maintain its Ca^{2+} store, the ER contains many Ca^{2+} binding folding enzymes and protein chaperones like calreticulin [1, 2]. The impact of calreticulin as a Ca^{2+} binding protein extends beyond ER Ca^{2+} storage capacity and affects processes such as ER Ca^{2+} release [3-5] and uptake [4, 6] and store-operated Ca^{2+} entry (SOCE) activity [7-10]. Furthermore, calreticulin as a multifunctional protein has been shown to play a role in cardiogenesis, immunity, cancer and most recently, cholesterol homeostasis [11, 12]. Importantly, recent studies have emerged establishing the role for STIM1, Orai1 and SOCE in lipid metabolism [13-15]. Specifically, it was shown that lipid accumulation in obese mice disrupted SOCE [15] and in turn, SOCE-deficient mice display an abnormal amount of lipid droplet accumulation, reduced fatty acid oxidation and impaired lipolysis [13]. Obese mice display a reduced ER Ca^{2+} store, disrupted STIM1 to plasma membrane translocation and defective SOCE, all of which can be improved upon overexpressing STIM1 and re-establishing proper SOCE activity [14]. Furthermore, cholesterol binding domains have been found in STIM1 and Orai1 and the accessibility of cholesterol to these sites plays a role in modulating SOCE [16, 17]. Therefore, there is a strong link between maintaining SOCE and proper Ca^{2+} signaling and maintaining lipid homeostasis.

To investigate the mechanism by which loss of calreticulin or ER Ca^{2+} reduction affects the distribution of cholesterol and thereby affect nSREBP activity (refer to chapter two and three), we also examined the role of SOCE and SOCE components, STIM1 and Orai1. We hypothesized that SOCE or its constituents, STIM1 and Orai1, may contribute to the observed increase in nSREBP activity seen in the absence of calreticulin or reduced total ER luminal Ca^{2+} (refer to

chapter two and three) [12]. First, we characterized the effect of calreticulin deficiency on STIM1, Orai1 and SOCE. Then we utilized STIM1- or Orai1-deficient mouse embryonic fibroblasts as an experimental model to investigate their effects on cholesterol metabolism and nSREBP activity. Special emphasis was on a role of the STIM1 EF hand [18] and the newly identified cholesterol binding region [16].

Materials and Methods

Cell Culture and Treatments

Wild-type and *Calr*$^{-/-}$ cells and culturing conditions were previously described in chapter two [1]. *Stim1*$^{-/-}$ mouse embryonic fibroblast (referred to as *Stim1*$^{-/-}$ cells) was previously described [19]. *Orai1*$^{-/-}$ mouse embryonic fibroblast (referred to as *Orai1*$^{-/-}$ cells) was a kind gift from Dr. Yousang Gwack and previously described [20].

SRE-luciferase [21] experiments were previously described in chapter two.

STIM1 Mutagenesis and Cloning

cDNA encoding human STIM1 (transcript variant 2 mRNA, NM_003156.3) was cloned into pcDNA3.1/Zeo(+) plasmid using restriction enzymes EcoRI and NotI cut sites. The restriction enzyme cut sites were introduced through PCR using the pCMV6 XL5 human STIM1 plasmid (previously generated in the lab) as a template with the following primers:

5’ CCGCGGAATTCATGGATGTATGCGTCCGTCTTGC 3’

5’ CGGCGGCGGCCGCCTACTTCTTAAGAGGCTTCTTAAAG 3’

The pcDNA3.1/Zeo(+) vector was double digested with EcoRI and NotI enzymes (New England BioLabs) followed by the ligation of cDNA encoding STIM1 using T4 DNA ligase (New England BioLabs). The ligation product was transformed into DH5α and ampicillin resistant colonies were selected and DNA sequence of all generated clones was confirmed by PCR analysis and DNA sequencing. The STIM1 expressing pcDNA3.1/Zeo(+) is referred to as STIM1-pcDNA (Zeo).

STIM1 (D76A)-pcDNA (Zeo) expression plasmid encoding the STIM1 EF hand mutant (D76A) was generated by site-directed mutagenesis of STIM1-pcDNA (Zeo) using the following primers:

Forward 5' CACAAACTGATGGCCGATGATGCCAATGGTGATGTG 3'

Reverse 5' CACATCACCATTGGCATCATCGGCCATCAGTTTGTG 3'

STIM1 (I364A)-pcDNA (Zeo) expression plasmid encoding the cholesterol binding domain mutant (I364A) in STIM1 was generated by site-directed mutagenesis of STIM1-pcDNA (Zeo) using the following primers:

Forward 5' CATGAGGTGGAGGTGCAATATTACAACGCCAAGAAGCAAAATGC 3'

Reverse 5' GCATTTTGCTTCTTGGCGTTGTAATATTGCACCTCCACCTCATG 3'

Stim1$^{-/-}$ cells were transfected with STIM1-pcDNA (Zeo), STIM1 (D76A)-pcDNA (Zeo) and STIM1 (I364A)-pcDNA (Zeo) using the NEON transfection system (Thermo Fisher Scientific). After 24 hours, cells were treated with 500 mg/mL of Zeocin™ (Thermo Fisher Scientific) for selection of stable cell lines.

Fura-2 AM Calcium Measurements

Ca^{2+} measurements were previously described in chapter three [9]. Measurement of peak Ca^{2+} influx during SOCE was obtained through the addiction of 2 mM $CaCl_2$ following thapsigargin induced ER Ca^{2+} depletion.

Immunoblot Analysis

Sample preparations and immunoblot analysis were previously described in chapter two [22]. Additional antibodies used were rabbit anti-STIM1 (1:1000; previously generated in the lab),

goat anti-ribophorin I (1:500; Santa Cruz Biotechnology sc-12164) and rabbit anti-SOAT 1 (1:500; Abcam ab39327).

Subcellular Fractionation

Subcellular Fractionation experiments were previously described in chapter three.

Lipid Measurement

Measurement of cellular lipids were previously described in chapter two [23].

Lipid Staining and Imaging

Cell preparation for lipid analysis was previously described in chapter two.

For nucleus and unesterified cholesterol staining, cells were incubated with NucRed® Live 647 (Thermo Fisher Scientific) at 2 drops/mL of normal media for 30 minutes at 37°C. Cells were then washed 3 times with PBS, fixed with 3.7% formaldehyde (in PBS) for 1 hour, washed 3 times with PBS, incubated with 1.5 mg/mL of glycine in PBS for 10 min at room temperature, stained with 0.05 mg/mL of filipin in PBS with 10% FBS for 2 hours at room temperature in the dark. Cells were then washed 3 times with PBS before visualization. NucRed was visualized with the Red HeNe laser, with excitation at 633 nm and emission peak at 661 nm. Filipin staining was visualized with the UV laser, with excitation at 405 nm and emission peak at 430 nm. Staining was visualized and imaged using a Leica TCS SP5 confocal microscope.

Quantitative Polymerase Chain Reaction Analysis

RNA isolation and QPCR experiments were previously described in chapter two.

Results and Discussions

Calreticulin deficiency reduces SOCE

Cells overexpressing calreticulin have increased Ca^{2+} concentration within the lumen of the ER and have reduced and delayed SOCE in response to total ER Ca^{2+} depletion triggered by thapsigargin [6, 8, 9]. Surprisingly, when we measured thapsigargin-induced SOCE in *Calr*$^{-/-}$ cells, we also observed a reduction in SOCE in the *Calr*$^{-/-}$ cells as compared to wild-type cells (Figure 4.1). We then examined the abundance of the ER associated protein STIM1 in the absence of calreticulin and discovered that there was a reduction in STIM1 protein abundance in *Calr*$^{-/-}$ cells as compared to wild-type (Figure 4.2A,C). Furthermore there was also a reduction in Orai1 protein abundance in the absence of calreticulin (Figure 4.2B.D). Reduced STIM1 and Orai1 protein levels in calreticulin deficient cells help explain the reduced SOCE response associated with the absence of calreticulin (Figure 4.1).

The distribution of STIM1 within the subcellular iodixanol gradients of wild-type and *Calr*$^{-/-}$ cells was also examined. First we characterized the gradient fractions for the presence of different ER markers, including calnexin, ribophorin I, SOAT1, SCAP and INSIG1. We found that calnexin and ribophorin I were found in the heavy fractions (6 to 10) whereas SOAT1, SCAP and INSIG1 were found in the light fractions (2 to 6) (Figure 4.3). In addition, a portion of SOAT1 were also found in fractions 10 and 11 and a portion of INSIG1 were found in fractions 8 to 11 (Figure 4.3), indicating that of these proteins were distributed across both the heavy and light ER membrane fractions. Next, we probed for the presence of STIM1. In wild-type cells STIM1 was distributed in the light fractions (2 to 6) containing SOAT1, SCAP and INSIG1 (Figure 4.3). In contrast, in *Calr*$^{-/-}$ cells, STIM1 was predominantly found in the heavy, calnexin

containing fractions (4 to 11) (Figure 4.3). A similar shift in STIM1 distribution was also seen in wild-type cells cultured in media with reduced Ca^{2+} (150 · M), with STIM1 appearing in fractions 2 to 4 and 8 to 12 (Figure 4.3). These data suggest that in the absence of calreticulin, there is reduced SOCE and this may in part be due to the reduction of Orai1 and STIM1 expression and the shift in STIM1 ER distribution. Furthermore, the shift in STIM1 ER distribution observed in the absence of calreticulin may be due to reduced total ER Ca^{2+} store.

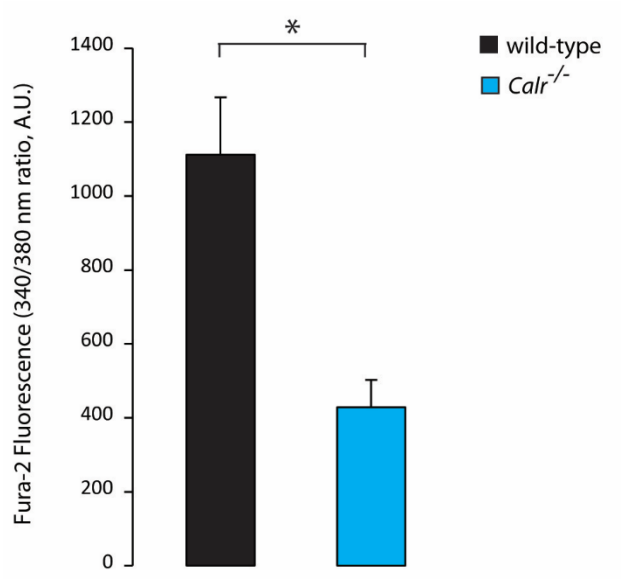

Figure 4.1 SOCE in wild-type and *Calr*$^{-/-}$ cells

SOCE was induced by thapsigargin-mediated total ER Ca^{2+} depletion in wild-type and *Calr*$^{-/-}$ mouse embryonic fibroblast cells. The graph summarizes the peak of Ca^{2+} entry immediately following the addition of Ca^{2+}. *Indicates statistically significant differences: *p*-value=0.0114. Representative of 4 biological experiments; 1 replicate per experiment (Student's t-test).

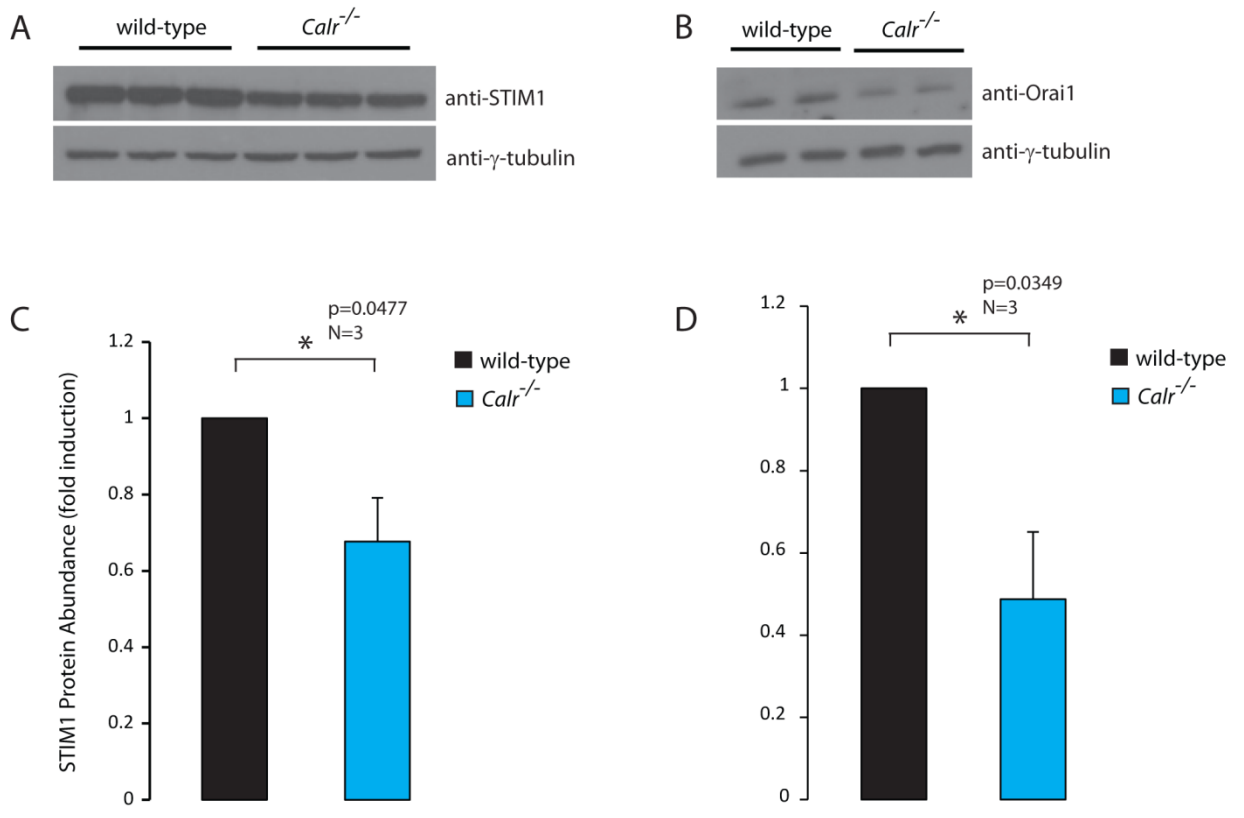

Figure 4.2 STIM1 and Orai1 abundance in the absence of calreticulin

A,B. Immunoblot of wild-type and *Calr*$^{-/-}$ mouse embryonic fibroblast cells probed with (**A)** anti-STIM1 and **(B)** anti-Orai1 antibodies. Anti-γ-tubulin antibodies were used as a loading control. Representative of 3 biological experiments; 1 replicate per experiment.

C,D. Quantitative analysis of immunoblots showing the abundance of **(C)** STIM1 and **(D)** Orai1 in wild-type and *Calr*$^{-/-}$ mouse embryonic fibroblast cells. *Indicates statistically significant differences: STIM1, *p*-value=0.0477; Orai1, *p*-value=0.0349. Representative of 3 biological experiments; 1 replicate per experiment (Student's t-test).

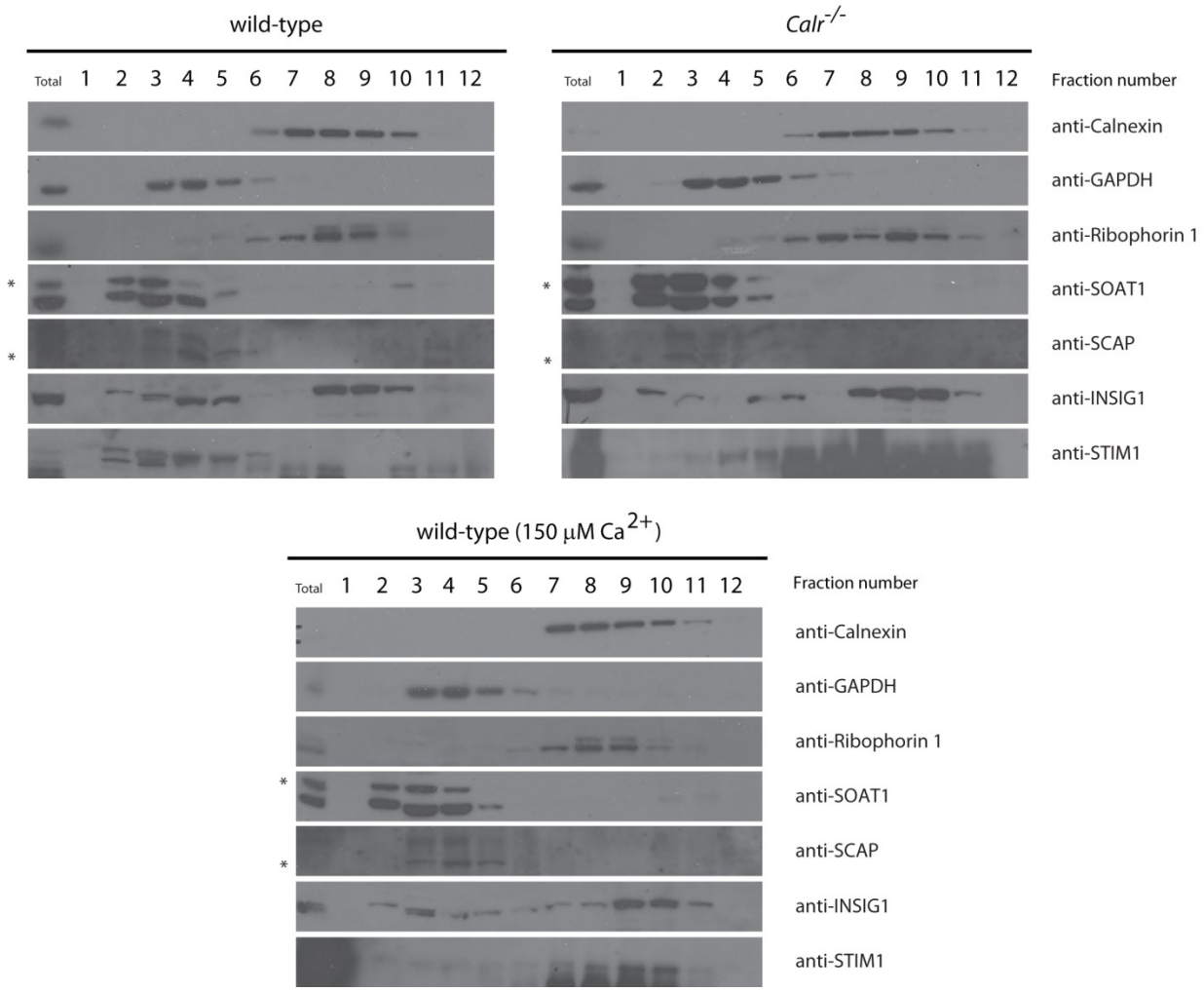

Figure 4.3 STIM1 distribution in the absence of calreticulin

Immunoblot analysis of subcellular fractions from wild-type, *Calr*$^{-/-}$ mouse embryonic fibroblast cells and wild-type mouse embryonic fibroblast cells treated with EGTA for a final extracellular Ca^{2+} concentration of 150 μM, probed with anti-calnexin, anti-GAPDH, anti-ribophorin I, anti-SOAT1, anti-SCAP, anti-INSIG1 and anti-STIM1 antibodies. *Indicates the correct protein band. Representative of 3 biological experiments; 1 replicate per experiment.

SOCE and Cholesterol Homeostasis

To examine whether the increase in nSREBP activity is due to the observed reduction in Ca^{2+} influx during SOCE in *Calr*$^{-/-}$ cells, we examined nSREBP activity in *Stim1*$^{-/-}$ and *Orai1*$^{-/-}$ cells. STIM1 deficient cells have reduced SOCE in response to thapsigargin triggered ER depletion [19, 24] and Orai1 deficient cells have abrogated SOCE in response to thapsigargin triggered ER depletion [24]. Activity of nSREBP was increased 2-fold in *Orai1*$^{-/-}$ cells as compared to wild-type (Figure 4.4). This increase in the nSREBP activity in the absence of Orai1 was similar to what was previously seen in *Calr*$^{-/-}$ cells (Figure 2.11). To confirm the increased nSREBP activity we examined SREBP-2 protein abundance with immunoblot analysis of *Orai1*$^{-/-}$ cells and showed an increase in both total and nuclear forms of SREBP-2 as compared to wild-type cells (Figure 4.5A). Furthermore, the mRNA abundance for SREBP-2 targeted genes HMG-CoA reductase and LDLR was also increased in the absence of Orai1 (Figure 4.5B). Therefore, the nSREBP activity in the absence of Orai1 mirrors what was observed in the absence of calreticulin (refer to chapter two), whether or not this observation is due to the same mechanism requires more investigation.

The level of nSREBP activity observed in *Calr*$^{-/-}$ (Figure 2.11) and *Orai1*$^{-/-}$ (Figure 4.4) cells suggests that reduced SOCE may be linked to the increase in nSREBP activity. Therefore, we tested STIM1-deficient cells or cells with reduced expression of STIM1 for nSREBP activity. First wild-type cells treated with STIM1 specific siRNA to knockdown STIM1 was measured for nSREBP activity. Cells with reduced expression of STIM1 showed a 20% decrease in the activity of nSREBP (Figure 4.4). In agreement with this observation, *Stim1*$^{-/-}$ cells exhibited a 50% reduction of nSREBP activity (Figure 4.4). This discrepancy between the increased

nSREBP activity in *Orai1*$^{-/-}$ cells and the reduced nSREBP activity in *Stim1*$^{-/-}$ cells suggest that the modulation of nSREBP activity in the absence of calreticulin was not simply a result of decrease in SOCE. The changes in nSREBP activity may therefore be independently specific to STIM1 or Orai1.

To further characterize the effect of STIM1 and Orai1 on lipid homeostasis, we measured the lipid composition within wild-type, *Stim1*$^{-/-}$ and *Orai1*$^{-/-}$ cells. There was no difference in the level of triacylglycerols between wild-type and *Stim1*$^{-/-}$ cells (Figure 4.6). In contrast, there was a significant increase the level of triacylglycerols in *Orai1*$^{-/-}$ cells as compared to wild-type cells (Figure 4.6). The level of unesterified and esterified cholesterol did not significantly change in the absence of STIM1 or Orai1, although there was a trend toward an increase in the level of esterified cholesterol in *Stim1*$^{-/-}$ cells as compared to wild-type cells (Figure 4.6). To examine whether the absence of STIM1 or Orai1 affected intracellular distribution of unesterified cholesterol, we used filipin staining. Compared to wild-type cells, *Stim1*$^{-/-}$ cells had a significantly more intense intracellular filipin staining, indicating an increased abundance of cholesterol-rich regions within the cell (Figure 4.7A,B). The abundance of intracellular unesterified cholesterol in the absence of STIM1 (Figure 4.7A,B) corresponds with the reduced nSREBP activity observed in *Stim1*$^{-/-}$ cells (Figure 4.4). In contrast, *Orai1*$^{-/-}$ cells showed a trend towards reduced intracellular filipin staining, revealing a reduced abundance of cholesterol-rich regions within the cell (Figure 4.7A,B). The low abundance of unesterified cholesterol in the absence of Orai1 (Figure 4.7A,B) also agrees with the increased nSREBP activity seen in *Orai1*$^{-/-}$ cells (Figure 4.4). These results indicate that STIM1 and Orai1 may differentially modulate cellular distribution of unesterified cholesterol and nSREBP activity.

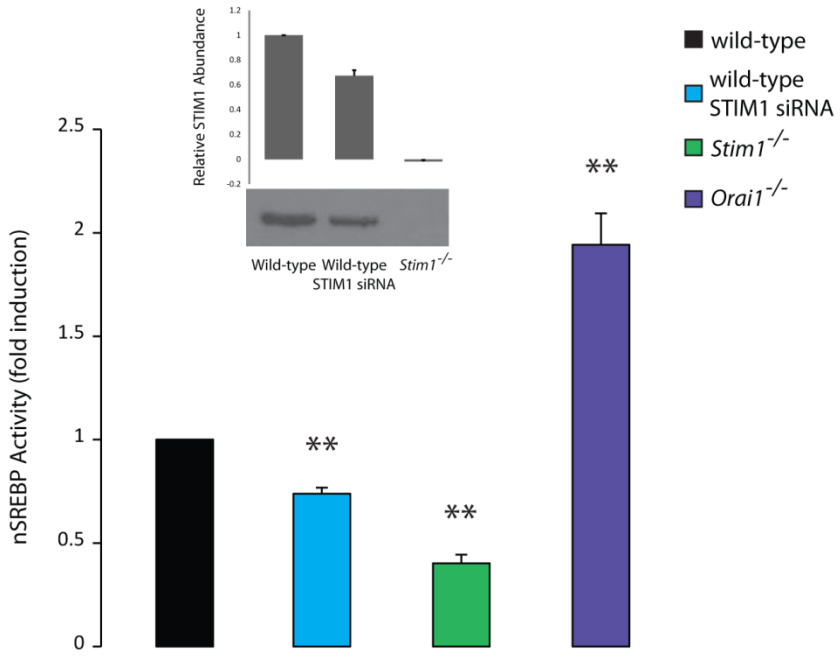

Figure 4.4 nSREBP activity and SOCE

nSREBP activity in wild-type mouse embryonic fibroblast cells transfected with scrambled or STIM1 specific siRNA, *Stim1*$^{-/-}$ and *Orai1*$^{-/-}$ mouse embryonic fibroblast cells. **Indicates statistically significant differences: wild-type vs. wild-type STIM1 siRNA, *p*-value=0.0008 (3 biological experiments; 2 replicates per experiment); wild-type vs. *Stim1*$^{-/-}$, *p*-value=0.0001 (12 biological experiments; 2 replicates per experiment); wild-type vs. *Orai1*$^{-/-}$, *p*-value=0.0001 (6 biological experiments; 2 replicates per experiment) (Student's t-test).

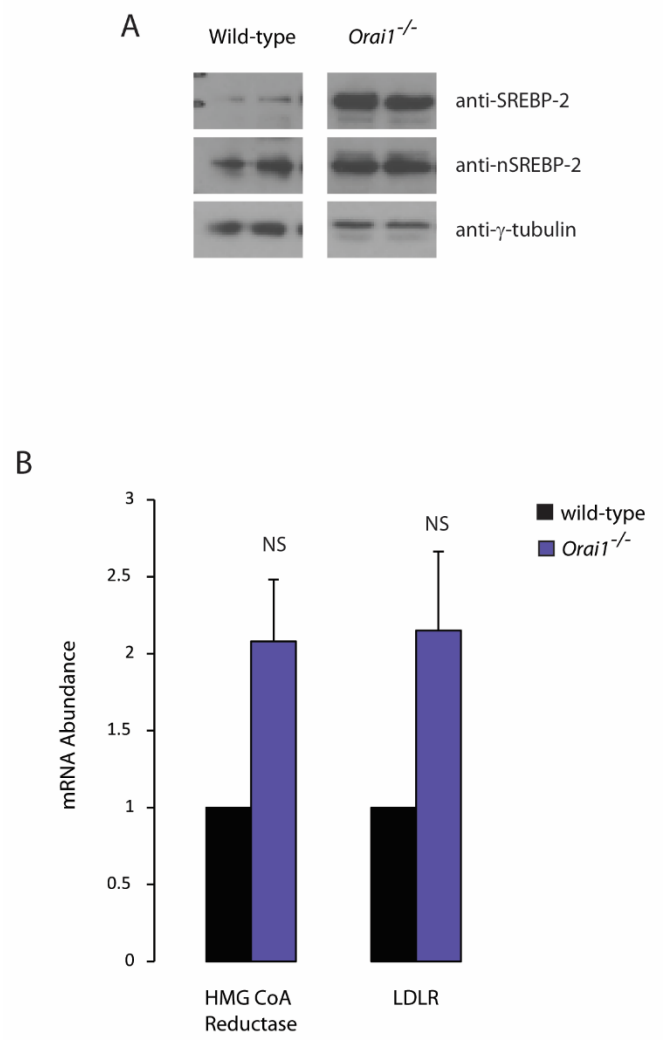

Figure 4.5 SREBP-2 in the absence of Orai1

A. Immunoblot analysis of wild-type and *Orai1*$^{-/-}$ mouse embryonic fibroblast cells probed with anti-SREBP-2 and anti-nSREBP-2 antibodies. Anti-γ-tubulin antibodies were used as a loading control. Representative of 3 biological experiments; 1 replicate per experiment.

B. Q-PCR analysis of HMG-CoA reductase and LDLR mRNA abundance in wild-type and *Orai1*$^{-/-}$ mouse embryonic fibroblast cells. Results were normalized to 18S rRNA (internal control). NS, not significant. Representative of 3 biological experiments; 1 replicate per experiment (Student's t-test).

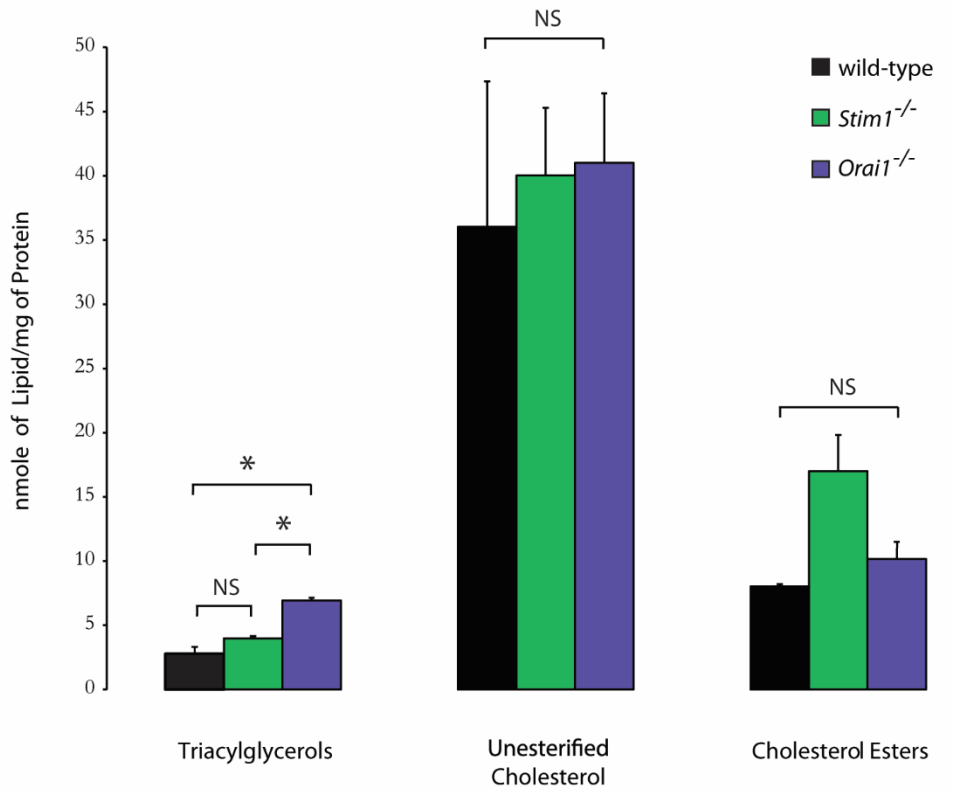

Figure 4.6 Lipid levels and SOCE

Triacylglycerols, unesterified cholesterol and cholesterol ester levels in wild-type, *Stim1*$^{-/-}$ and *Orai1*$^{-/-}$ mouse embryonic fibroblast cells. *Indicates statistically significant differences: wild-type vs. *Orai1*$^{-/-}$ triacylglycerols, $p<0.05$; *Stim1*$^{-/-}$ vs *Orai1*$^{-/-}$ triacylglycerols, $p<0.05$. NS, not significant. Representative of 3 biological experiments; 1 replicate per experiment (ANOVA).

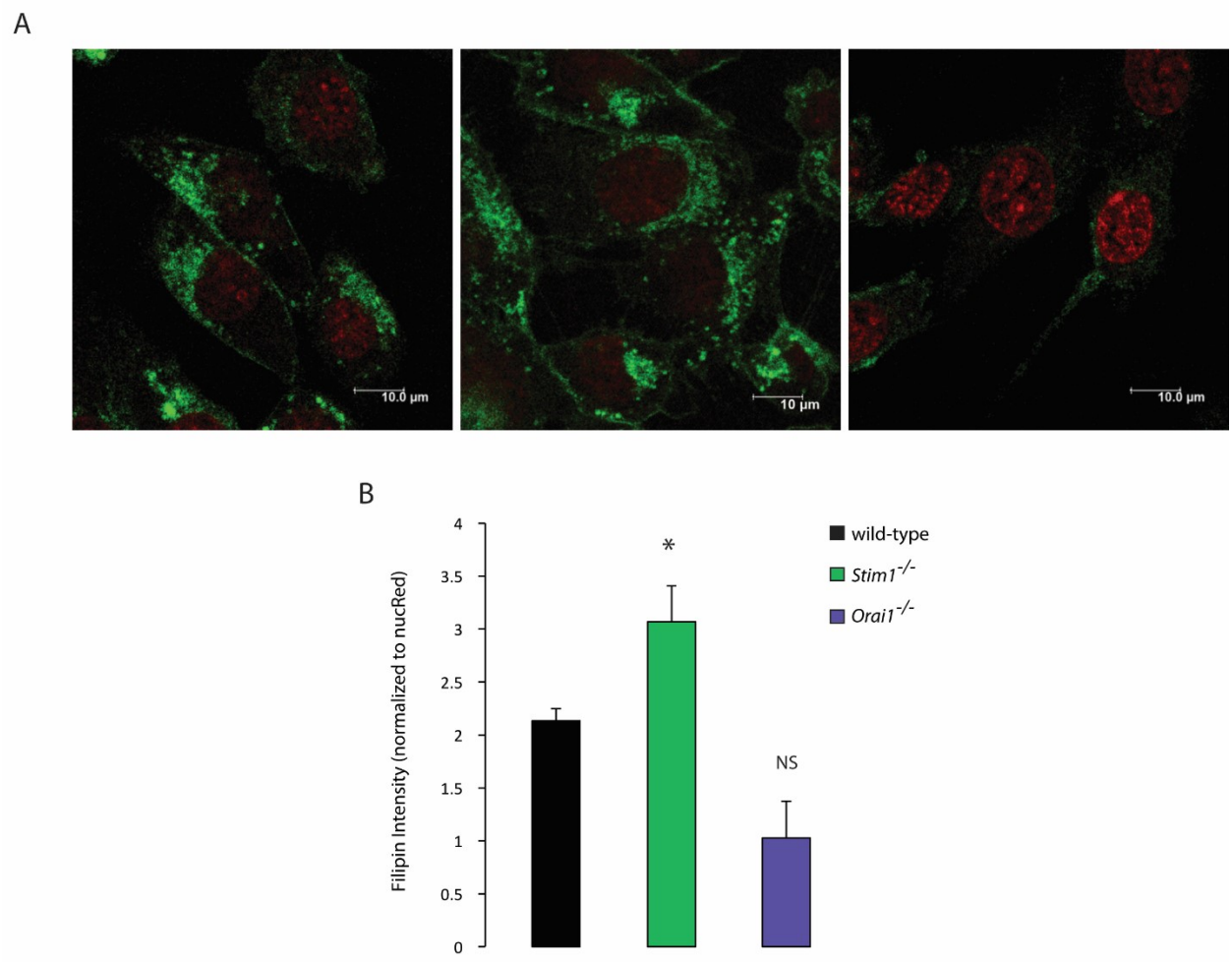

Figure 4.7 Distribution of unesterified cholesterol and SOCE

A. Wild-type (*left panel*), *Stim1*$^{-/-}$ (*middle panel*) and *Orai1*$^{-/-}$ (*right panel*) cells stained with Nucleus Red (NucRed) and filipin. A representative of 3 independent analyses is presented.

B. Graphic representation of filipin intensity normalized to NucRed intensity in wild-type, *Stim1*$^{-/-}$ and *Orai1*$^{-/-}$ cells. *Indicates statistically significant differences: wild-type vs. *Stim1*$^{-/-}$ cells, $p<0.05$. NS, not significant. Representative of 3 biological experiments; at least 3 images per experiment (ANOVA).

Analysis of STIM1 Mutants and SREBP Activity

Due to the unique effect of STIM1 deficiency on nSREBP activity as compared to the observed nSREBP activity in the absence of calreticulin or Orai1, we decided to further investigate, the role of STIM1 in modulating cholesterol distribution and nSREBP activity. In particular, we examined whether the reduction in nSREBP activity in the absence of STIM1 was dependent upon the ability of STIM1 to sense ER Ca^{2+} or the ability of STIM1 to bind membrane cholesterol. We created *Stim1*$^{-/-}$ cells that stably expressed wild-type STIM1, STIM1 with an EF hand mutation (D76A) [18] or STIM1 with a cholesterol binding domain mutation (I364A) [16]. The cells were examined for STIM1 expression and function in SOCE. Expression of STIM1 and STIM1 mutants was confirmed by immunoblot analysis (Figure 4.8). As expected SOCE activity was significantly higher in *Stim1*$^{-/-}$ cells expressing STIM1, STIM1 D76A or STIM1 I364A mutants as compared to *Stim1*$^{-/-}$ cells (Figure 4.9). These findings were in agreement with previous reports [16, 18]. STIM1 with the D76A EF hand mutation is constitutively active due to the inability to detect ER Ca^{2+} and therefore expression of STIM D76A in *Stim1*$^{-/-}$ cells will reconstitute activity of SOCE [18]. The cholesterol binding domain mutant of STIM1 decreases SOCE as induced by ER Ca^{2+} depletion, however expression of STIM I364A in *Stim1*$^{-/-}$ cells will reconstitute activity of SOCE, although not to the same extent as wild-type STIM1 [16].

Next we examined the effect of the absence of STIM1 on nSREBP in *Stim1*$^{-/-}$ cells stably expressing STIM1, STIM1 D76A or STIM1 I364A mutants. The reduced nSREBP activity was restored in cells expressing STIM1 and the STIM1 D76A mutant but not in cells expressing the STIM1 I364A mutant (Figure 4.10). These preliminary findings indicate that the cholesterol binding domain of STIM1 might be involved in modulating nSREBP activity (Figure 4.10).

Furthermore, when cultured in lipid free media, there was a corresponding increase in nSREBP activity in wild-type cells and *Stim1*$^{-/-}$ cells stably expressing STIM1 and STIM1 D76A, but not in *Stim1*$^{-/-}$ cells or *Stim1*$^{-/-}$ cells expressing STIM1 I364A (Figure 4.10), indicating that the cholesterol binding domain of STIM1 may play a role in the ability of the SREBP-SCAP complex to sense ER membrane cholesterol.

These preliminary results indicate that in the absence of STIM1, there is a reduced nSREBP activity and an increased abundance of intracellular cholesterol-rich regions. The reduced nSREBP activity was observed in both cells deficient of STIM1 and cells expressing STIM1 with a mutation in the cholesterol binding domain. Therefore the cholesterol binding domain of STIM1 may play a role in modulating unesterified cholesterol distribution within the ER, affecting the cholesterol sensing ability of the SREBP-SCAP complex and nSREBP activity.

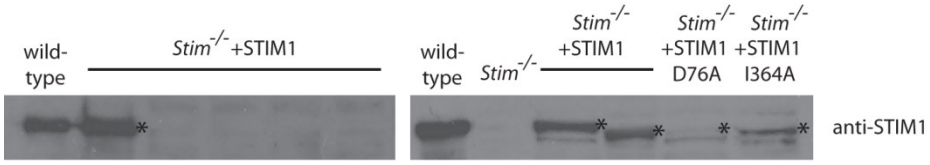

Figure 4.8 STIM1 wild-type, D76A and I364A mutant expression in *Stim1*$^{-/-}$ cells

Immunoblot analysis of *Stim1*$^{-/-}$ mouse embryonic fibroblast cells stably transfected with STIM1-pcDNA (Zeo) (*Stim1*$^{-/-}$ +STIM1), STIM1 (D76A)-pcDNA (Zeo) (*Stim1*$^{-/-}$ +STIM1 D76A) and STIM1 (I364A)-pcDNA (Zeo) (*Stim1*$^{-/-}$ +STIM1 I364A) expression vectors, probed with anit-STIM1 antibodies. *Indicates cell lines positive for STIM1 or STIM1 mutant expression and the correct protein band.

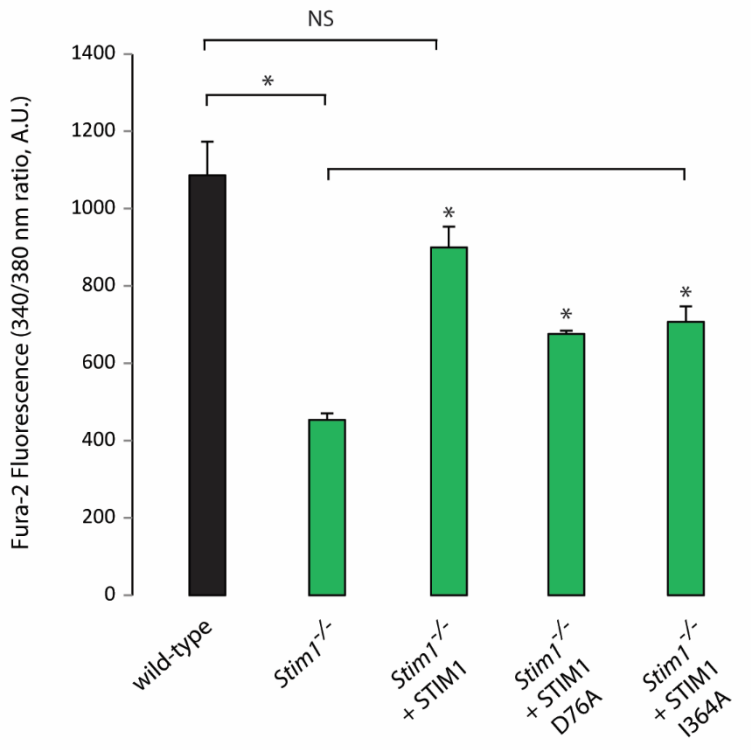

Figure 4.9 SOCE function in cells expressing STIM1 and STIM1 mutants

SOCE was induced by thapsigargin-mediated total ER Ca^{2+} depletion in wild-type cells, *Stim1*$^{-/-}$ mouse embryonic fibroblast cells and *Stim1*$^{-/-}$ mouse embryonic fibroblast cells stably expressing STIM1 (*Stim1*$^{-/-}$ +STIM1), STIM1 D76A (*Stim1*$^{-/-}$ +STIM1 D76A) and STIM1 I364A (*Stim1*$^{-/-}$ +STIM1 I364A). The graph shows the peak of Ca^{2+} entry immediately following the addition of Ca^{2+}. *Indicates statistically significant differences: wild-type vs. *Stim1*$^{-/-}$, p-value<0.05; *Stim1*$^{-/-}$ vs. *Stim1*$^{-/-}$ +STIM1, p-value<0.05; *Stim*$^{-/-}$ vs. *Stim1*$^{-/-}$ +STIM1 D76A, p-value<0.05; *Stim1*$^{-/-}$ vs. *Stim1*$^{-/-}$ +STIM1 I364A, p-value<0.05. NS, not significant. Representative of 3 biological experiments; 1 replicate per experiment (ANOVA).

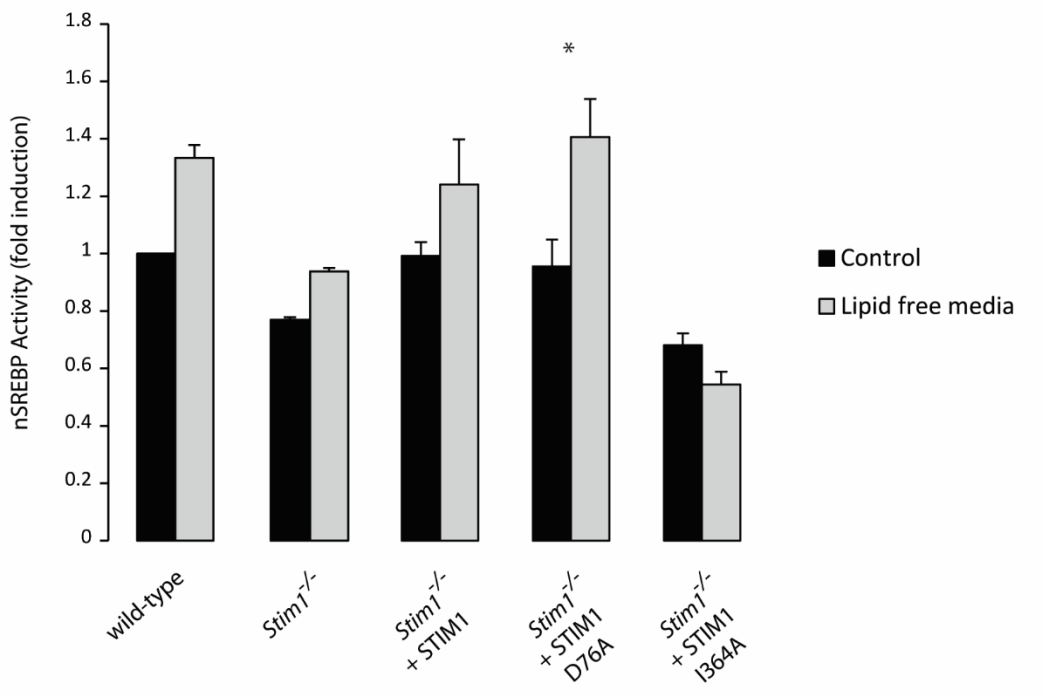

Figure 4.10 nSREBP activity in cells expressing STIM1 mutants

nSREBP activity in wild-type, *Stim1*$^{-/-}$ mouse embryonic fibroblast cells and *Stim1*$^{-/-}$ mouse embryonic fibroblast cells stably expressing STIM1 (*Stim1*$^{-/-}$ +STIM1), STIM1 D76A (*Stim1*$^{-/-}$ +STIM1 D76A) and STIM1 I364A (*Stim1*$^{-/-}$ +STIM1 I364A). *Indicates statistically significant differences: *Stim1*$^{-/-}$ +STIM1 D76A cultured with control vs. lipid free media, p-value<0.05. Representative of 3 biological experiments; 2 replicates per experiment (ANOVA).

References

[1] K. Nakamura, A. Zuppini, S. Arnaudeau, J. Lynch, I. Ahsan, R. Krause, S. Papp, H. De Smedt, J.B. Parys, W. Muller-Esterl, D.P. Lew, K.H. Krause, N. Demaurex, M. Opas, M. Michalak, Functional specialization of calreticulin domains, The Journal of cell biology, 154 (2001) 961-972.

[2] D. Prins, M. Michalak, Organellar calcium buffers, Cold Spring Harbor perspectives in biology, 3 (2011) 197-212.

[3] N. Mesaeli, K. Nakamura, E. Zvaritch, P. Dickie, E. Dziak, K.H. Krause, M. Opas, D.H. MacLennan, M. Michalak, Calreticulin is essential for cardiac development, The Journal of cell biology, 144 (1999) 857-868.

[4] P. Camacho, J.D. Lechleiter, Calreticulin inhibits repetitive intracellular Ca^{2+} waves, Cell, 82 (1995) 765-771.

[5] S. Naaby-Hansen, M.J. Wolkowicz, K. Klotz, L.A. Bush, V.A. Westbrook, H. Shibahara, J. Shetty, S.A. Coonrod, P.P. Reddi, J. Shannon, M. Kinter, N.E. Sherman, J. Fox, C.J. Flickinger, J.C. Herr, Co-localization of the inositol 1,4,5-trisphosphate receptor and calreticulin in the equatorial segment and in membrane bounded vesicles in the cytoplasmic droplet of human spermatozoa, Molecular human reproduction, 7 (2001) 923-933.

[6] S. Arnaudeau, M. Frieden, K. Nakamura, C. Castelbou, M. Michalak, N. Demaurex, Calreticulin differentially modulates calcium uptake and release in the endoplasmic reticulum and mitochondria, The Journal of biological chemistry, 277 (2002) 46696-46705.

[7] C. Fasolato, P. Pizzo, T. Pozzan, Delayed activation of the store-operated calcium current induced by calreticulin overexpression in RBL-1 cells, Molecular biology of the cell, 9 (1998) 1513-1522.

[8] C. Bastianutto, E. Clementi, F. Codazzi, P. Podini, F. De Giorgi, R. Rizzuto, J. Meldolesi, T. Pozzan, Overexpression of calreticulin increases the Ca^{2+} capacity of rapidly exchanging Ca^{2+} stores and reveals aspects of their lumenal microenvironment and function, The Journal of cell biology, 130 (1995) 847-855.

[9] L. Mery, N. Mesaeli, M. Michalak, M. Opas, D.P. Lew, K.H. Krause, Overexpression of calreticulin increases intracellular Ca^{2+} storage and decreases store-operated Ca^{2+} influx, The Journal of biological chemistry, 271 (1996) 9332-9339.

[10] W. Xu, F.J. Longo, M.R. Wintermantel, X. Jiang, R.A. Clark, S. DeLisle, Calreticulin modulates capacitative Ca^{2+} influx by controlling the extent of inositol 1,4,5-trisphosphate-induced Ca^{2+} store depletion, The Journal of biological chemistry, 275 (2000) 36676-36682.

[11] W.A. Wang, J. Groenendyk, M. Michalak, Calreticulin signaling in health and disease, The international journal of biochemistry & cell biology, 44 (2012) 842-846.

[12] W.A. Wang, W.X. Liu, S. Durnaoglu, S.K. Lee, J. Lian, R. Lehner, J. Ahnn, L.B. Agellon, M. Michalak, Loss of Calreticulin Uncovers a Critical Role for Calcium in Regulating Cellular Lipid Homeostasis, Scientific reports, 7 (2017) s41598.

[13] M. Maus, M. Cuk, B. Patel, J. Lian, M. Ouimet, U. Kaufmann, J. Yang, R. Horvath, H.T. Hornig-Do, Z.M. Chrzanowska-Lightowlers, K.J. Moore, A.M. Cuervo, S. Feske, Store-Operated Ca(2+) Entry Controls Induction of Lipolysis and the Transcriptional Reprogramming to Lipid Metabolism, Cell metabolism, 25 (2017) 698-712.

[14] A.P. Arruda, B.M. Pers, G. Parlakgul, E. Guney, T. Goh, E. Cagampan, G.Y. Lee, R.L. Goncalves, G.S. Hotamisligil, Defective STIM-mediated store operated Ca(2+) entry in hepatocytes leads to metabolic dysfunction in obesity, eLife, 6 (2017) e29968.
[15] C.H. Wilson, E.S. Ali, N. Scrimgeour, A.M. Martin, J. Hua, G.A. Tallis, G.Y. Rychkov, G.J. Barritt, Steatosis inhibits liver cell store-operated Ca(2)(+) entry and reduces ER Ca(2)(+) through a protein kinase C-dependent mechanism, The Biochemical journal, 466 (2015) 379-390.
[16] J. Pacheco, L. Dominguez, A. Bohorquez-Hernandez, A. Asanov, L. Vaca, A cholesterol-binding domain in STIM1 modulates STIM1-Orai1 physical and functional interactions, Scientific reports, 6 (2016) srep29634.
[17] I. Derler, I. Jardin, P.B. Stathopulos, M. Muik, M. Fahrner, V. Zayats, S.K. Pandey, M. Poteser, B. Lackner, M. Absolonova, R. Schindl, K. Groschner, R. Ettrich, M. Ikura, C. Romanin, Cholesterol modulates Orai1 channel function, Science signaling, 9 (2016) ra10.
[18] T. Hewavitharana, X. Deng, Y. Wang, M.F. Ritchie, G.V. Girish, J. Soboloff, D.L. Gill, Location and function of STIM1 in the activation of Ca^{2+} entry signals, The Journal of biological chemistry, 283 (2008) 26252-26262.
[19] D. Prins, J. Groenendyk, N. Touret, M. Michalak, Modulation of STIM1 and capacitative Ca^{2+} entry by the endoplasmic reticulum luminal oxidoreductase ERp57, EMBO reports, 12 (2011) 1182-1188.
[20] Y. Gwack, S. Srikanth, M. Oh-Hora, P.G. Hogan, E.D. Lamperti, M. Yamashita, C. Gelinas, D.S. Neems, Y. Sasaki, S. Feske, M. Prakriya, K. Rajewsky, A. Rao, Hair loss and defective T- and B-cell function in mice lacking ORAI1, Molecular and cellular biology, 28 (2008) 5209-5222.
[21] R.D. Bell, R. Deane, N. Chow, X. Long, A. Sagare, I. Singh, J.W. Streb, H. Guo, A. Rubio, W. Van Nostrand, J.M. Miano, B.V. Zlokovic, SRF and myocardin regulate LRP-mediated amyloid-beta clearance in brain vascular cells, Nature cell biology, 11 (2009) 143-153.
[22] S.H. Back, K. Lee, E. Vink, R.J. Kaufman, Cytoplasmic IRE1alpha-mediated XBP1 mRNA splicing in the absence of nuclear processing and endoplasmic reticulum stress, The Journal of biological chemistry, 281 (2006) 18691-18706.
[23] J. Folch, M. Lees, G.H. Sloane Stanley, A simple method for the isolation and purification of total lipides from animal tissues, The Journal of biological chemistry, 226 (1957) 497-509.
[24] M. Vig, C. Peinelt, A. Beck, D.L. Koomoa, D. Rabah, M. Koblan-Huberson, S. Kraft, H. Turner, A. Fleig, R. Penner, J.P. Kinet, CRACM1 is a plasma membrane protein essential for store-operated Ca^{2+} entry, Science, 312 (2006) 1220-1223.

Chapter Five: General Discussion

ER Ca^{2+} and cholesterol homeostasis

Although it is well established that the ER plays an important role in intracellular Ca^{2+} signaling and that it is a key organelle involved in lipid homeostasis, including cholesterol metabolism, there has been no evidence for a direct link between ER Ca^{2+} and lipid homeostasis. The discovery of an elevated content of lipid in *Calr*$^{-/-}$ mice rescued by cardiac-specific expression of activated calcineurin [1] helped to uncover a crosstalk between Ca^{2+} and lipid homeostasis [2] and, more specifically, to identify a link between total ER luminal Ca^{2+} and the SREBP processing and signaling pathway.

The surprising finding is that the reduction of total ER luminal Ca^{2+} increases nSREBP activity when the level of total cellular unesterified cholesterol is not changed [2]. This is because the decrease in total ER Ca^{2+} or loss of calreticulin, which reduced total ER luminal Ca^{2+} [3, 4], caused a shift in intracellular distribution of unesterified cholesterol away from the SREBP-SCAP sensing mechanism and, therefore, increased SREBP processing and nSREBP activity even under abundant cholesterol conditions. Taken together my findings indicate that ER Ca^{2+} status must be an important, previously not recognized, determinant of the basal sensitivity of the sterol sensing mechanism inherent to the SREBP processing pathway.

Intracellular movement of cholesterol

The conundrum lies with how fluctuations of total ER luminal Ca^{2+} affect the distribution and/or trafficking of intracellular unesterified cholesterol and the ability for the SREBP-SCAP complex to sense intracellular cholesterol status. There are three pools of plasma membrane unesterified cholesterol: 1. cholesterol available for ER transport and accounts for 16% of total plasma membrane lipids; 2. cholesterol sequestered by sphingomyelin, (not available for ER transport)

accounting for 10-23% of total plasma membrane lipids and, 3. cholesterol complexed with the phospholipid bilayer, essential for plasma membrane integrity (not available for ER transport) accounting for 12 % of total plasma membrane lipids [5]. When LDL-derived cholesterol is in abundance, it moves from lysosomes to the plasma membrane and contributes to the rise of the first pool of cholesterol, the accessible cholesterol [6]. A fraction of this accessible cholesterol is then transported to the ER where transcriptional regulation of cholesterol uptake and biosynthesis is controlled [6]. It is not known at present how total ER Ca^{2+} affects the movement and buildup of the different plasma membrane pools of cholesterol.

Vesicular-dependent pathway

The ER is the main site of control over cholesterol homeostasis; yet only ~1% of a cell's total cholesterol remains at the ER, the majority, ~60-90% of the cell's total cholesterol, is distributed at the plasma membrane [5]. Intracellular movement of cholesterol is carried out by either a vesicular-dependent or vesicular-independent pathway [7]. With respect to the vesicular-dependent pathway, the endosomal/lysosomal pathway, being one of the major processes that facilitate the transfer of contents and signals from the extracellular environment for intracellular distribution, plays a central role in the transport of lipids and more specifically cholesterol [7]. During exogenous uptake of cholesterol, LDLs carrying cholesterol in the blood stream binds to the LDLR on the plasma membrane and initiates endocytosis of the lipoprotein [8, 9] (Figure 5.1). The contents of the LDL particles are mainly consisted of esterified cholesterol, which is eventually hydrolyzed by acidic lipases to unesterified cholesterol and distributed to the plasma membrane [6, 10]. Levels of unesterified cholesterol within the cell are detected at the ER where the transcription factor SREBP-2, which regulates the expression of genes involved in

cholesterol uptake and biosynthesis, is controlled [11]. When cholesterol levels are in abundance, excess unesterified cholesterol from the plasma membrane traffics to the ER membrane, where it supresses SREBP-2 and HMG-CoA reductase activity, is esterified by SOAT1 for lipid droplet storage, transports back to the plasma membrane or is distributed to other organelles [6, 12].

Ca^{2+} crosstalk between the ER and endosomes play an important role in the maturation and function of endosomes and endo-lysosomal fusion, and consequently in the intracellular trafficking/delivery of cholesterol (Figure 5.1). Initial endosomes formed through endocytosis contain similar Ca^{2+} concentrations as the extracellular environment, around 1 mM [13]. This is followed by rapid release of Ca^{2+} from the endosome and within 20 min Ca^{2+} levels fall to 3-40 μM [14]. As endosomes mature and fuse with lysosomes, Ca^{2+} levels rise to around 500 μM, similar to what is seen in the ER [15-17]. This change in Ca^{2+} levels within the endosomal/lysosomal pathway are majorly affected by the Ca^{2+} stores within the ER [18-20] (Figure 5.1). Moreover, this exchange of Ca^{2+} between the ER and the endosomal/lysosomal pathway are dependent upon a number of ER, endosomal and lysosomal Ca^{2+}channels. These include the $InsP_3R$ [18, 21], transient receptor potential (TRP) channels [22-27], mucolipin-3 [28], presenilin1 [29] and two-pore channels (TPCs) [30]. All of which, when disrupted, leads to a disruption in endosomal/lysosomal progression and cholesterol trafficking.

Therefore, the Ca^{2+} signaling events and the transfer of cholesterol between the ER and the endosomal/lysosomal pathway are interdependent. Furthermore, both of these processes occur at MCSs [21, 31, 32] and may be involved in affecting the basal cholesterol sensitivity of the SREBP-SCAP complex (Figure 5.2).

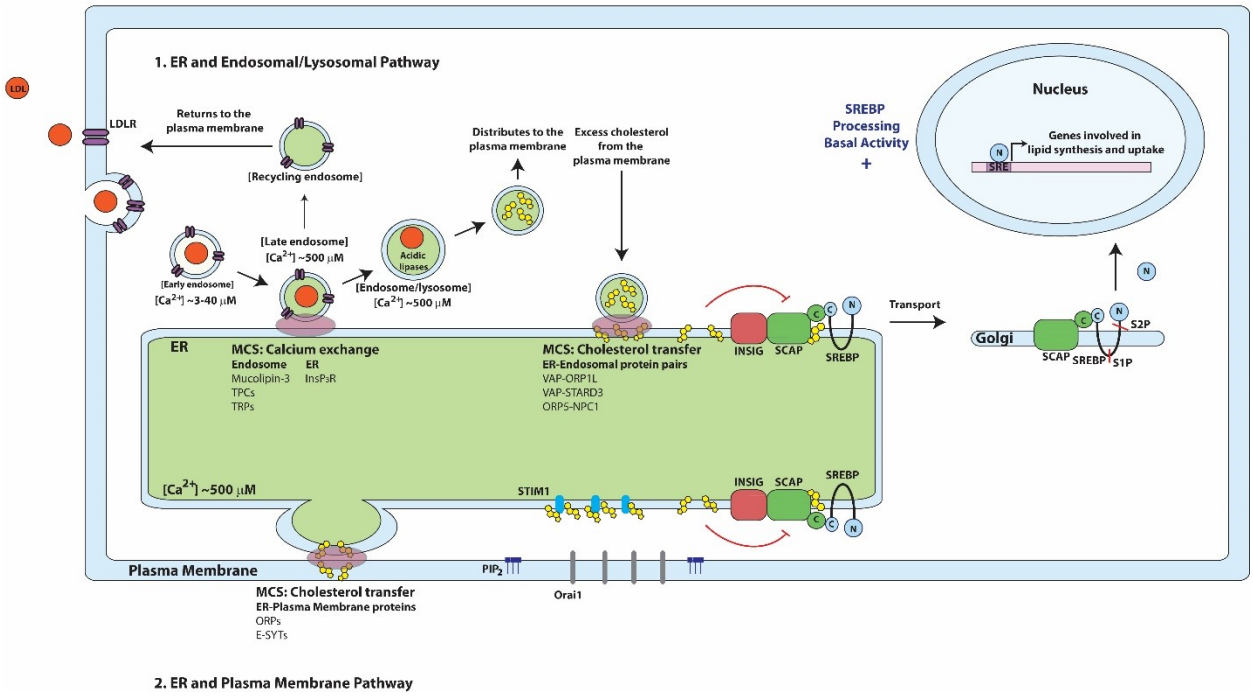

Figure 5.1 Graphic representation of the intracellular pathway of LDL-derived and *de novo* synthesized cholesterol

(1) Exogenous cholesterol enters the cell through low density lipoprotein (LDL) receptor (LDLR) mediated endocytosis. The early endosomes progresses into late endosomes and eventually fuses with lysosomes. This process is dependent upon Ca^{2+} crosstalk with the ER which relies upon ER Ca^{2+} release from inositol trisphosphate receptor ($InsP_3R$) and Ca^{2+} channels like mucolipin-3, the two-pore channels (TPCs) and the transient receptor potential (TRP) channels on endosomes and lysosomes. The refilling of endosome Ca^{2+} is important for endo/lysosomal fusion which allows for hydrolysis of LDL derived cholesterol esters by acidic lipases. The resulting unesterified cholesterol is then distributed to the plasma membrane. Excess cholesterol moves from the plasma membrane to the ER through membrane contact sites (MCSs) and involves cholesterol binding proteins vesicle-associated membrane protein (VAP) and oxysterol-binding

proteins (ORPs) on the ER membrane and ORP1L, steroidogenic acute regulatory-related lipid transfer domain 3 (STARD3) and Niemann-Pick type C1 (NPC1) on endosomes. (2) Exchange of cholesterol, including *de novo* synthesized cholesterol, between the ER and plasma membrane can also occur through MCSs between the ER and plasma membrane. This exchange is dependent upon cholesterol transferring proteins; ORPs and synaptotagmins (E-SYTs). The cholesterol at the ER is sensed by the SREBP-SCAP complex, which remains bound to INSIG1 in the presence of cholesterol and there is limited transport of the SREBP-SCAP to the Golgi, S1P and S2P processing and nSREBP transcriptional activity.

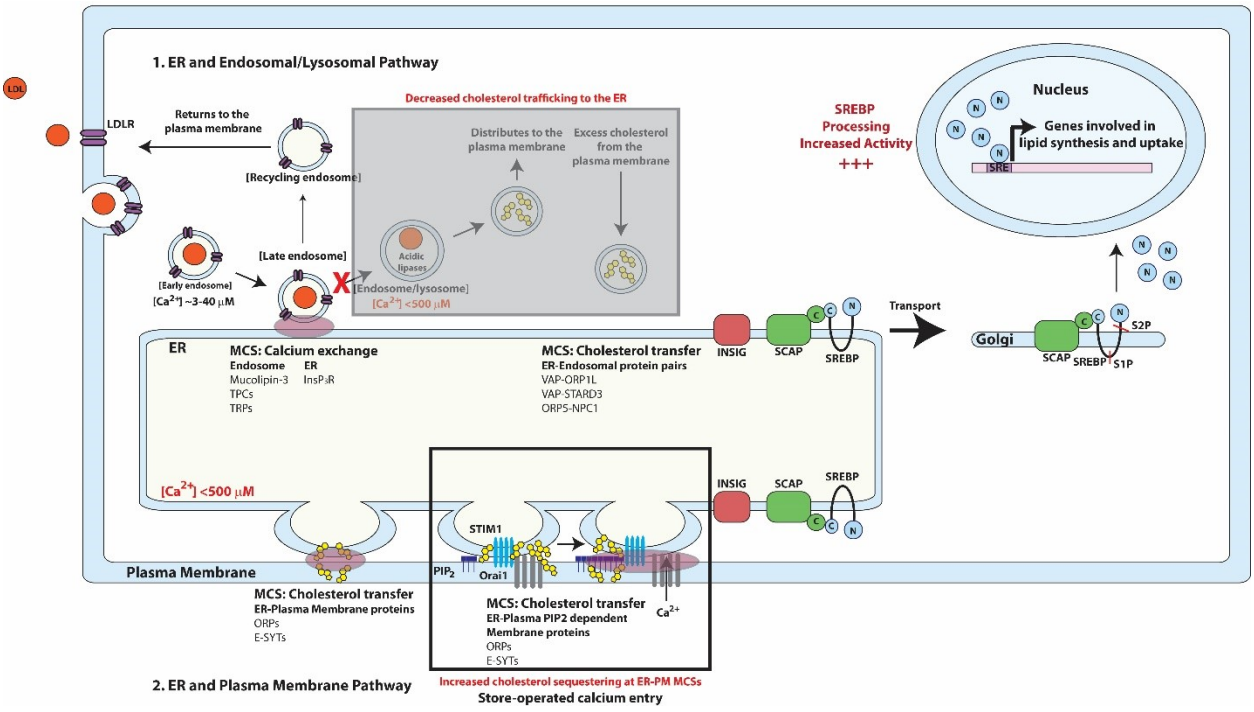

Figure 5.2 Graphic representation of the intracellular pathway of LDL-derived and *de novo* synthesized cholesterol under conditions where ER Ca^{2+} is low

(1) The progression of the endosomal/lysosomal pathway depends upon the release of ER Ca^{2+} and the refilling and accumulation of Ca^{2+} within the acidic compartments. Therefore, when ER Ca^{2+} is low there is a disruption in the endosomal/lysosomal pathway, specifically where the endosomes and lysosomes fuse. This may prevent the complete hydrolysis of LDL particles through LDLR-mediated endocytosis. The trafficking of cholesterol to the plasma membrane and then to the ER decreases and the SREBP-SCAP complex at the ER no longer senses cellular cholesterol. (2) The decrease in ER Ca^{2+} triggers a process known as store-operated Ca^{2+} entry (SOCE). This process involves STIM1, which senses the decrease in ER Ca^{2+} oligomerize and extends in conformation to interact with the plasma membrane and form ER-plasma membrane MCSs. STIM1 binds to and triggers the oligomerization and activation of Orai1, the plasma membrane Ca^{2+} channel. Studies have shown that STIM1-Orai1 moves from a

phosphatidylinositol (4,5) bisphosphate (PIP_2) poor region to a PIP_2 rich region. STIM1 and Orai1 both have cholesterol binding domains. Therefore, the hypothesis is that STIM1 and Orai1 binds to and sequester cholesterol at the MCSs and brings the cholesterol to PIP_2 rich regions where PIP_2 dependent cholesterol transfer proteins are located. The sequestering of cholesterol at SOCE-mediated MCSs also prevents the SREBP-SCAP complex from sensing cellular cholesterol.

Vesicular-independent pathway and MCS

The majority of cholesterol trafficked between the ER and plasma membrane likely occurs via a vesicular-independent pathway and involves ER-plasma membrane MCSs (Figure 5.1). This is evident from studies which show that blocking the secretory pathway only partially blocked (~20%) the transport of newly synthesized cholesterol from the ER to the plasma membrane [33, 34]. In yeast, C28 sterol or ergosterol is synthesized instead of cholesterol and transport of ergosterol between the ER and the plasma membrane occurs through a bidirectional non-vesicular equilibration process at ER-plasma membrane MCSs [35]. Transfer of newly synthesized ergosterol from the ER to the plasma membrane occurred rapidly (within minutes) and independently of Sec18p, a vesicular trafficking protein [35].

The exact mechanism or route for the vesicular-independent transfer of cholesterol is still not fully understood but may involve cytosolic lipid transfer proteins or occur via direct MCSs (two membranes of ≤30 nm in proximity) or a combination of both. The ER itself forms multiple MCSs with the plasma membrane and other organelles including the Golgi apparatus, lysosomes, membranous components of the endocytic pathway, peroxisomes, and the mitochondria [36]. These MCSs are tethered together by the interacting proteins of both membranes and allow functions such as signaling, sensing and content transferring.

The distribution of cholesterol through MCSs involves a number of cholesterol binding proteins (Figure 5.1). These proteins are found in the ER, plasma membrane, endosomes and lysosomes. Within the endosomal/lysosomal pathway, there is a difference in the proteins involved and the degree of cholesterol transfer based on the progression and maturity of vesicles. The ER protein vesicle-associated membrane protein (VAP) interacts with oxysterol-binding protein-related

protein 1L (ORP1L) and steroidogenic acute regulatory-related lipid transfer domain 3 (STARD3) on late endosomes and facilitates ER-endosomal MCSs [37]. ORP1L is a cholesterol sensor present on a subset of late endosomes carrying the cholesterol exporter Niemann-Pick type C1 (NPC1) and forms ER-endosome MCSs, when cholesterol levels are low [38]. STARD3 is involved in MCSs between late endosomes and the ER and is present in endosomes containing the ATP binding cassette class A 3 (ABCA3) cholesterol transporter [39]. ER protein ORP5 and the endosomal NPC1 is another pair that facilitates MCS formation and cholesterol transfer [37]. NPC2, an endosomal luminal protein, binds unesterified cholesterol, transfers it to NPC1 at the membrane [40], which along with ORP5, facilitate the exit of unesterified cholesterol from the endosome and its insertion into the ER membrane [41].

The transfer of cholesterol also occurs at MCSs between the ER and plasma membrane and involves a number of lipid transfer proteins that are phosphoinositide (PIP)-dependent [42, 43]. Osh4p, a member of the ORPs that transfer sterols in yeast, has multiple membrane binding sites and binds to PIP on the plasma membrane [42, 43]. Specifically, the presence of phosphatidylinositol (4,5) bisphosphate ($PI(4,5)P_2$), a lipid enriched at the plasma membrane, stimulated sterol transport by Osh4p [42]. In mammalian cells the transport of cholesterol between the plasma membrane and the ER is partly also facilitated by ORPs, specifically ORP1S and ORP2 [44].

The extended synaptotagmins (E-SYTs) are another group of ER anchored proteins that bind to and functions in the transfer of lipids at ER-plasma membrane MCSs [45]. The interaction between E-SYTs with the plasma membrane also require $PI(4,5)P_2$ enriched microdomains and occurs in a Ca^{2+}-dependent manner [46]. Depletion of $PI(4,5)P_2$ disrupted the normal distribution of E-SYT2 and E-SYT3 isoforms at MCSs between the ER and plasma membrane and resultein

an usual ER network distribution [46]. Recruitment of E-SYT1 to MCSs between the ER and plasma membrane on the other hand, occurred through ER Ca^{2+} release or more specifically, through cytoplasmic Ca^{2+} increase [46]. The formation of ER and plasma membrane tethers by E-SYTs, are similar to the process of SOCE as both are Ca^{2+}-dependent, however, it remains to be seen how these two distinct MCS formation processes may affect cholesterol trafficking between the ER and plasma membrane [46].

Ca^{2+} signaling and ER-plasma membrane MCSs

The MCSs formed between STIM1 and Orai1 at the ER/plasma membrane interface, play a major role in Ca^{2+} signaling driving SOCE, a major route of Ca^{2+} entry into the cell. The STIM1 cytoplasmic domain contains a polybasic region that promotes its binding to the phosphatidylinositol within the plasma membrane to facilitate MCS formation between the plasma membrane and the ER [47]. Recently, both STIM1 [48] and Orai1 [49] have been identified as cholesterol binding proteins. Furthermore, we have been able to show that STIM1 and Orai1 differentially affect unesterified cholesterol distribution and nSREBP activity. Specifically, the effect of STIM1 on nSREBP activity was shown to be mediated by its cholesterol binding domain. Therefore the components of SOCE may play a role in intracellular cholesterol distribution and more importantly, cholesterol movement between the ER and plasma membrane.

During SOCE, STIM1 interacts with the plasma membrane by binding to $PI(4,5)P_2$ and there is movement of the STIM1-Orai1 complex during SOCE from a $PI(4,5)P_2$-poor region to a $PI(4,5)P_2$-rich region [45]. The $PI(4,5)P_2$ microdomains are suggested to be important for clustering the STIM1-Orai1 complex with proteins involved in Ca^{2+}-dependent inactivation of

SOCE [45]. However, this role of $PI(4,5)P_2$ microdomains in SOCE has been challenged and it remains to be established [50]. The fact that both ER-plasma membrane MCSs involved in cholesterol transfer and SOCE occur at $PI(4,5)P_2$-rich regions suggest that there may be a link between the two signaling pathways.

So far the idea that cholesterol transfer between the ER and plasma membrane can occur through MCSs in a vesicle-independent manner has led to the discovery of many lipid transferring proteins that can form tethers between the two membranes. However, what activates these tether formation and where they form are still unclear. E-SYT-mediated MCS formation between the ER and plasma membrane is the only known lipid transferring mechanism dependent upon cytoplasmic Ca^{2+} increase [46]. The effect of total ER Ca^{2+} observed on cholesterol homeostasis in our recent report [2] may be due to the effect of total ER Ca^{2+} on STIM1, Orai1 and ultimately the activity of SOCE. As hypothesized in the Figure 5.2 Graphic representation of the intracellular pathway of LDL-derived and *de novo* synthesized cholesterol under conditions where ER Ca^{2+} is low, depletion of total ER Ca^{2+} may induce SOCE and the sequestering of membrane cholesterol, by STIM1 and Orai1 cholesterol binding sites, at ER-plasma membrane MCSs, evading detection from the SREBP-SCAP sensing mechanism. Furthermore, the sequestering of cholesterol at ER-plasma membrane MCSs during SOCE, occurs in $PI(4,5)P_2$-rich regions, which may be a mechanism by which $PI(4,5)P_2$-dependent cholesterol transfer proteins access cholesterol for transfer between the ER and plasma membrane. It would be interesting to investigate the effect of lowered ER Ca^{2+} on STIM1-Orai1-mediated MCSs and how this can affect cholesterol transfer between the ER and the plasma membrane.

Calreticulin has been shown to modulate the activity of SOCE [51]. Overexpression of calreticulin increases total ER Ca^{2+} stores, disrupts STIM1 Ca^{2+} sensing capacity and reduces

Ca^{2+} influx through SOCE [52]. We have shown that in the absence of calreticulin, where total ER Ca^{2+} is reduced, STIM1 distribution, STIM1 and Orai1 expression and the activity of SOCE are greatly affected (refer to chapter four). In particular, in the absence of calreticulin, there is reduced Ca^{2+} influx during SOCE (Figure 4.1) which is a result likely due to the decreased protein expression of both STIM1 and Orai1 (Figure 4.2). Furthermore, the distribution of STIM1 within the ER membrane is shifted from the lighter fractions marked by SCAP in the absence of calreticulin (Figure 4.3). In light of a recent study showing the binding of cholesterol by STIM1 [48], the change in STIM1 distribution may result in the sequestering of cholesterol away from the SREBP-SCAP complex. Therefore, in the absence of STIM1 and ER cholesterol binding, cholesterol may be more available for SREBP-SCAP sensing and therefore cause the observed reduction in nSREBP activity in our experiments with *Stim1*$^{-/-}$ cells (Figure 4.4). Overall, our results indicate that there is an established link between ER Ca^{2+} dynamics and cholesterol homeostasis, mediated through ER Ca^{2+} binding proteins calreticulin, STIM1 and the plasma membrane Ca^{2+} channel Orai1.

Conclusion

Ca^{2+} is a versatile signaling molecule involved in a wide variety of cellular processes and it is able to do this because of the many different Ca^{2+} interacting proteins. Recently, Ca^{2+} has emerged as an important player in cholesterol metabolism. The idea of MCSs and its ability to act as a bridge between membranes for cholesterol transfer has identified many old and new proteins that can potentially interact with both Ca^{2+} and cholesterol. This provides a new avenue of study that investigates the ways in which Ca^{2+} plays a role in governing cholesterol homeostasis.

Reference

[1] L. Guo, K. Nakamura, J. Lynch, M. Opas, E.N. Olson, L.B. Agellon, M. Michalak, Cardiac-specific expression of calcineurin reverses embryonic lethality in calreticulin-deficient mouse, The Journal of biological chemistry, 277 (2002) 50776-50779.
[2] W.A. Wang, W.X. Liu, S. Durnaoglu, S.K. Lee, J. Lian, R. Lehner, J. Ahnn, L.B. Agellon, M. Michalak, Loss of Calreticulin Uncovers a Critical Role for Calcium in Regulating Cellular Lipid Homeostasis, Scientific reports, 7 (2017) s41598.
[3] N. Mesaeli, K. Nakamura, E. Zvaritch, P. Dickie, E. Dziak, K.H. Krause, M. Opas, D.H. MacLennan, M. Michalak, Calreticulin is essential for cardiac development, The Journal of cell biology, 144 (1999) 857-868.
[4] K. Nakamura, A. Zuppini, S. Arnaudeau, J. Lynch, I. Ahsan, R. Krause, S. Papp, H. De Smedt, J.B. Parys, W. Muller-Esterl, D.P. Lew, K.H. Krause, N. Demaurex, M. Opas, M. Michalak, Functional specialization of calreticulin domains, The Journal of cell biology, 154 (2001) 961-972.
[5] A. Das, M.S. Brown, D.D. Anderson, J.L. Goldstein, A. Radhakrishnan, Three pools of plasma membrane cholesterol and their relation to cholesterol homeostasis, eLife, 3 (2014) e02882.
[6] R.E. Infante, A. Radhakrishnan, Continuous transport of a small fraction of plasma membrane cholesterol to endoplasmic reticulum regulates total cellular cholesterol, eLife, 6 (2017) e25466.
[7] T.Y. Chang, C.C. Chang, N. Ohgami, Y. Yamauchi, Cholesterol sensing, trafficking, and esterification, Annual review of cell and developmental biology, 22 (2006) 129-157.
[8] M.S. Brown, S.E. Dana, J.L. Goldstein, Receptor-dependent hydrolysis of cholesteryl esters contained in plasma low density lipoprotein, Proceedings of the National Academy of Sciences of the United States of America, 72 (1975) 2925-2929.
[9] M.S. Brown, J.L. Goldstein, A receptor-mediated pathway for cholesterol homeostasis, Science, 232 (1986) 34-47.
[10] E.B. Neufeld, A.M. Cooney, J. Pitha, E.A. Dawidowicz, N.K. Dwyer, P.G. Pentchev, E.J. Blanchette-Mackie, Intracellular trafficking of cholesterol monitored with a cyclodextrin, The Journal of biological chemistry, 271 (1996) 21604-21613.
[11] T. Yang, P.J. Espenshade, M.E. Wright, D. Yabe, Y. Gong, R. Aebersold, J.L. Goldstein, M.S. Brown, Crucial step in cholesterol homeostasis: sterols promote binding of SCAP to INSIG-1, a membrane protein that facilitates retention of SREBPs in ER, Cell, 110 (2002) 489-500.
[12] T.Y. Chang, C.C. Chang, D. Cheng, Acyl-coenzyme A:cholesterol acyltransferase, Annual review of biochemistry, 66 (1997) 613-638.
[13] S. Patel, R. Docampo, Acidic calcium stores open for business: expanding the potential for intracellular Ca^{2+} signaling, Trends in cell biology, 20 (2010) 277-286.
[14] J.V. Gerasimenko, A.V. Tepikin, O.H. Petersen, O.V. Gerasimenko, Calcium uptake via endocytosis with rapid release from acidifying endosomes, Current biology: CB, 8 (1998) 1335-1338.
[15] J.P. Luzio, N.A. Bright, P.R. Pryor, The role of calcium and other ions in sorting and delivery in the late endocytic pathway, Biochemical Society transactions, 35 (2007) 1088-1091.

[16] K.A. Christensen, J.T. Myers, J.A. Swanson, pH-dependent regulation of lysosomal calcium in macrophages, Journal of cell science, 115 (2002) 599-607.
[17] T. Albrecht, Y. Zhao, T.H. Nguyen, R.E. Campbell, J.D. Johnson, Fluorescent biosensors illuminate calcium levels within defined beta-cell endosome subpopulations, Cell calcium, 57 (2015) 263-274.
[18] C.I. Lopez-Sanjurjo, S.C. Tovey, D.L. Prole, C.W. Taylor, Lysosomes shape Ins(1,4,5)P3-evoked Ca^{2+} signals by selectively sequestering Ca^{2+} released from the endoplasmic reticulum, Journal of cell science, 126 (2013) 289-300.
[19] A.G. Garrity, W. Wang, C.M. Collier, S.A. Levey, Q. Gao, H. Xu, The endoplasmic reticulum, not the pH gradient, drives calcium refilling of lysosomes, eLife, 5 (2016) e15887.
[20] V. Ronco, D.M. Potenza, F. Denti, S. Vullo, G. Gagliano, M. Tognolina, G. Guerra, P. Pinton, A.A. Genazzani, L. Mapelli, D. Lim, F. Moccia, A novel Ca(2)(+)-mediated cross-talk between endoplasmic reticulum and acidic organelles: implications for NAADP-dependent Ca(2)(+) signalling, Cell calcium, 57 (2015) 89-100.
[21] B.S. Kilpatrick, E.R. Eden, A.H. Schapira, C.E. Futter, S. Patel, Direct mobilisation of lysosomal Ca^{2+} triggers complex Ca^{2+} signals, Journal of cell science, 126 (2013) 60-66.
[22] K. Abe, R. Puertollano, Role of TRP channels in the regulation of the endosomal pathway, Physiology, 26 (2011) 14-22.
[23] M. Sun, E. Goldin, S. Stahl, J.L. Falardeau, J.C. Kennedy, J.S. Acierno, Jr., C. Bove, C.R. Kaneski, J. Nagle, M.C. Bromley, M. Colman, R. Schiffmann, S.A. Slaugenhaupt, Mucolipidosis type IV is caused by mutations in a gene encoding a novel transient receptor potential channel, Human molecular genetics, 9 (2000) 2471-2478.
[24] D. Shen, X. Wang, X. Li, X. Zhang, Z. Yao, S. Dibble, X.P. Dong, T. Yu, A.P. Lieberman, H.D. Showalter, H. Xu, Lipid storage disorders block lysosomal trafficking by inhibiting a TRP channel and lysosomal calcium release, Nature communications, 3 (2012) 731.
[25] D.A. Zeevi, A. Frumkin, V. Offen-Glasner, A. Kogot-Levin, G. Bach, A potentially dynamic lysosomal role for the endogenous TRPML proteins, The Journal of pathology, 219 (2009) 153-162.
[26] C. Karacsonyi, A.S. Miguel, R. Puertollano, Mucolipin-2 localizes to the Arf6-associated pathway and regulates recycling of GPI-APs, Traffic, 8 (2007) 1404-1414.
[27] J.A. Martina, B. Lelouvier, R. Puertollano, The calcium channel mucolipin-3 is a novel regulator of trafficking along the endosomal pathway, Traffic, 10 (2009) 1143-1156.
[28] B. Lelouvier, R. Puertollano, Mucolipin-3 regulates luminal calcium, acidification, and membrane fusion in the endosomal pathway, The Journal of biological chemistry, 286 (2011) 9826-9832.
[29] K. Coen, R.S. Flannagan, S. Baron, L.R. Carraro-Lacroix, D. Wang, W. Vermeire, C. Michiels, S. Munck, V. Baert, S. Sugita, F. Wuytack, P.R. Hiesinger, S. Grinstein, W. Annaert, Lysosomal calcium homeostasis defects, not proton pump defects, cause endo-lysosomal dysfunction in PSEN-deficient cells, The Journal of cell biology, 198 (2012) 23-35.
[30] M. Ruas, K. Rietdorf, A. Arredouani, L.C. Davis, E. Lloyd-Evans, H. Koegel, T.M. Funnell, A.J. Morgan, J.A. Ward, K. Watanabe, X. Cheng, G.C. Churchill, M.X. Zhu, F.M. Platt, G.M. Wessel, J. Parrington, A. Galione, Purified TPC isoforms form NAADP receptors with distinct roles for Ca(2+) signaling and endolysosomal trafficking, Current biology: CB, 20 (2010) 703-709.

[31] A.J. Morgan, L.C. Davis, S.K. Wagner, A.M. Lewis, J. Parrington, G.C. Churchill, A. Galione, Bidirectional Ca(2)(+) signaling occurs between the endoplasmic reticulum and acidic organelles, The Journal of cell biology, 200 (2013) 789-805.
[32] R. van der Kant, J. Neefjes, Small regulators, major consequences - Ca(2)(+) and cholesterol at the endosome-ER interface, Journal of cell science, 127 (2014) 929-938.
[33] L. Urbani, R.D. Simoni, Cholesterol and vesicular stomatitis virus G protein take separate routes from the endoplasmic reticulum to the plasma membrane, The Journal of biological chemistry, 265 (1990) 1919-1923.
[34] S. Heino, S. Lusa, P. Somerharju, C. Ehnholm, V.M. Olkkonen, E. Ikonen, Dissecting the role of the golgi complex and lipid rafts in biosynthetic transport of cholesterol to the cell surface, Proceedings of the National Academy of Sciences of the United States of America, 97 (2000) 8375-8380.
[35] N.A. Baumann, D.P. Sullivan, H. Ohvo-Rekila, C. Simonot, A. Pottekat, Z. Klaassen, C.T. Beh, A.K. Menon, Transport of newly synthesized sterol to the sterol-enriched plasma membrane occurs via nonvesicular equilibration, Biochemistry, 44 (2005) 5816-5826.
[36] M.J. Phillips, G.K. Voeltz, Structure and function of ER membrane contact sites with other organelles, Nature reviews. Molecular cell biology, 17 (2016) 69-82.
[37] E.R. Eden, The formation and function of ER-endosome membrane contact sites, Biochimica et biophysica acta, 1861 (2016) 874-879.
[38] N. Rocha, C. Kuijl, R. van der Kant, L. Janssen, D. Houben, H. Janssen, W. Zwart, J. Neefjes, Cholesterol sensor ORP1L contacts the ER protein VAP to control Rab7-RILP-p150 Glued and late endosome positioning, The Journal of cell biology, 185 (2009) 1209-1225.
[39] R. van der Kant, I. Zondervan, L. Janssen, J. Neefjes, Cholesterol-binding molecules MLN64 and ORP1L mark distinct late endosomes with transporters ABCA3 and NPC1, Journal of lipid research, 54 (2013) 2153-2165.
[40] D.E. Sleat, J.A. Wiseman, M. El-Banna, S.M. Price, L. Verot, M.M. Shen, G.S. Tint, M.T. Vanier, S.U. Walkley, P. Lobel, Genetic evidence for nonredundant functional cooperativity between NPC1 and NPC2 in lipid transport, Proceedings of the National Academy of Sciences of the United States of America, 101 (2004) 5886-5891.
[41] X. Du, J. Kumar, C. Ferguson, T.A. Schulz, Y.S. Ong, W. Hong, W.A. Prinz, R.G. Parton, A.J. Brown, H. Yang, A role for oxysterol-binding protein-related protein 5 in endosomal cholesterol trafficking, The Journal of cell biology, 192 (2011) 121-135.
[42] S. Raychaudhuri, Y.J. Im, J.H. Hurley, W.A. Prinz, Nonvesicular sterol movement from plasma membrane to ER requires oxysterol-binding protein-related proteins and phosphoinositides, The Journal of cell biology, 173 (2006) 107-119.
[43] T.A. Schulz, M.G. Choi, S. Raychaudhuri, J.A. Mears, R. Ghirlando, J.E. Hinshaw, W.A. Prinz, Lipid-regulated sterol transfer between closely apposed membranes by oxysterol-binding protein homologues, The Journal of cell biology, 187 (2009) 889-903.
[44] M. Jansen, Y. Ohsaki, L.R. Rega, R. Bittman, V.M. Olkkonen, E. Ikonen, Role of ORPs in sterol transport from plasma membrane to ER and lipid droplets in mammalian cells, Traffic, 12 (2011) 218-231.
[45] J. Maleth, S. Choi, S. Muallem, M. Ahuja, Translocation between PI(4,5)P2-poor and PI(4,5)P2-rich microdomains during store depletion determines STIM1 conformation and Orai1 gating, Nature communications, 5 (2014) 5843.

[46] F. Giordano, Y. Saheki, O. Idevall-Hagren, S.F. Colombo, M. Pirruccello, I. Milosevic, E.O. Gracheva, S.N. Bagriantsev, N. Borgese, P. De Camilli, PI(4,5)P(2)-dependent and Ca(2+)-regulated ER-PM interactions mediated by the extended synaptotagmins, Cell, 153 (2013) 1494-1509.
[47] W.D. Heo, T. Inoue, W.S. Park, M.L. Kim, B.O. Park, T.J. Wandless, T. Meyer, PI(3,4,5)P3 and PI(4,5)P2 lipids target proteins with polybasic clusters to the plasma membrane, Science, 314 (2006) 1458-1461.
[48] J. Pacheco, L. Dominguez, A. Bohorquez-Hernandez, A. Asanov, L. Vaca, A cholesterol-binding domain in STIM1 modulates STIM1-Orai1 physical and functional interactions, Scientific reports, 6 (2016) 29634.
[49] I. Derler, I. Jardin, P.B. Stathopulos, M. Muik, M. Fahrner, V. Zayats, S.K. Pandey, M. Poteser, B. Lackner, M. Absolonova, R. Schindl, K. Groschner, R. Ettrich, M. Ikura, C. Romanin, Cholesterol modulates Orai1 channel function, Science signaling, 9 (2016) ra10.
[50] M.K. Korzeniowski, M.A. Popovic, Z. Szentpetery, P. Varnai, S.S. Stojilkovic, T. Balla, Dependence of STIM1/Orai1-mediated calcium entry on plasma membrane phosphoinositides, The Journal of biological chemistry, 284 (2009) 21027-21035.
[51] S. Arnaudeau, M. Frieden, K. Nakamura, C. Castelbou, M. Michalak, N. Demaurex, Calreticulin differentially modulates calcium uptake and release in the endoplasmic reticulum and mitochondria, The Journal of biological chemistry, 277 (2002) 46696-46705.
[52] L. Mery, N. Mesaeli, M. Michalak, M. Opas, D.P. Lew, K.H. Krause, Overexpression of calreticulin increases intracellular Ca^{2+} storage and decreases store-operated Ca^{2+} influx, The Journal of biological chemistry, 271 (1996) 9332-9339.

Bibliography

ABE, K. & PUERTOLLANO, R. 2011. Role of TRP channels in the regulation of the endosomal pathway. *Physiology (Bethesda),* 26**,** 14-22.

ALBRECHT, T., ZHAO, Y., NGUYEN, T. H., CAMPBELL, R. E. & JOHNSON, J. D. 2015. Fluorescent biosensors illuminate calcium levels within defined beta-cell endosome subpopulations. *Cell Calcium,* 57**,** 263-74.

AMEMIYA-KUDO, M., SHIMANO, H., HASTY, A. H., YAHAGI, N., YOSHIKAWA, T., MATSUZAKA, T., OKAZAKI, H., TAMURA, Y., IIZUKA, Y., OHASHI, K., OSUGA, J., HARADA, K., GOTODA, T., SATO, R., KIMURA, S., ISHIBASHI, S. & YAMADA, N. 2002. Transcriptional activities of nuclear SREBP-1a, -1c, and -2 to different target promoters of lipogenic and cholesterogenic genes. *J Lipid Res,* 43**,** 1220-35.

AMODIO, G., RENNA, M., PALADINO, S., VENTURI, C., TACCHETTI, C., MOLTEDO, O., FRANCESCHELLI, S., MALLARDO, M., BONATTI, S. & REMONDELLI, P. 2009. Endoplasmic reticulum stress reduces the export from the ER and alters the architecture of post-ER compartments. *Int J Biochem Cell Biol,* 41**,** 2511-21.

ANDERSON, R. G. 2003. Joe Goldstein and Mike Brown: from cholesterol homeostasis to new paradigms in membrane biology. *Trends Cell Biol,* 13**,** 534-9.

ARNAUDEAU, S., FRIEDEN, M., NAKAMURA, K., CASTELBOU, C., MICHALAK, M. & DEMAUREX, N. 2002. Calreticulin differentially modulates calcium uptake and release in the endoplasmic reticulum and mitochondria. *J Biol Chem,* 277**,** 46696-705.

ARRUDA, A. P., PERS, B. M., PARLAKGUL, G., GUNEY, E., GOH, T., CAGAMPAN, E., LEE, G. Y., GONCALVES, R. L. & HOTAMISLIGIL, G. S. 2017. Defective STIM-mediated store operated Ca(2+) entry in hepatocytes leads to metabolic dysfunction in obesity. *Elife,* 6 pii: e29968.

BABA, Y., HAYASHI, K., FUJII, Y., MIZUSHIMA, A., WATARAI, H., WAKAMORI, M., NUMAGA, T., MORI, Y., IINO, M., HIKIDA, M. & KUROSAKI, T. 2006. Coupling of STIM1 to store-operated Ca^{2+} entry through its constitutive and inducible movement in the endoplasmic reticulum. *Proc Natl Acad Sci U S A,* 103**,** 16704-9.

BACK, S. H., LEE, K., VINK, E. & KAUFMAN, R. J. 2006. Cytoplasmic IRE1alpha-mediated XBP1 mRNA splicing in the absence of nuclear processing and endoplasmic reticulum stress. *J Biol Chem,* 281**,** 18691-706.

BAKSH, S. & MICHALAK, M. 1991. Expression of calreticulin in Escherichia coli and identification of its Ca^{2+} binding domains. *J Biol Chem,* 266**,** 21458-65.

BASTIANUTTO, C., CLEMENTI, E., CODAZZI, F., PODINI, P., DE GIORGI, F., RIZZUTO, R., MELDOLESI, J. & POZZAN, T. 1995. Overexpression of calreticulin increases the Ca^{2+} capacity of rapidly exchanging Ca^{2+} stores and reveals aspects of their lumenal microenvironment and function. *J Cell Biol,* 130**,** 847-55.

BAUMANN, N. A., SULLIVAN, D. P., OHVO-REKILA, H., SIMONOT, C., POTTEKAT, A., KLAASSEN, Z., BEH, C. T. & MENON, A. K. 2005. Transport of newly synthesized sterol to the sterol-enriched plasma membrane occurs via nonvesicular equilibration. *Biochemistry,* 44**,** 5816-26.

BAUMANN, O. & WALZ, B. 2001. Endoplasmic reticulum of animal cells and its organization into structural and functional domains. *Int Rev Cytol,* 205**,** 149-214.

BELL, R. D., DEANE, R., CHOW, N., LONG, X., SAGARE, A., SINGH, I., STREB, J. W., GUO, H., RUBIO, A., VAN NOSTRAND, W., MIANO, J. M. & ZLOKOVIC, B. V. 2009. SRF and myocardin regulate LRP-mediated amyloid-beta clearance in brain vascular cells. *Nat Cell Biol,* 11**,** 143-53.

BERRIDGE, M. J. 1993. Inositol trisphosphate and calcium signalling. *Nature,* 361**,** 315-25.

BERRIDGE, M. J., BOOTMAN, M. D. & RODERICK, H. L. 2003. Calcium signalling: dynamics, homeostasis and remodelling. *Nat Rev Mol Cell Biol,* 4**,** 517-29.

BERTOLOTTI, A., ZHANG, Y., HENDERSHOT, L. M., HARDING, H. P. & RON, D. 2000. Dynamic interaction of BiP and ER stress transducers in the unfolded-protein response. *Nat Cell Biol,* 2**,** 326-32.

BRAAKMAN, I. & HEBERT, D. N. 2013. Protein folding in the endoplasmic reticulum. *Cold Spring Harb Perspect Biol,* 5**,** a013201.

BROWN, M. S., DANA, S. E. & GOLDSTEIN, J. L. 1975. Receptor-dependent hydrolysis of cholesteryl esters contained in plasma low density lipoprotein. *Proc Natl Acad Sci U S A,* 72**,** 2925-9.

BROWN, M. S. & GOLDSTEIN, J. L. 1986. A receptor-mediated pathway for cholesterol homeostasis. *Science,* 232**,** 34-47.

BROWN, M. S. & GOLDSTEIN, J. L. 1997. The SREBP pathway: regulation of cholesterol metabolism by proteolysis of a membrane-bound transcription factor. *Cell,* 89**,** 331-40.

CAMACHO, P. & LECHLEITER, J. D. 1995. Calreticulin inhibits repetitive intracellular Ca^{2+} waves. *Cell,* 82**,** 765-71.

CERQUEIRA, N. M., OLIVEIRA, E. F., GESTO, D. S., SANTOS-MARTINS, D., MOREIRA, C., MOORTHY, H. N., RAMOS, M. J. & FERNANDES, P. A. 2016. Cholesterol Biosynthesis: A Mechanistic Overview. *Biochemistry,* 55**,** 5483-5506.

CHANG, C. C., MIYAZAKI, A., DONG, R., KHEIROLLAH, A., YU, C., GENG, Y., HIGGS, H. N. & CHANG, T. Y. 2010. Purification of recombinant acyl-coenzyme A:cholesterol acyltransferase 1 (ACAT1) from H293 cells and binding studies between the enzyme and substrates using difference intrinsic fluorescence spectroscopy. *Biochemistry,* 49**,** 9957-63.

CHANG, T. Y., CHANG, C. C. & CHENG, D. 1997. Acyl-coenzyme A:cholesterol acyltransferase. *Annu Rev Biochem,* 66**,** 613-38.

CHANG, T. Y., CHANG, C. C., OHGAMI, N. & YAMAUCHI, Y. 2006. Cholesterol sensing, trafficking, and esterification. *Annu Rev Cell Dev Biol,* 22**,** 129-57.

CHENG, C., RU, P., GENG, F., LIU, J., YOO, J. Y., WU, X., CHENG, X., EUTHINE, V., HU, P., GUO, J. Y., LEFAI, E., KAUR, B., NOHTURFFT, A., MA, J., CHAKRAVARTI, A. & GUO, D. 2015. Glucose-Mediated N-glycosylation of SCAP Is Essential for SREBP-1 Activation and Tumor Growth. *Cancer Cell,* 28**,** 569-581.

CHENG, D., ESPENSHADE, P. J., SLAUGHTER, C. A., JAEN, J. C., BROWN, M. S. & GOLDSTEIN, J. L. 1999. Secreted site-1 protease cleaves peptides corresponding to luminal loop of sterol regulatory element-binding proteins. *J Biol Chem,* 274**,** 22805-12.

CHRISTENSEN, K. A., MYERS, J. T. & SWANSON, J. A. 2002. pH-dependent regulation of lysosomal calcium in macrophages. *J Cell Sci,* 115**,** 599-607.

CLAPHAM, D. E. 2007. Calcium signaling. *Cell,* 131**,** 1047-58.

COEN, K., FLANNAGAN, R. S., BARON, S., CARRARO-LACROIX, L. R., WANG, D., VERMEIRE, W., MICHIELS, C., MUNCK, S., BAERT, V., SUGITA, S., WUYTACK,

F., HIESINGER, P. R., GRINSTEIN, S. & ANNAERT, W. 2012. Lysosomal calcium homeostasis defects, not proton pump defects, cause endo-lysosomal dysfunction in PSEN-deficient cells. *J Cell Biol,* 198**,** 23-35.

COLGAN, S. M., TANG, D., WERSTUCK, G. H. & AUSTIN, R. C. 2007. Endoplasmic reticulum stress causes the activation of sterol regulatory element binding protein-2. *Int J Biochem Cell Biol,* 39**,** 1843-51.

CORBETT, E. F., MICHALAK, K. M., OIKAWA, K., JOHNSON, S., CAMPBELL, I. D., EGGLETON, P., KAY, C. & MICHALAK, M. 2000. The conformation of calreticulin is influenced by the endoplasmic reticulum luminal environment. *J Biol Chem,* 275**,** 27177-85.

CORBETT, E. F. & MICHALAK, M. 2000. Calcium, a signaling molecule in the endoplasmic reticulum? *Trends Biochem Sci,* 25**,** 307-11.

DAS, A., BROWN, M. S., ANDERSON, D. D., GOLDSTEIN, J. L. & RADHAKRISHNAN, A. 2014. Three pools of plasma membrane cholesterol and their relation to cholesterol homeostasis. *Elife,* 3 e02882.

DEBOSE-BOYD, R. A., BROWN, M. S., LI, W. P., NOHTURFFT, A., GOLDSTEIN, J. L. & ESPENSHADE, P. J. 1999. Transport-dependent proteolysis of SREBP: relocation of site-1 protease from Golgi to ER obviates the need for SREBP transport to Golgi. *Cell,* 99**,** 703-12.

DERLER, I., JARDIN, I., STATHOPULOS, P. B., MUIK, M., FAHRNER, M., ZAYATS, V., PANDEY, S. K., POTESER, M., LACKNER, B., ABSOLONOVA, M., SCHINDL, R., GROSCHNER, K., ETTRICH, R., IKURA, M. & ROMANIN, C. 2016. Cholesterol modulates Orai1 channel function. *Sci Signal,* 9**,** ra10.

DU, X., KUMAR, J., FERGUSON, C., SCHULZ, T. A., ONG, Y. S., HONG, W., PRINZ, W. A., PARTON, R. G., BROWN, A. J. & YANG, H. 2011. A role for oxysterol-binding protein-related protein 5 in endosomal cholesterol trafficking. *J Cell Biol,* 192**,** 121-35.

EDEN, E. R. 2016. The formation and function of ER-endosome membrane contact sites. *Biochim Biophys Acta,* 1861**,** 874-879.

FAHRNER, M., MUIK, M., SCHINDL, R., BUTORAC, C., STATHOPULOS, P., ZHENG, L., JARDIN, I., IKURA, M. & ROMANIN, C. 2014. A coiled-coil clamp controls both conformation and clustering of stromal interaction molecule 1 (STIM1). *J Biol Chem,* 289**,** 33231-44.

FASOLATO, C., PIZZO, P. & POZZAN, T. 1998. Delayed activation of the store-operated calcium current induced by calreticulin overexpression in RBL-1 cells. *Mol Biol Cell,* 9**,** 1513-22.

FESKE, S., GWACK, Y., PRAKRIYA, M., SRIKANTH, S., PUPPEL, S. H., TANASA, B., HOGAN, P. G., LEWIS, R. S., DALY, M. & RAO, A. 2006. A mutation in Orai1 causes immune deficiency by abrogating CRAC channel function. *Nature,* 441**,** 179-85.

FOLCH, J., LEES, M. & SLOANE STANLEY, G. H. 1957. A simple method for the isolation and purification of total lipides from animal tissues. *J Biol Chem,* 226**,** 497-509.

GAO, S. & ZHEN, M. 2011. Action potentials drive body wall muscle contractions in Caenorhabditis elegans. *Proc Natl Acad Sci U S A,* 108**,** 2557-62.

GARRITY, A. G., WANG, W., COLLIER, C. M., LEVEY, S. A., GAO, Q. & XU, H. 2016. The endoplasmic reticulum, not the pH gradient, drives calcium refilling of lysosomes. *Elife,* 5 pii: e5887.

GEORGIADES, P., ALLAN, V. J., WRIGHT, G. D., WOODMAN, P. G., UDOMMAI, P., CHUNG, M. A. & WAIGH, T. A. 2017. The flexibility and dynamics of the tubules in the endoplasmic reticulum. *Sci Rep,* 7**,** 16474.

GERASIMENKO, J. V., TEPIKIN, A. V., PETERSEN, O. H. & GERASIMENKO, O. V. 1998. Calcium uptake via endocytosis with rapid release from acidifying endosomes. *Curr Biol,* 8**,** 1335-8.

GIORDANO, F., SAHEKI, Y., IDEVALL-HAGREN, O., COLOMBO, S. F., PIRRUCCELLO, M., MILOSEVIC, I., GRACHEVA, E. O., BAGRIANTSEV, S. N., BORGESE, N. & DE CAMILLI, P. 2013. PI(4,5)P(2)-dependent and Ca(2+)-regulated ER-PM interactions mediated by the extended synaptotagmins. *Cell,* 153**,** 1494-509.

GOLDSTEIN, J. L., DEBOSE-BOYD, R. A. & BROWN, M. S. 2006. Protein sensors for membrane sterols. *Cell,* 124**,** 35-46.

GROENENDYK, J., AGELLON, L. B. & MICHALAK, M. 2013. Coping with endoplasmic reticulum stress in the cardiovascular system. *Annu Rev Physiol,* 75**,** 49-67.

GROENENDYK, J., LYNCH, J. & MICHALAK, M. 2004. Calreticulin, Ca^{2+}, and calcineurin - signaling from the endoplasmic reticulum. *Mol Cells,* 17**,** 383-9.

GUO, L., NAKAMURA, K., LYNCH, J., OPAS, M., OLSON, E. N., AGELLON, L. B. & MICHALAK, M. 2002. Cardiac-specific expression of calcineurin reverses embryonic lethality in calreticulin-deficient mouse. *J Biol Chem,* 277**,** 50776-9.

GWACK, Y., SRIKANTH, S., OH-HORA, M., HOGAN, P. G., LAMPERTI, E. D., YAMASHITA, M., GELINAS, C., NEEMS, D. S., SASAKI, Y., FESKE, S., PRAKRIYA, M., RAJEWSKY, K. & RAO, A. 2008. Hair loss and defective T- and B-cell function in mice lacking ORAI1. *Mol Cell Biol,* 28**,** 5209-22.

HAN, D., LERNER, A. G., VANDE WALLE, L., UPTON, J. P., XU, W., HAGEN, A., BACKES, B. J., OAKES, S. A. & PAPA, F. R. 2009. IRE1alpha kinase activation modes control alternate endoribonuclease outputs to determine divergent cell fates. *Cell,* 138**,** 562-75.

HARDING, H. P., ZHANG, Y., BERTOLOTTI, A., ZENG, H. & RON, D. 2000. Perk is essential for translational regulation and cell survival during the unfolded protein response. *Mol Cell,* 5**,** 897-904.

HAZE, K., YOSHIDA, H., YANAGI, H., YURA, T. & MORI, K. 1999. Mammalian transcription factor ATF6 is synthesized as a transmembrane protein and activated by proteolysis in response to endoplasmic reticulum stress. *Mol Biol Cell,* 10**,** 3787-99.

HEINO, S., LUSA, S., SOMERHARJU, P., EHNHOLM, C., OLKKONEN, V. M. & IKONEN, E. 2000. Dissecting the role of the golgi complex and lipid rafts in biosynthetic transport of cholesterol to the cell surface. *Proc Natl Acad Sci U S A,* 97**,** 8375-80.

HEO, W. D., INOUE, T., PARK, W. S., KIM, M. L., PARK, B. O., WANDLESS, T. J. & MEYER, T. 2006. PI(3,4,5)P3 and PI(4,5)P2 lipids target proteins with polybasic clusters to the plasma membrane. *Science,* 314**,** 1458-61.

HETZ, C. 2012. The unfolded protein response: controlling cell fate decisions under ER stress and beyond. *Nat Rev Mol Cell Biol,* 13**,** 89-102.

HETZ, C. & GLIMCHER, L. H. 2009. Fine-tuning of the unfolded protein response: Assembling the IRE1alpha interactome. *Mol Cell,* 35**,** 551-61.

HEVONOJA, T., PENTIKAINEN, M. O., HYVONEN, M. T., KOVANEN, P. T. & ALA-KORPELA, M. 2000. Structure of low density lipoprotein (LDL) particles: basis for

understanding molecular changes in modified LDL. *Biochim Biophys Acta,* 1488**,** 189-210.
HEWAVITHARANA, T., DENG, X., WANG, Y., RITCHIE, M. F., GIRISH, G. V., SOBOLOFF, J. & GILL, D. L. 2008. Location and function of STIM1 in the activation of Ca^{2+} entry signals. *J Biol Chem,* 283**,** 26252-62.
HOLLIEN, J., LIN, J. H., LI, H., STEVENS, N., WALTER, P. & WEISSMAN, J. S. 2009. Regulated Ire1-dependent decay of messenger RNAs in mammalian cells. *J Cell Biol,* 186**,** 323-31.
HORTON, J. D., GOLDSTEIN, J. L. & BROWN, M. S. 2002. SREBPs: activators of the complete program of cholesterol and fatty acid synthesis in the liver. *J Clin Invest,* 109**,** 1125-31.
HORTON, J. D., SHIMOMURA, I., BROWN, M. S., HAMMER, R. E., GOLDSTEIN, J. L. & SHIMANO, H. 1998. Activation of cholesterol synthesis in preference to fatty acid synthesis in liver and adipose tissue of transgenic mice overproducing sterol regulatory element-binding protein-2. *J Clin Invest,* 101**,** 2331-9.
HOU, X., PEDI, L., DIVER, M. M. & LONG, S. B. 2012. Crystal structure of the calcium release-activated calcium channel Orai. *Science,* 338**,** 1308-13.
HUA, X., WU, J., GOLDSTEIN, J. L., BROWN, M. S. & HOBBS, H. H. 1995. Structure of the human gene encoding sterol regulatory element binding protein-1 (SREBF1) and localization of SREBF1 and SREBF2 to chromosomes 17p11.2 and 22q13. *Genomics,* 25**,** 667-73.
INFANTE, R. E. & RADHAKRISHNAN, A. 2017. Continuous transport of a small fraction of plasma membrane cholesterol to endoplasmic reticulum regulates total cellular cholesterol. *Elife,* 6 pii: e25466.
JANSEN, M., OHSAKI, Y., REGA, L. R., BITTMAN, R., OLKKONEN, V. M. & IKONEN, E. 2011. Role of ORPs in sterol transport from plasma membrane to ER and lipid droplets in mammalian cells. *Traffic,* 12**,** 218-31.
KAMMOUN, H. L., CHABANON, H., HAINAULT, I., LUQUET, S., MAGNAN, C., KOIKE, T., FERRE, P. & FOUFELLE, F. 2009. GRP78 expression inhibits insulin and ER stress-induced SREBP-1c activation and reduces hepatic steatosis in mice. *J Clin Invest,* 119**,** 1201-15.
KARACSONYI, C., MIGUEL, A. S. & PUERTOLLANO, R. 2007. Mucolipin-2 localizes to the Arf6-associated pathway and regulates recycling of GPI-APs. *Traffic,* 8**,** 1404-14.
KILPATRICK, B. S., EDEN, E. R., SCHAPIRA, A. H., FUTTER, C. E. & PATEL, S. 2013. Direct mobilisation of lysosomal Ca^{2+} triggers complex Ca^{2+} signals. *J Cell Sci,* 126**,** 60-6.
KORZENIOWSKI, M. K., POPOVIC, M. A., SZENTPETERY, Z., VARNAI, P., STOJILKOVIC, S. S. & BALLA, T. 2009. Dependence of STIM1/Orai1-mediated calcium entry on plasma membrane phosphoinositides. *J Biol Chem,* 284**,** 21027-35.
KREBS, J., AGELLON, L. B. & MICHALAK, M. 2015. Ca(2+) homeostasis and endoplasmic reticulum (ER) stress: An integrated view of calcium signaling. *Biochem Biophys Res Commun,* 460**,** 114-21.
LAMRIBEN, L., GRAHAM, J. B., ADAMS, B. M. & HEBERT, D. N. 2016. N-Glycan-based ER Molecular Chaperone and Protein Quality Control System: The Calnexin Binding Cycle. *Traffic,* 17**,** 308-26.

LEE, D., SINGARAVELU, G., PARK, B. J. & AHNN, J. 2007. Differential requirement of unfolded protein response pathway for calreticulin expression in Caenorhabditis elegans. *J Mol Biol,* 372**,** 331-40.

LEE, J. N. & YE, J. 2004. Proteolytic activation of sterol regulatory element-binding protein induced by cellular stress through depletion of Insig-1. *J Biol Chem,* 279**,** 45257-65.

LEE, T. H. & LINSTEDT, A. D. 1999. Osmotically induced cell volume changes alter anterograde and retrograde transport, Golgi structure, and COPI dissociation. *Mol Biol Cell,* 10**,** 1445-62.

LEE, W., KIM, K. R., SINGARAVELU, G., PARK, B. J., KIM, D. H., AHNN, J. & YOO, Y. J. 2006. Alternative chaperone machinery may compensate for calreticulin/calnexin deficiency in Caenorhabditis elegans. *Proteomics,* 6**,** 1329-39.

LELOUVIER, B. & PUERTOLLANO, R. 2011. Mucolipin-3 regulates luminal calcium, acidification, and membrane fusion in the endosomal pathway. *J Biol Chem,* 286**,** 9826-32.

LIOU, J., KIM, M. L., HEO, W. D., JONES, J. T., MYERS, J. W., FERRELL, J. E., JR. & MEYER, T. 2005. STIM is a Ca^{2+} sensor essential for Ca^{2+}-store-depletion-triggered Ca^{2+} influx. *Curr Biol,* 15**,** 1235-41.

LOPEZ-SANJURJO, C. I., TOVEY, S. C., PROLE, D. L. & TAYLOR, C. W. 2013. Lysosomes shape Ins(1,4,5)P3-evoked Ca2+ signals by selectively sequestering Ca^{2+} released from the endoplasmic reticulum. *J Cell Sci,* 126**,** 289-300.

LUIK, R. M., WANG, B., PRAKRIYA, M., WU, M. M. & LEWIS, R. S. 2008. Oligomerization of STIM1 couples ER calcium depletion to CRAC channel activation. *Nature,* 454**,** 538-42.

LUIK, R. M., WU, M. M., BUCHANAN, J. & LEWIS, R. S. 2006. The elementary unit of store-operated Ca^{2+} entry: local activation of CRAC channels by STIM1 at ER-plasma membrane junctions. *J Cell Biol,* 174**,** 815-25.

LUO, S., BAUMEISTER, P., YANG, S., ABCOUWER, S. F. & LEE, A. S. 2003. Induction of Grp78/BiP by translational block: activation of the Grp78 promoter by ATF4 through and upstream ATF/CRE site independent of the endoplasmic reticulum stress elements. *J Biol Chem,* 278**,** 37375-85.

LUZIO, J. P., BRIGHT, N. A. & PRYOR, P. R. 2007. The role of calcium and other ions in sorting and delivery in the late endocytic pathway. *Biochem Soc Trans,* 35**,** 1088-91.

LYNCH, J. & MICHALAK, M. 2003. Calreticulin is an upstream regulator of calcineurin. *Biochem Biophys Res Commun,* 311**,** 1173-9.

MALETH, J., CHOI, S., MUALLEM, S. & AHUJA, M. 2014. Translocation between PI(4,5)P2-poor and PI(4,5)P2-rich microdomains during store depletion determines STIM1 conformation and Orai1 gating. *Nat Commun,* 5**,** 5843.

MARTIN, V., GROENENDYK, J., STEINER, S. S., GUO, L., DABROWSKA, M., PARKER, J. M., MULLER-ESTERL, W., OPAS, M. & MICHALAK, M. 2006. Identification by mutational analysis of amino acid residues essential in the chaperone function of calreticulin. *J Biol Chem,* 281**,** 2338-46.

MARTINA, J. A., LELOUVIER, B. & PUERTOLLANO, R. 2009. The calcium channel mucolipin-3 is a novel regulator of trafficking along the endosomal pathway. *Traffic,* 10**,** 1143-56.

MATSUDA, M., KORN, B. S., HAMMER, R. E., MOON, Y. A., KOMURO, R., HORTON, J. D., GOLDSTEIN, J. L., BROWN, M. S. & SHIMOMURA, I. 2001. SREBP cleavage-activating protein (SCAP) is required for increased lipid synthesis in liver induced by cholesterol deprivation and insulin elevation. *Genes Dev,* 15**,** 1206-16.

MAUS, M., CUK, M., PATEL, B., LIAN, J., OUIMET, M., KAUFMANN, U., YANG, J., HORVATH, R., HORNIG-DO, H. T., CHRZANOWSKA-LIGHTOWLERS, Z. M., MOORE, K. J., CUERVO, A. M. & FESKE, S. 2017. Store-Operated Ca(2+) Entry Controls Induction of Lipolysis and the Transcriptional Reprogramming to Lipid Metabolism. *Cell Metab,* 25**,** 698-712.

MERY, L., MESAELI, N., MICHALAK, M., OPAS, M., LEW, D. P. & KRAUSE, K. H. 1996. Overexpression of calreticulin increases intracellular Ca^{2+} storage and decreases store-operated Ca^{2+} influx. *J Biol Chem,* 271**,** 9332-9.

MESAELI, N., NAKAMURA, K., ZVARITCH, E., DICKIE, P., DZIAK, E., KRAUSE, K. H., OPAS, M., MACLENNAN, D. H. & MICHALAK, M. 1999. Calreticulin is essential for cardiac development. *J Cell Biol,* 144**,** 857-68.

MICHALAK, M., GROENENDYK, J., SZABO, E., GOLD, L. I. & OPAS, M. 2009. Calreticulin, a multi-process calcium-buffering chaperone of the endoplasmic reticulum. *Biochem J,* 417**,** 651-66.

MICHALAK, M., LYNCH, J., GROENENDYK, J., GUO, L., ROBERT PARKER, J. M. & OPAS, M. 2002. Calreticulin in cardiac development and pathology. *Biochim Biophys Acta,* 1600**,** 32-7.

MICHALAK, M., MILNER, R. E., BURNS, K. & OPAS, M. 1992. Calreticulin. *Biochem J,* 285 (Pt 3)**,** 681-92.

MIGNEN, O., THOMPSON, J. L. & SHUTTLEWORTH, T. J. 2008. Orai1 subunit stoichiometry of the mammalian CRAC channel pore. *J Physiol,* 586**,** 419-25.

MIKOSHIBA, K. & HATTORI, M. 2000. IP3 receptor-operated calcium entry. *Sci STKE,* 2000**,** pe1.

MOLINARI, M., ERIKSSON, K. K., CALANCA, V., GALLI, C., CRESSWELL, P., MICHALAK, M. & HELENIUS, A. 2004. Contrasting functions of calreticulin and calnexin in glycoprotein folding and ER quality control. *Mol Cell,* 13**,** 125-35.

MORGAN, A. J., DAVIS, L. C., WAGNER, S. K., LEWIS, A. M., PARRINGTON, J., CHURCHILL, G. C. & GALIONE, A. 2013. Bidirectional Ca(2)(+) signaling occurs between the endoplasmic reticulum and acidic organelles. *J Cell Biol,* 200**,** 789-805.

MUIK, M., FRISCHAUF, I., DERLER, I., FAHRNER, M., BERGSMANN, J., EDER, P., SCHINDL, R., HESCH, C., POLZINGER, B., FRITSCH, R., KAHR, H., MADL, J., GRUBER, H., GROSCHNER, K. & ROMANIN, C. 2008. Dynamic coupling of the putative coiled-coil domain of ORAI1 with STIM1 mediates ORAI1 channel activation. *J Biol Chem,* 283**,** 8014-22.

MUKHERJEE, S., ZHA, X., TABAS, I. & MAXFIELD, F. R. 1998. Cholesterol distribution in living cells: fluorescence imaging using dehydroergosterol as a fluorescent cholesterol analog. *Biophys J,* 75**,** 1915-25.

MULLANEY, B. C. & ASHRAFI, K. 2009. C. elegans fat storage and metabolic regulation. *Biochim Biophys Acta,* 1791**,** 474-8.

NAABY-HANSEN, S., WOLKOWICZ, M. J., KLOTZ, K., BUSH, L. A., WESTBROOK, V. A., SHIBAHARA, H., SHETTY, J., COONROD, S. A., REDDI, P. P., SHANNON, J.,

KINTER, M., SHERMAN, N. E., FOX, J., FLICKINGER, C. J. & HERR, J. C. 2001. Co-localization of the inositol 1,4,5-trisphosphate receptor and calreticulin in the equatorial segment and in membrane bounded vesicles in the cytoplasmic droplet of human spermatozoa. *Mol Hum Reprod,* 7**,** 923-33.

NAKAMURA, K., ZUPPINI, A., ARNAUDEAU, S., LYNCH, J., AHSAN, I., KRAUSE, R., PAPP, S., DE SMEDT, H., PARYS, J. B., MULLER-ESTERL, W., LEW, D. P., KRAUSE, K. H., DEMAUREX, N., OPAS, M. & MICHALAK, M. 2001. Functional specialization of calreticulin domains. *J Cell Biol,* 154**,** 961-72.

NEUFELD, E. B., COONEY, A. M., PITHA, J., DAWIDOWICZ, E. A., DWYER, N. K., PENTCHEV, P. G. & BLANCHETTE-MACKIE, E. J. 1996. Intracellular trafficking of cholesterol monitored with a cyclodextrin. *J Biol Chem,* 271**,** 21604-13.

NIXON-ABELL, J., OBARA, C. J., WEIGEL, A. V., LI, D., LEGANT, W. R., XU, C. S., PASOLLI, H. A., HARVEY, K., HESS, H. F., BETZIG, E., BLACKSTONE, C. & LIPPINCOTT-SCHWARTZ, J. 2016. Increased spatiotemporal resolution reveals highly dynamic dense tubular matrices in the peripheral ER. *Science,* 354.

NOHTURFFT, A., DEBOSE-BOYD, R. A., SCHEEK, S., GOLDSTEIN, J. L. & BROWN, M. S. 1999. Sterols regulate cycling of SREBP cleavage-activating protein (SCAP) between endoplasmic reticulum and Golgi. *Proc Natl Acad Sci U S A,* 96**,** 11235-40.

NUNES-HASLER, P. & DEMAUREX, N. 2017. The ER phagosome connection in the era of membrane contact sites. *Biochim Biophys Acta,* 1864**,** 1513-1524.

OHSAKI, Y., SOLTYSIK, K. & FUJIMOTO, T. 2017. The Lipid Droplet and the Endoplasmic Reticulum. *Adv Exp Med Biol,* 997**,** 111-120.

OKAMURA, K., KIMATA, Y., HIGASHIO, H., TSURU, A. & KOHNO, K. 2000. Dissociation of Kar2p/BiP from an ER sensory molecule, Ire1p, triggers the unfolded protein response in yeast. *Biochem Biophys Res Commun,* 279**,** 445-50.

OSTWALD, T. J. & MACLENNAN, D. H. 1974. Isolation of a high affinity calcium-binding protein from sarcoplasmic reticulum. *J Biol Chem,* 249**,** 974-9.

PACHECO, J., DOMINGUEZ, L., BOHORQUEZ-HERNANDEZ, A., ASANOV, A. & VACA, L. 2016. A cholesterol-binding domain in STIM1 modulates STIM1-Orai1 physical and functional interactions. *Sci Rep,* 6**,** 29634.

PARK, B. J., LEE, D. G., YU, J. R., JUNG, S. K., CHOI, K., LEE, J., LEE, J., KIM, Y. S., LEE, J. I., KWON, J. Y., LEE, J., SINGSON, A., SONG, W. K., EOM, S. H., PARK, C. S., KIM, D. H., BANDYOPADHYAY, J. & AHNN, J. 2001. Calreticulin, a calcium-binding molecular chaperone, is required for stress response and fertility in Caenorhabditis elegans. *Mol Biol Cell,* 12**,** 2835-45.

PARK, C. Y., HOOVER, P. J., MULLINS, F. M., BACHHAWAT, P., COVINGTON, E. D., RAUNSER, S., WALZ, T., GARCIA, K. C., DOLMETSCH, R. E. & LEWIS, R. S. 2009. STIM1 clusters and activates CRAC channels via direct binding of a cytosolic domain to Orai1. *Cell,* 136**,** 876-90.

PATEL, S. & DOCAMPO, R. 2010. Acidic calcium stores open for business: expanding the potential for intracellular Ca^{2+} signaling. *Trends Cell Biol,* 20**,** 277-86.

PEINELT, C., VIG, M., KOOMOA, D. L., BECK, A., NADLER, M. J., KOBLAN-HUBERSON, M., LIS, A., FLEIG, A., PENNER, R. & KINET, J. P. 2006. Amplification of CRAC current by STIM1 and CRACM1 (Orai1). *Nat Cell Biol,* 8**,** 771-3.

PENNA, A., DEMURO, A., YEROMIN, A. V., ZHANG, S. L., SAFRINA, O., PARKER, I. & CAHALAN, M. D. 2008. The CRAC channel consists of a tetramer formed by Stim-induced dimerization of Orai dimers. *Nature,* 456**,** 116-20.

PHILLIPS, M. J. & VOELTZ, G. K. 2016. Structure and function of ER membrane contact sites with other organelles. *Nat Rev Mol Cell Biol,* 17**,** 69-82.

PINTON, P., FERRARI, D., RAPIZZI, E., DI VIRGILIO, F., POZZAN, T. & RIZZUTO, R. 2001. The Ca^{2+} concentration of the endoplasmic reticulum is a key determinant of ceramide-induced apoptosis: significance for the molecular mechanism of Bcl-2 action. *EMBO J,* 20**,** 2690-701.

POCANSCHI, C. L., KOZLOV, G., BROCKMEIER, U., BROCKMEIER, A., WILLIAMS, D. B. & GEHRING, K. 2011. Structural and functional relationships between the lectin and arm domains of calreticulin. *J Biol Chem,* 286**,** 27266-77.

PRAKRIYA, M., FESKE, S., GWACK, Y., SRIKANTH, S., RAO, A. & HOGAN, P. G. 2006. Orai1 is an essential pore subunit of the CRAC channel. *Nature,* 443**,** 230-3.

PRINS, D., GROENENDYK, J., TOURET, N. & MICHALAK, M. 2011. Modulation of STIM1 and capacitative Ca^{2+} entry by the endoplasmic reticulum luminal oxidoreductase ERp57. *EMBO Rep,* 12**,** 1182-8.

PRINS, D. & MICHALAK, M. 2011. Organellar calcium buffers. *Cold Spring Harb Perspect Biol,* 3, 197-212.

PRUDENT, J. & MCBRIDE, H. M. 2017. The mitochondria-endoplasmic reticulum contact sites: a signalling platform for cell death. *Curr Opin Cell Biol,* 47**,** 52-63.

RADHAKRISHNAN, A., GOLDSTEIN, J. L., MCDONALD, J. G. & BROWN, M. S. 2008. Switch-like control of SREBP-2 transport triggered by small changes in ER cholesterol: a delicate balance. *Cell Metab,* 8**,** 512-21.

RAYCHAUDHURI, S., IM, Y. J., HURLEY, J. H. & PRINZ, W. A. 2006. Nonvesicular sterol movement from plasma membrane to ER requires oxysterol-binding protein-related proteins and phosphoinositides. *J Cell Biol,* 173**,** 107-19.

REID, P. C., SAKASHITA, N., SUGII, S., OHNO-IWASHITA, Y., SHIMADA, Y., HICKEY, W. F. & CHANG, T. Y. 2004. A novel cholesterol stain reveals early neuronal cholesterol accumulation in the Niemann-Pick type C1 mouse brain. *J Lipid Res,* 45**,** 582-91.

ROCHA, N., KUIJL, C., VAN DER KANT, R., JANSSEN, L., HOUBEN, D., JANSSEN, H., ZWART, W. & NEEFJES, J. 2009. Cholesterol sensor ORP1L contacts the ER protein VAP to control Rab7-RILP-p150 Glued and late endosome positioning. *J Cell Biol,* 185**,** 1209-25.

ROGERS, M. A., LIU, J., SONG, B. L., LI, B. L., CHANG, C. C. & CHANG, T. Y. 2015. Acyl-CoA:cholesterol acyltransferases (ACATs/SOATs): Enzymes with multiple sterols as substrates and as activators. *J Steroid Biochem Mol Biol,* 151**,** 102-7.

RONCO, V., POTENZA, D. M., DENTI, F., VULLO, S., GAGLIANO, G., TOGNOLINA, M., GUERRA, G., PINTON, P., GENAZZANI, A. A., MAPELLI, L., LIM, D. & MOCCIA, F. 2015. A novel Ca(2)(+)-mediated cross-talk between endoplasmic reticulum and acidic organelles: implications for NAADP-dependent Ca(2)(+) signalling. *Cell Calcium,* 57**,** 89-100.

ROOS, J., DIGREGORIO, P. J., YEROMIN, A. V., OHLSEN, K., LIOUDYNO, M., ZHANG, S., SAFRINA, O., KOZAK, J. A., WAGNER, S. L., CAHALAN, M. D., VELICELEBI,

G. & STAUDERMAN, K. A. 2005. STIM1, an essential and conserved component of store-operated Ca^{2+} channel function. *J Cell Biol,* 169**,** 435-45.

RUAS, M., RIETDORF, K., ARREDOUANI, A., DAVIS, L. C., LLOYD-EVANS, E., KOEGEL, H., FUNNELL, T. M., MORGAN, A. J., WARD, J. A., WATANABE, K., CHENG, X., CHURCHILL, G. C., ZHU, M. X., PLATT, F. M., WESSEL, G. M., PARRINGTON, J. & GALIONE, A. 2010. Purified TPC isoforms form NAADP receptors with distinct roles for Ca(2+) signaling and endolysosomal trafficking. *Curr Biol,* 20**,** 703-9.

SAHOO, D., TRISCHUK, T. C., CHAN, T., DROVER, V. A., HO, S., CHIMINI, G., AGELLON, L. B., AGNIHOTRI, R., FRANCIS, G. A. & LEHNER, R. 2004. ABCA1-dependent lipid efflux to apolipoprotein A-I mediates HDL particle formation and decreases VLDL secretion from murine hepatocytes. *J Lipid Res,* 45**,** 1122-31.

SAKAI, J., NOHTURFFT, A., CHENG, D., HO, Y. K., BROWN, M. S. & GOLDSTEIN, J. L. 1997. Identification of complexes between the COOH-terminal domains of sterol regulatory element-binding proteins (SREBPs) and SREBP cleavage-activating protein. *J Biol Chem,* 272**,** 20213-21.

SAMBROOK, J. F. 1990. The involvement of calcium in transport of secretory proteins from the endoplasmic reticulum. *Cell,* 61**,** 197-9.

SATO, R., INOUE, J., KAWABE, Y., KODAMA, T., TAKANO, T. & MAEDA, M. 1996. Sterol-dependent transcriptional regulation of sterol regulatory element-binding protein-2. *J Biol Chem,* 271**,** 26461-4.

SCHULZ, T. A., CHOI, M. G., RAYCHAUDHURI, S., MEARS, J. A., GHIRLANDO, R., HINSHAW, J. E. & PRINZ, W. A. 2009. Lipid-regulated sterol transfer between closely apposed membranes by oxysterol-binding protein homologues. *J Cell Biol,* 187**,** 889-903.

SEVER, N., YANG, T., BROWN, M. S., GOLDSTEIN, J. L. & DEBOSE-BOYD, R. A. 2003. Accelerated degradation of HMG CoA reductase mediated by binding of insig-1 to its sterol-sensing domain. *Mol Cell,* 11**,** 25-33.

SHAMU, C. E. & WALTER, P. 1996. Oligomerization and phosphorylation of the Ire1p kinase during intracellular signaling from the endoplasmic reticulum to the nucleus. *EMBO J,* 15**,** 3028-39.

SHEN, D., WANG, X., LI, X., ZHANG, X., YAO, Z., DIBBLE, S., DONG, X. P., YU, T., LIEBERMAN, A. P., SHOWALTER, H. D. & XU, H. 2012. Lipid storage disorders block lysosomal trafficking by inhibiting a TRP channel and lysosomal calcium release. *Nat Commun,* 3**,** 731.

SHEN, J., CHEN, X., HENDERSHOT, L. & PRYWES, R. 2002. ER stress regulation of ATF6 localization by dissociation of BiP/GRP78 binding and unmasking of Golgi localization signals. *Dev Cell,* 3**,** 99-111.

SHIBATA, Y., VOELTZ, G. K. & RAPOPORT, T. A. 2006. Rough sheets and smooth tubules. *Cell,* 126**,** 435-9.

SHIMANO, H. 2002. Sterol regulatory element-binding protein family as global regulators of lipid synthetic genes in energy metabolism. *Vitam Horm,* 65**,** 167-94.

SHIMANO, H., HORTON, J. D., HAMMER, R. E., SHIMOMURA, I., BROWN, M. S. & GOLDSTEIN, J. L. 1996. Overproduction of cholesterol and fatty acids causes massive liver enlargement in transgenic mice expressing truncated SREBP-1a. *J Clin Invest,* 98**,** 1575-84.

SHIMANO, H., HORTON, J. D., SHIMOMURA, I., HAMMER, R. E., BROWN, M. S. & GOLDSTEIN, J. L. 1997. Isoform 1c of sterol regulatory element binding protein is less active than isoform 1a in livers of transgenic mice and in cultured cells. *J Clin Invest,* 99**,** 846-54.

SIDRAUSKI, C. & WALTER, P. 1997. The transmembrane kinase Ire1p is a site-specific endonuclease that initiates mRNA splicing in the unfolded protein response. *Cell,* 90**,** 1031-9.

SLEAT, D. E., WISEMAN, J. A., EL-BANNA, M., PRICE, S. M., VEROT, L., SHEN, M. M., TINT, G. S., VANIER, M. T., WALKLEY, S. U. & LOBEL, P. 2004. Genetic evidence for nonredundant functional cooperativity between NPC1 and NPC2 in lipid transport. *Proc Natl Acad Sci U S A,* 101**,** 5886-91.

SOKOLOV, A. & RADHAKRISHNAN, A. 2010. Accessibility of cholesterol in endoplasmic reticulum membranes and activation of SREBP-2 switch abruptly at a common cholesterol threshold. *J Biol Chem,* 285**,** 29480-90.

SOLOVYOVA, N., VESELOVSKY, N., TOESCU, E. C. & VERKHRATSKY, A. 2002. Ca(2+) dynamics in the lumen of the endoplasmic reticulum in sensory neurons: direct visualization of Ca(2+)-induced Ca(2+) release triggered by physiological Ca(2+) entry. *EMBO J,* 21**,** 622-30.

SONG, B. L., JAVITT, N. B. & DEBOSE-BOYD, R. A. 2005. Insig-mediated degradation of HMG CoA reductase stimulated by lanosterol, an intermediate in the synthesis of cholesterol. *Cell Metab,* 1**,** 179-89.

STATHOPULOS, P. B., LI, G. Y., PLEVIN, M. J., AMES, J. B. & IKURA, M. 2006. Stored Ca^{2+} depletion-induced oligomerization of stromal interaction molecule 1 (STIM1) via the EF-SAM region: An initiation mechanism for capacitive Ca^{2+} entry. *J Biol Chem,* 281**,** 35855-62.

SUGII, S., REID, P. C., OHGAMI, N., DU, H. & CHANG, T. Y. 2003. Distinct endosomal compartments in early trafficking of low density lipoprotein-derived cholesterol. *J Biol Chem,* 278**,** 27180-9.

SUN, L. P., LI, L., GOLDSTEIN, J. L. & BROWN, M. S. 2005. Insig required for sterol-mediated inhibition of Scap/SREBP binding to COPII proteins in vitro. *J Biol Chem,* 280**,** 26483-90.

SUN, M., GOLDIN, E., STAHL, S., FALARDEAU, J. L., KENNEDY, J. C., ACIERNO, J. S., JR., BOVE, C., KANESKI, C. R., NAGLE, J., BROMLEY, M. C., COLMAN, M., SCHIFFMANN, R. & SLAUGENHAUPT, S. A. 2000. Mucolipidosis type IV is caused by mutations in a gene encoding a novel transient receptor potential channel. *Hum Mol Genet,* 9**,** 2471-8.

SUNDQVIST, A., BENGOECHEA-ALONSO, M. T., YE, X., LUKIYANCHUK, V., JIN, J., HARPER, J. W. & ERICSSON, J. 2005. Control of lipid metabolism by phosphorylation-dependent degradation of the SREBP family of transcription factors by SCF(Fbw7). *Cell Metab,* 1**,** 379-91.

SUZUKI, M. 2017. Regulation of lipid metabolism via a connection between the endoplasmic reticulum and lipid droplets. *Anat Sci Int,* 92**,** 50-54.

TAUCHI-SATO, K., OZEKI, S., HOUJOU, T., TAGUCHI, R. & FUJIMOTO, T. 2002. The surface of lipid droplets is a phospholipid monolayer with a unique Fatty Acid composition. *J Biol Chem,* 277**,** 44507-12.

THIAM, A. R., FARESE, R. V., JR. & WALTHER, T. C. 2013. The biophysics and cell biology of lipid droplets. *Nat Rev Mol Cell Biol,* 14**,** 775-86.

TREIMAN, M., CASPERSEN, C. & CHRISTENSEN, S. B. 1998. A tool coming of age: thapsigargin as an inhibitor of sarco-endoplasmic reticulum Ca(2+)-ATPases. *Trends Pharmacol Sci,* 19**,** 131-5.

URBANI, L. & SIMONI, R. D. 1990. Cholesterol and vesicular stomatitis virus G protein take separate routes from the endoplasmic reticulum to the plasma membrane. *J Biol Chem,* 265**,** 1919-23.

VAN DER KANT, R. & NEEFJES, J. 2014. Small regulators, major consequences - Ca(2)(+) and cholesterol at the endosome-ER interface. *J Cell Sci,* 127**,** 929-38.

VAN DER KANT, R., ZONDERVAN, I., JANSSEN, L. & NEEFJES, J. 2013. Cholesterol-binding molecules MLN64 and ORP1L mark distinct late endosomes with transporters ABCA3 and NPC1. *J Lipid Res,* 54**,** 2153-65.

VIG, M., BECK, A., BILLINGSLEY, J. M., LIS, A., PARVEZ, S., PEINELT, C., KOOMOA, D. L., SOBOLOFF, J., GILL, D. L., FLEIG, A., KINET, J. P. & PENNER, R. 2006a. CRACM1 multimers form the ion-selective pore of the CRAC channel. *Curr Biol,* 16**,** 2073-9.

VIG, M., PEINELT, C., BECK, A., KOOMOA, D. L., RABAH, D., KOBLAN-HUBERSON, M., KRAFT, S., TURNER, H., FLEIG, A., PENNER, R. & KINET, J. P. 2006b. CRACM1 is a plasma membrane protein essential for store-operated Ca^{2+} entry. *Science,* 312**,** 1220-3.

WALKER, A. K., JACOBS, R. L., WATTS, J. L., ROTTIERS, V., JIANG, K., FINNEGAN, D. M., SHIODA, T., HANSEN, M., YANG, F., NIEBERGALL, L. J., VANCE, D. E., TZONEVA, M., HART, A. C. & NAAR, A. M. 2011. A conserved SREBP-1/phosphatidylcholine feedback circuit regulates lipogenesis in metazoans. *Cell,* 147**,** 840-52.

WALKER, A. K., YANG, F., JIANG, K., JI, J. Y., WATTS, J. L., PURUSHOTHAM, A., BOSS, O., HIRSCH, M. L., RIBICH, S., SMITH, J. J., ISRAELIAN, K., WESTPHAL, C. H., RODGERS, J. T., SHIODA, T., ELSON, S. L., MULLIGAN, P., NAJAFI-SHOUSHTARI, H., BLACK, J. C., THAKUR, J. K., KADYK, L. C., WHETSTINE, J. R., MOSTOSLAVSKY, R., PUIGSERVER, P., LI, X., DYSON, N. J., HART, A. C. & NAAR, A. M. 2010. Conserved role of SIRT1 orthologs in fasting-dependent inhibition of the lipid/cholesterol regulator SREBP. *Genes Dev,* 24**,** 1403-17.

WANG, W. A., GROENENDYK, J. & MICHALAK, M. 2012. Calreticulin signaling in health and disease. *Int J Biochem Cell Biol,* 44**,** 842-6.

WANG, W. A., LIU, W. X., DURNAOGLU, S., LEE, S. K., LIAN, J., LEHNER, R., AHNN, J., AGELLON, L. B. & MICHALAK, M. 2017. Loss of Calreticulin Uncovers a Critical Role for Calcium in Regulating Cellular Lipid Homeostasis. *Sci Rep,* 7**,** 5941.

WILSON, C. H., ALI, E. S., SCRIMGEOUR, N., MARTIN, A. M., HUA, J., TALLIS, G. A., RYCHKOV, G. Y. & BARRITT, G. J. 2015. Steatosis inhibits liver cell store-operated Ca(2)(+) entry and reduces ER Ca(2)(+) through a protein kinase C-dependent mechanism. *Biochem J,* 466**,** 379-90.

XU, W., LONGO, F. J., WINTERMANTEL, M. R., JIANG, X., CLARK, R. A. & DELISLE, S. 2000. Calreticulin modulates capacitative Ca^{2+} influx by controlling the extent of inositol 1,4,5-trisphosphate-induced Ca^{2+} store depletion. *J Biol Chem,* 275**,** 36676-82.

YANG, T., ESPENSHADE, P. J., WRIGHT, M. E., YABE, D., GONG, Y., AEBERSOLD, R., GOLDSTEIN, J. L. & BROWN, M. S. 2002. Crucial step in cholesterol homeostasis: sterols promote binding of SCAP to INSIG-1, a membrane protein that facilitates retention of SREBPs in ER. *Cell,* 110**,** 489-500.

YANG, X., JIN, H., CAI, X., LI, S. & SHEN, Y. 2012. Structural and mechanistic insights into the activation of Stromal interaction molecule 1 (STIM1). *Proc Natl Acad Sci U S A,* 109**,** 5657-62.

YE, J., RAWSON, R. B., KOMURO, R., CHEN, X., DAVE, U. P., PRYWES, R., BROWN, M. S. & GOLDSTEIN, J. L. 2000. ER stress induces cleavage of membrane-bound ATF6 by the same proteases that process SREBPs. *Mol Cell,* 6**,** 1355-64.

YOSHIDA, H., MATSUI, T., YAMAMOTO, A., OKADA, T. & MORI, K. 2001. XBP1 mRNA is induced by ATF6 and spliced by IRE1 in response to ER stress to produce a highly active transcription factor. *Cell,* 107**,** 881-91.

YOSHIDA, H., OKADA, T., HAZE, K., YANAGI, H., YURA, T., NEGISHI, M. & MORI, K. 2000. ATF6 activated by proteolysis binds in the presence of NF-Y (CBF) directly to the cis-acting element responsible for the mammalian unfolded protein response. *Mol Cell Biol,* 20**,** 6755-67.

YU, R. & HINKLE, P. M. 2000. Rapid turnover of calcium in the endoplasmic reticulum during signaling. Studies with cameleon calcium indicators. *J Biol Chem,* 275**,** 23648-53.

ZEEVI, D. A., FRUMKIN, A., OFFEN-GLASNER, V., KOGOT-LEVIN, A. & BACH, G. 2009. A potentially dynamic lysosomal role for the endogenous TRPML proteins. *J Pathol,* 219**,** 153-62.

ZELENSKI, N. G., RAWSON, R. B., BROWN, M. S. & GOLDSTEIN, J. L. 1999. Membrane topology of S2P, a protein required for intramembranous cleavage of sterol regulatory element-binding proteins. *J Biol Chem,* 274**,** 21973-80.

ZHANG, H. & HU, J. 2016. Shaping the Endoplasmic Reticulum into a Social Network. *Trends Cell Biol,* 26**,** 934-943.

ZHANG, S. L., YU, Y., ROOS, J., KOZAK, J. A., DEERINCK, T. J., ELLISMAN, M. H., STAUDERMAN, K. A. & CAHALAN, M. D. 2005. STIM1 is a Ca^{2+} sensor that activates CRAC channels and migrates from the Ca^{2+} store to the plasma membrane. *Nature,* 437**,** 902-5.

ZHANG, Y., YU, C., LIU, J., SPENCER, T. A., CHANG, C. C. & CHANG, T. Y. 2003. Cholesterol is superior to 7-ketocholesterol or 7 alpha-hydroxycholesterol as an allosteric activator for acyl-coenzyme A:cholesterol acyltransferase 1. *J Biol Chem,* 278**,** 11642-7.

ZHENG, L., STATHOPULOS, P. B., LI, G. Y. & IKURA, M. 2008. Biophysical characterization of the EF-hand and SAM domain containing Ca^{2+} sensory region of STIM1 and STIM2. *Biochem Biophys Res Commun,* 369**,** 240-6.

Appendix I – Purification of Calreticulin Domains Using Mammalian Cells

Calreticulin is a multifunctional protein reportedly to have many functions within and outside of the ER [1]. It has been shown that exogenous calreticulin have wound healing properties and specifically enhances cellular migration and proliferation [2]. This was done with purified calreticulin from bacteria and yeast [2, 3]. There are a number of benefits to purifying calreticulin in the yeast system, including the presence of an ER and the lack of bacterial lipopolysaccharide.As calreticulin is an ER protein, expression in a system in the presence of an ER will allow for high quality folding of the protein [3]. The presence of lipopolysaccharide or endotoxins in the protein preparation purified from bacteria is problematic due to its proinflammatory properties [4]. Furthermore, lipopolysaccharides have been shown to induce cell proliferation and migration, effects that may interfere with the direct functional study of exogenous calreticulin [5, 6]. Therefore, testing different preparations of purified proteins from different expression systems allows for further validation of the functional studies of calreticulin. We were able to clone the calreticulin gene into the bacterial expressing plasmid pET22b (+) and the mammalian expressing plasmid pED. Furthermore, we expressed distinct calreticulin domains within these 2 plasmid systems and using cos-1 cells we expressed and purified the full length and NP-domain of calreticulin for further functional studies.

For the *E. coli* expressing plasmid pET22b(+), we cloned the following calreticulin constructs between the cut sites XhoI and NcoI. We cloned full length human calreticulin (NM_004343.3) (amino acids 18-417) without the signal sequence (first 17 amino acids), the N-domain of human calreticulin (amino acids 18-210), which corresponds to vasostatin, an endogenous fragment of the calreticulin N-domain and an inhibitor of angiogenesis [7], the PC-domain of human calreticulin (amino residues 181-417) and just the P-domain of calreticulin (amino residues 181-290).

For the mammalian cell expressing plasmid pED, we cloned the following calreticulin constructs between cut sites PstI and EcoRI. We cloned full length human calreticulin (NM_004343.3) (amino acids 1-417) with the signal sequence and a C-terminus His tag followed by the KDEL sequence, the NP-domain of calreticulin (amino residues 18-290) the N-domain of calreticulin (vasostatin) (amino residues 18-210) [7] and the PC-domain of calreticulin (amino residues 181-417).

Cos-1 cells were transfected with the full length human calreticulin (Figure AI.1) or NP-domain (Figure AI.2) of calreticulin containing pED vector using Lipofectamine (Thermo Fisher Scientific) as previously described [8]. Cells were harvested 60 hours post-transfection and lysed in Nonidet P-40 lysis buffer (25 mM Tris-Cl, pH 8.0, 150 mM NaCl, 1% Nonidet P-40). Cell lysates were centrifuged at 20,000 × g for 15 minutes at 4°C. Cell extracts were used for protein purification using the nickel-nitrilotriacetec acid (Ni-NTA)-agarose chromatography column. Ni-NTA-agarose chromatography was performed with a binding buffer (50 mM Tris-Cl, pH 8.0, 500 mM NaCl, and 5 mM imidazole). The full length and N-domain of calreticulin were eluted with elution buffer (100 mM imidazole) and concentrated. The expression of full length calreticulin in cos-1 cells are shown in Figure AI.1A and B and the purified full length calreticulin fractions are shown in Figure AI.1C. The expression of the NP-domain of calreticulin in cos-1 cells are shown in Figure AI.2B and C and the purified NP-domain fractions are shown in Figure AI.2A.

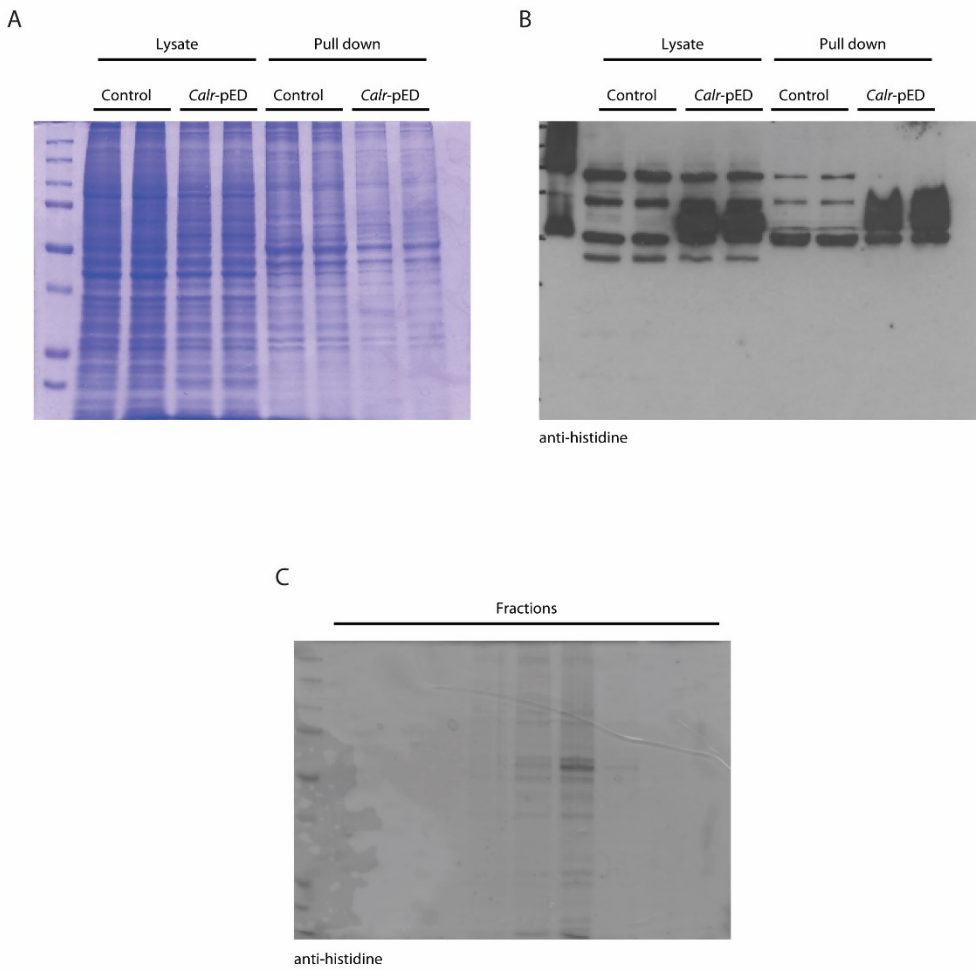

Figure AI.1 Expression and purification of full-length calreticulin

A. Coomassie blue staining of cell lysate and anti-His antibody pull down of Cos-1 cells (control) and Cos-1 cells transfected with the full-length human calreticulin containing pED vector (*Calr*-pED).

B. Immunoblot of cell lysate and anti-His antibody pull down of Cos-1 cells (control) and Cos-1 cells transfected with the full length human calreticulin containing pED vector (*Calr*-pED), probed with anit-histidine antibody.

C. Immunoblot of fractions from Ni-NTA agarose resin column purified full-length human calreticulin, probed with anti-histidine antibody.

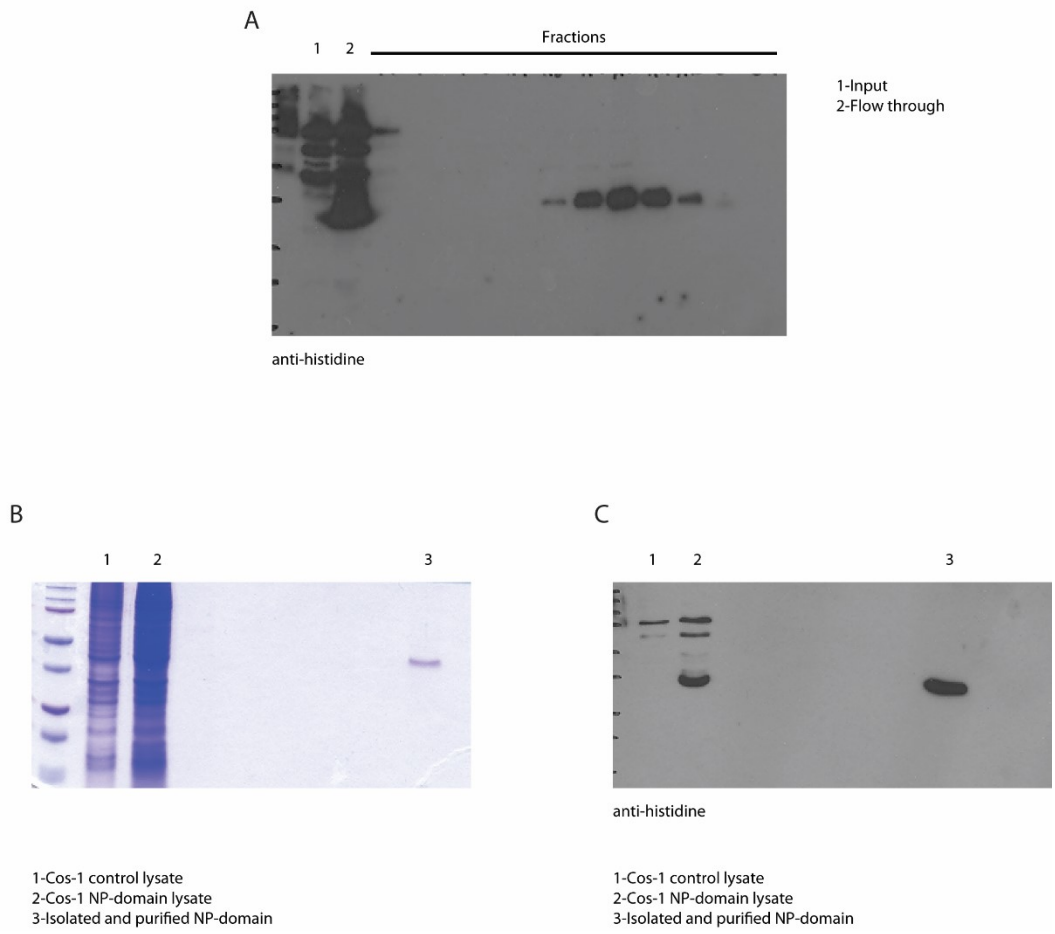

Figure AI.2 Expression and purification of NP-domain of calreticulin

A. Immunoblot of (1) input, (2) flow through and fractions from Ni-NTA agarose resin column purified NP-domain of calreticulin, probed with anti-histidine antibody.

B. Coomassie blue staining of (1) untransfected Cos-1 cell lysate, (2) NP-domain containing pED vector expressing cos-1 cell lysate and (3) purified and concentrated NP-domain of calreticulin.

C. Immunoblot of (1) untransfected Cos-1 cell lysate, (2) NP-domain containing pED vector expressing Cos-1 cell lysate and (3) purified and concentrated NP-domain of calreticulin, probed with anti-histidine antibody.

References

[1] M. Michalak, J. Groenendyk, E. Szabo, L.I. Gold, M. Opas, Calreticulin, a multi-process calcium-buffering chaperone of the endoplasmic reticulum, The Biochemical journal, 417 (2009) 651-666.
[2] M.R. Greives, F. Samra, S.C. Pavlides, K.M. Blechman, S.M. Naylor, C.D. Woodrell, C. Cadacio, J.P. Levine, T.A. Bancroft, M. Michalak, S.M. Warren, L.I. Gold, Exogenous calreticulin improves diabetic wound healing, Wound repair and regeneration: official publication of the Wound Healing Society [and] the European Tissue Repair Society, 20 (2012) 715-730.
[3] E. Ciplys, E. Zitkus, L.I. Gold, J. Daubriac, S.C. Pavlides, P. Hojrup, G. Houen, W.A. Wang, M. Michalak, R. Slibinskas, High-level secretion of native recombinant human calreticulin in yeast, Microbial cell factories, 14 (2015) 165.
[4] L. Mack, B. Brill, N. Delis, B. Groner, Endotoxin depletion of recombinant protein preparations through their preferential binding to histidine tags, Analytical biochemistry, 466 (2014) 83-88.
[5] K. Hattar, R. Savai, F.S. Subtil, J. Wilhelm, A. Schmall, D.S. Lang, T. Goldmann, B. Eul, G. Dahlem, L. Fink, R.T. Schermuly, G.A. Banat, U. Sibelius, F. Grimminger, E. Vollmer, W. Seeger, U. Grandel, Endotoxin induces proliferation of NSCLC in vitro and in vivo: role of COX-2 and EGFR activation, Cancer immunology, immunotherapy, 62 (2013) 309-320.
[6] V.S. Sharova, M.S. Izvol'skaia, S.N. Voronova, L.A. Zakharova, Effect of bacterial endotoxin on migration of gonadotropin-releasing, hormone producing neurons in rat embryogenesis, Ontogenez, 42 (2011) 439-446.
[7] S.E. Pike, L. Yao, K.D. Jones, B. Cherney, E. Appella, K. Sakaguchi, H. Nakhasi, J. Teruya-Feldstein, P. Wirth, G. Gupta, G. Tosato, Vasostatin, a calreticulin fragment, inhibits angiogenesis and suppresses tumor growth, The Journal of experimental medicine, 188 (1998) 2349-2356.
[8] C.Y. Liu, H.N. Wong, J.A. Schauerte, R.J. Kaufman, The protein kinase/endoribonuclease IRE1alpha that signals the unfolded protein response has a luminal N-terminal ligand-independent dimerization domain, The Journal of biological chemistry, 277 (2002) 18346-18356.

Appendix II – Tissue Specific Calreticulin Knockout in the Heart of Adult Mice

Calreticulin is an essential protein elevated during embryogenesis for cardiac development and therefore, knockout of calreticulin is embryonic lethal due to impaired cardiac development [1]. After birth however, the expression of calreticulin is rapidly down-regulated and maintained at a low level [1]. Transgenic mice overexpressing calreticulin in the heart have been shown to disrupt cardiac function, induced cardiomyopathy and eventual heart failure [2, 3]. Altogether, the data suggests that the downregulation of calreticulin expression is necessary for proper cardiac functioning in the adult mice. We therefore investigated the effect of knocking out calreticulin in the heart of adult mice using the cyclization recombination (Cre)/lox sit- specific recombination system [4]. Mice expressing loxP sites within introns 2 and 5 of the calreticulin gene were bred with mice expressing the cardiac specific α-myosin heavy chain (α-MHC) promoter controlled CreER (Cre fused to the mutated hormone-binding domain of estrogen receptor) [5].

Mice containing the wild-type calreticulin allele were genotyped with the following primers:

5’-GAGTGGAAACCACGTCAAATTGACAACC-3’

5’-CTTCTCTGATAAGTTTTCCTCTGACCTC-3’

The “floxed mice” containing the loxP sites in the calreticulin gene were genotyped with the following primers:

5’-GAGTGGAAACCACGTCAAATTGACAACC-3’

5’-AGGGTTCCGGATCCGATGAAGTTCC-3’

The cardiac specific “Cre mice” containing the gene for α-MHC-CreER were genotyped with the following primers:

5’-GTCTGACTAGGTGTCCTTCT-3’

5’-CGTCCTCCTGCTGGTATAG-3’

Once the transgenic offspring homozygous for the floxed calreticulin gene and heterozygous for α-MHC-CreER are generated, they are fed with 4-hydroxytamoxifen (OHT) containing food for 2-3 weeks to induce Cre movement into the nucleus, excise the floxed site within the calreticulin gene and create calreticulin null mice [4].

The cardiac specific calreticulin null mice were genotyped with the following primers:

5'-AATGACCAGAGTTGATTCCAAGG-3'

5'-CCAGAATGCTGATCTTCATACCATGG-3'

We obtained five mice homozygous for the floxed calreticulin gene and heterozygous for α-MHC-CreER (genotype results are in Figure AII.1); they were littermates 3, 11, 60, 61 and 64. Mice homozygous for the floxed calreticulin gene number 257, 258, 293 and 299 were used as controls. Mice 257, 258, 3 and 11 were sent for echocardiogram testing on day 0 and again 2 weeks after tamoxifen treatment. Mouse 11 died during echocardiogram testing while under gas. The results are summarized in Table AII.1. Mice 293, 299, 60, 61 and 64 were sent for echocardiogram testing on day 0 and again 3 weeks after tamoxifen treatment. The results are summarized in Table AII.1.

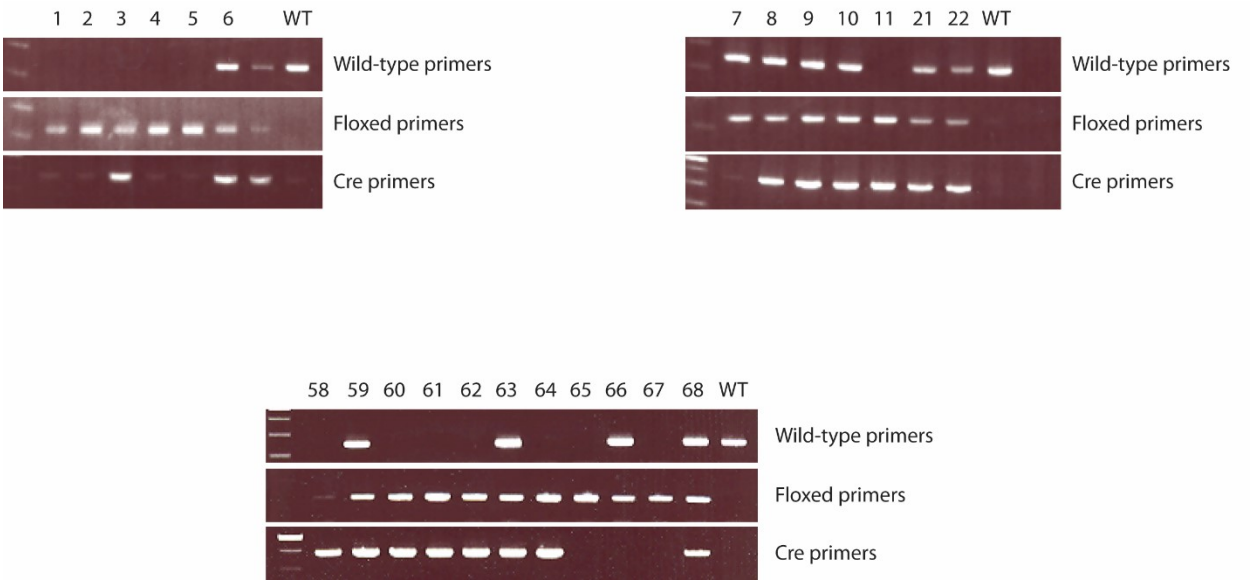

Figure AII.1 Genotype of mice offspring

Genotype of potential mice homozygous for the floxed calreticulin gene and heterozygous for α-MHC-CreER. Screening by PCR of genomic DNA was carried out with the wild-type, floxed and Cre primers.WT, wild-type control. Genotype performed by Alison Robinson.

		Before Tamoxifen		After Tamoxifen	
Measurement	**Unit**	**Control (n=4)**	***Calr*KO (n=5)**	**Control (n=4)**	***Calr*KO (n=5)**
Body weight	g	19.75±0.60	19.75±0.76	21.08±0.23	16.11±0.37
Heart Rate	bpm	441.45±16.48	458±4.86	484.07±14.91	515±16.01
LV dimensions and functions					
IVSd	mm	0.77±0.02	0.77±0.06	0.78±0.07	0.53±0.04
LVIDd	mm	3.79±0.12	3.46±0.10	3.30±0.20	4.07±0.19
LVPWd	mm	0.77±0.03	0.73±0.06	0.78±0.07	0.57±0.05
IVSs	mm	1.07±0.02	1.21±0.10	1.22±0.09	0.66±0.04
LVIDs	mm	2.72±0.10	2.03±0.11	1.71±0.31	3.61±0.26
LVPWs	mm	1.11±0.03	1.12±0.07	1.21±0.06	0.73±0.10
%EF		56.09±1.62	72.81±2.27	80.08±3.70	29.89±3.90
LV mass/bodyweight	mg/g	3.13±0.10	3.48±0.18	3.23±0.54	3.69±0.24
Mitral inflow					
E velocity	mm/sec	603.56±43.93	546.68±30.81	656.78±48.04	409.50±43.18
ME/A ratio	mm/sec	1.70±0.10	1.70±0.10	1.53±0.14	1.22*
Tei index		0.74±0.03	0.66±0.07	0.70±0.04	1.12±0.10
Pulmonary vein flow					
D wave	mm/sec	615.34±14.68	621.92±51.05	657.37±58.21	306.77±99.00
Ar duration time	msec	8.75±0.72	10.50±0.07	10.00±1.02	21.88±6.00

Numbers are mean ± standard error mean (SEM), LV, left ventricle; IVSd, intraventricular septum diastolic; LVIDd, left ventricle inner diameter diastolic; LVPWd, left ventricle posterior wall diastolic; IVSs, intraventricular septum systolic; LVIDd, left ventricle inner diameter systolic; LVPWd, left ventricle posterior wall systolic; %EF, percentage of ejection fraction; Tei index, an index of myocardial performance in systolic and diastolic fraction; Ar, arterial reverse.
*No SEM reported due to insufficient data from death of mice during experiment

Table AII.1 Summary of echocardiogram data

Summary of echocardiogram of control (mice homozygous for the floxed calreticulin gene) and Calr KO (mice homozygous for the floxed calreticulin gene and expressing cardiac specific αMHC-Cre) before tamoxifen and 2-3 weeks after tamoxifen treatment.

References

[1] N. Mesaeli, K. Nakamura, E. Zvaritch, P. Dickie, E. Dziak, K.H. Krause, M. Opas, D.H. MacLennan, M. Michalak, Calreticulin is essential for cardiac development, The Journal of cell biology, 144 (1999) 857-868.
[2] K. Nakamura, M. Robertson, G. Liu, P. Dickie, K. Nakamura, J.Q. Guo, H.J. Duff, M. Opas, K. Kavanagh, M. Michalak, Complete heart block and sudden death in mice overexpressing calreticulin, The Journal of clinical investigation, 107 (2001) 1245-1253.
[3] D. Lee, T. Oka, B. Hunter, A. Robinson, S. Papp, K. Nakamura, W. Srisakuldee, B.E. Nickel, P.E. Light, J.R. Dyck, G.D. Lopaschuk, E. Kardami, M. Opas, M. Michalak, Calreticulin induces dilated cardiomyopathy, PloS one, 8 (2013) e56387.
[4] S. Feil, N. Valtcheva, R. Feil, Inducible Cre mice, Methods in molecular biology, 530 (2009) 343-363.
[5] E. Szabo, J. Soboloff, E. Dziak, M. Opas, Tamoxifen-inducible Cre-mediated calreticulin excision to study mouse embryonic stem cell differentiation, Stem cells and development, 18 (2009) 187-193.

Appendix III – Analysis of Calcium Signaling in Mouse Ovarian Cancer Cell Lines

Ovarian cancer is a leading cause of death from gynecological cancers globally. The conventional treatment of ovarian cancer is surgery and chemo/radiotherapy and survival rate within the first 5 years is only 45%. Therefore, it is necessary to investigate new therapies that aim at eradicating cancer cells and target specific cancers such as ovarian cancer. Recent studies suggest that induction of cell surface exposure of the ER protein chaperone calreticulin can trigger anticancer immune responses [1-3]. In particular, calreticulin on the cell surface acts as a signal to dendritic and phagocytic cells for removal of the dying or apoptotic cell [1, 2]. Moreover, chemotherapeutic agents, such as anthracyclines, induce both pre-apoptotic tumor cell surface exposure of calreticulin and triggers immunogenic cell death [3]. Therefore, we characterized a variety of ovarian cancer cell lines and tumor samples (obtained as a kind gift from Dr. Vanderhyden from the University of Ottawa) as a potential model to investigate the physiological role of calreticulin in the immune response against cancer.

The ovarian cancer cell lines included the following: control mouse ovarian surface epithelial cells were designated M0510 and M1102; cell lines obtained from cre-loxP mice with induced oncogene SV40 large T-Antigen in mouse ovarian surface epithelial cells were designated MASC2 and MASE2 and tumor samples 2979 and 2983 were obtained; mouse ovarian epithelial cells expressing SV40 under the control of the mullerian inhibiting substance type II receptor promoter were designated MR TAG1 and MR TAG2 and tumor samples CG68 and CG70 were obtained; and lastly, spontaneously transformed ovarian cancer cell lines from a culture of mouse ovarian epithelial cells were designated STose and tumor samples 1505 and 1506 were obtained.

We characterized these ovarian cell lines and tumor samples by measuring the mRNA and levels of ER stress markers calreticulin, calnexin, PDIA3, IRE1, PERK, ATF6 and CHOP (Figure AIII.1). We also measured the mRNA levels spliced XBP1 in ovarian cell lines under control or

thapsigargin (0.5 μM for 24 hours) treated conditions (Figure AIII.2). The levels of mRNA were measured with the following primers:

Calreticulin forward – 5'-CGGGTGAGAGGTAGGTGAATA-3'

Calreticulin reverse – 5'-GTCCAAACCACTCGGAAACA-3'

Calnexin forward – 5'-GGCTTTGGGTGGTCTACATT-3'

Calnexin reverse – 5'-GAGCATCCGTCTTCTTGTACTC-3'

PDIA3 forward – 5'-GGTTCCTGTTGTGGCTATCA-3'

PDIA3 reverse – 5'-GATGGGTTCAGACTTCAGGTATC-3'

IRE1 forward – 5'-CCCAAATGTGATCCGCTACT-3'

IRE1 reverse – 5'-CCTTCTGCTCCACATACTCTTG-3'

XBP1 spliced forward – 5'-GAGTCCGCAGCAGGTG-3'

XBP1 spliced reverse – 5'-GTGTCAGAGTCCATGGGA-3'

PERK forward – 5'-CCCAGGCATTGTGAGGTATT-3'

PERK reverse – 5'-CCAGTCTGTGCTTTCGTCTT-3'

ATF6 forward – 5'-GGAGTGAGCTGCAAGTGTATTA-3'

ATF6 reverse – 5'-CTTCATAGTCCTGCCCATTGAT-3'

CHOP forward – 5'-TCACACGCACATCCCAAA-3'

CHOP reverse – 5'-CCTAAGTTCTTCCTTGCTCTTCC-3'

The mRNA abundance measurements are presented in the Figure AIII.1 and Figure AIII.2.

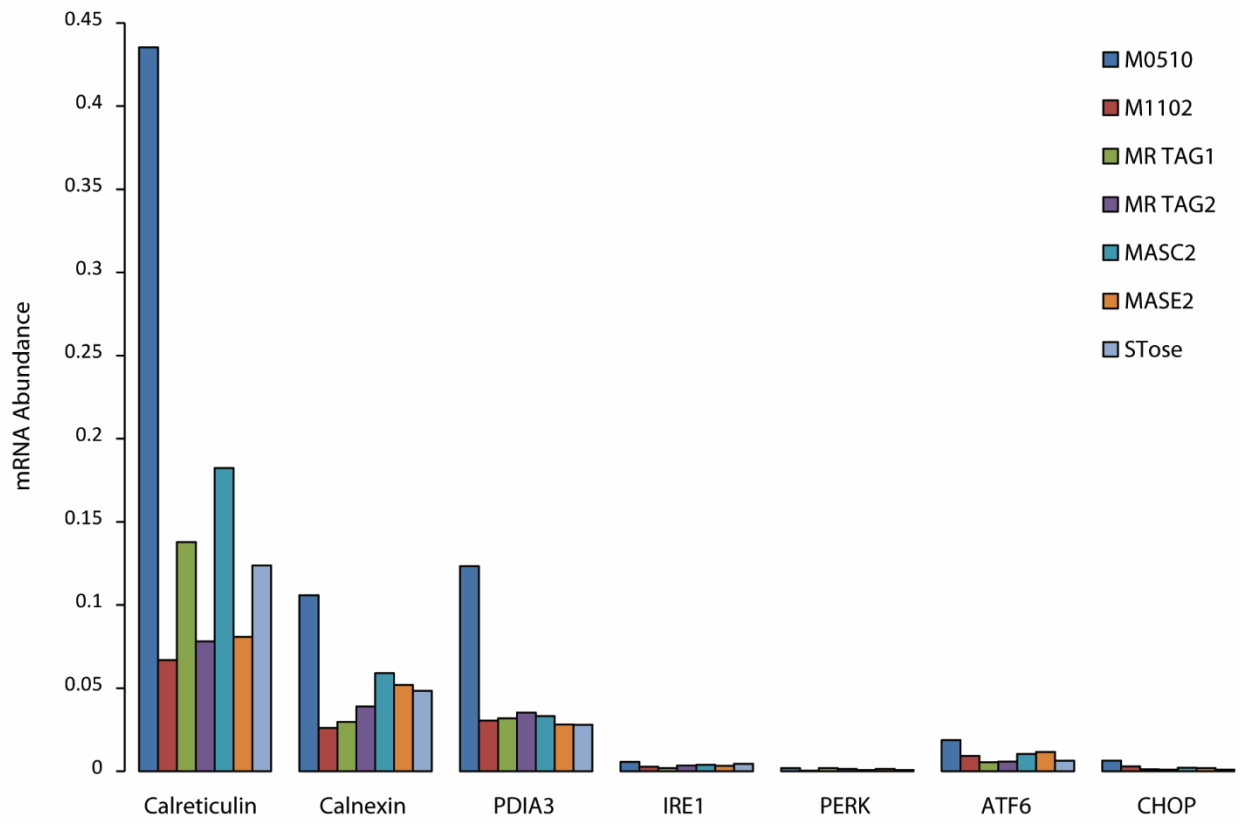

Figure AIII.1 ER stress markers in ovarian cancer cell lines

Abundance of mRNA of ER stress markers calreticulin, calnexin, PDIA3, IRE1, PERK, ATF6 and CHOP in M0510, M1102, MASC2, MASE2, MR TAG1, MR TAG2 and STose cell lines.

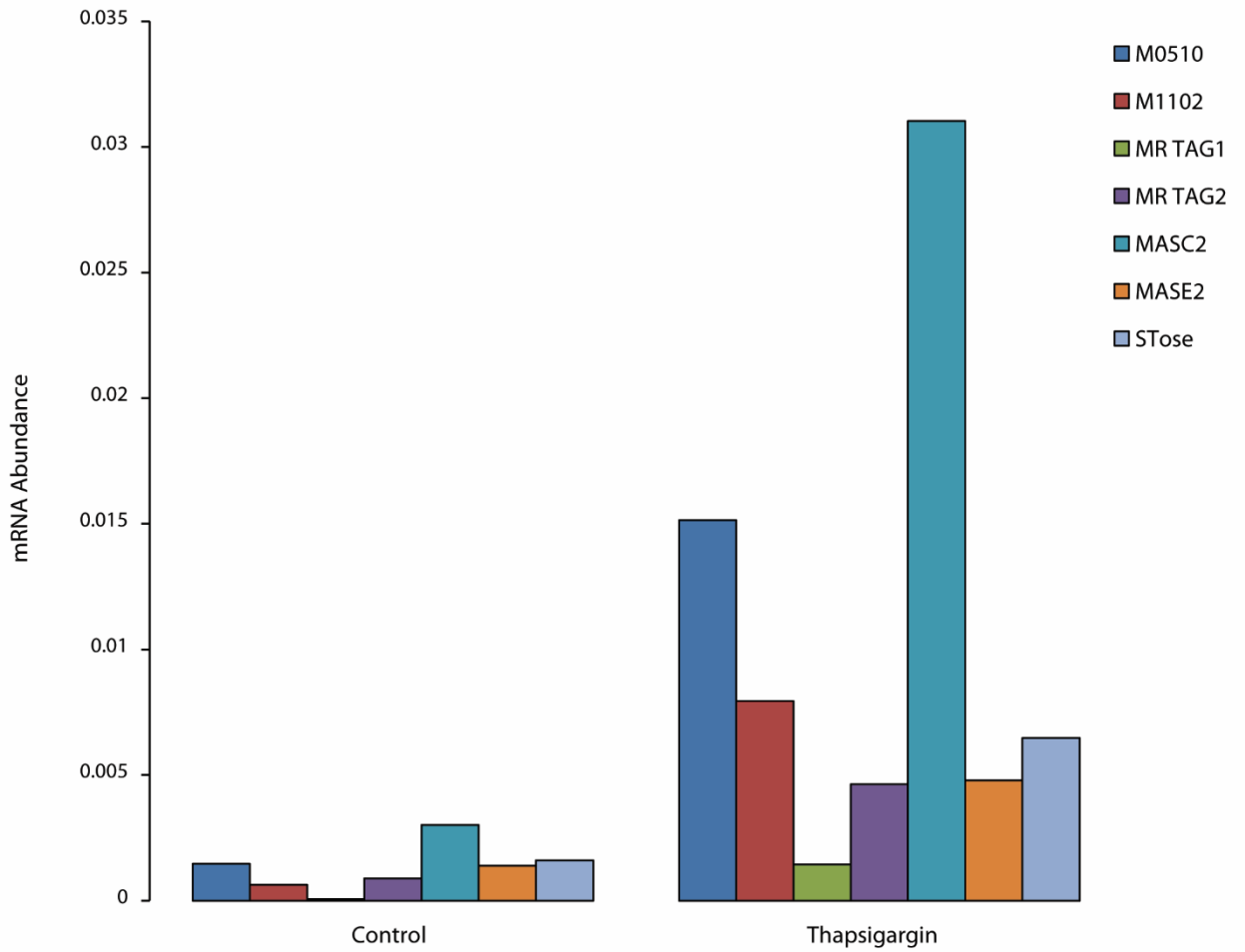

Figure AIII.2 XBP-1 splicing in ovarian cancer cell lines

Abundance of spliced XBP1 mRNA in M0510, M1102, MASC2, MASE2, MR TAG1, MR TAG2 and STose cell lines with or without thapsigargin treatment (0.5 μM for 24 hours).

Next we characterized the protein level of calreticulin within the ovarian cancer cell lines or derived tumors (Figure AIII.3). We also measured Ca^{2+} dynamics in response to ATP and thapsigargin in the ovarian cancer cell lines (Figure AIII.4) and characterized the level of STIM1 and STIM1 degradation or cleavage in response to MG-132, a proteasome inhibitor (Figure AIII.5).

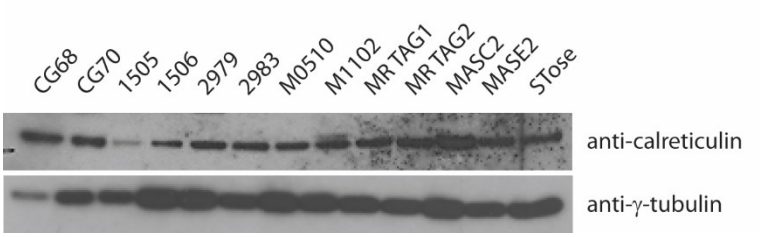

Figure AIII.3 Calreticulin protein levels in ovarian cancer cells and tumors

Immunoblot of ovarian cancer tumors CG68, CG70, 1505, 1506, 2979 and 2983 and cell lines M0510, M1102, MASC2, MASE2, MR TAG1, MR TAG2 and STose, probed with anti-calreticulin and anti-γ-tubulin antibodies.

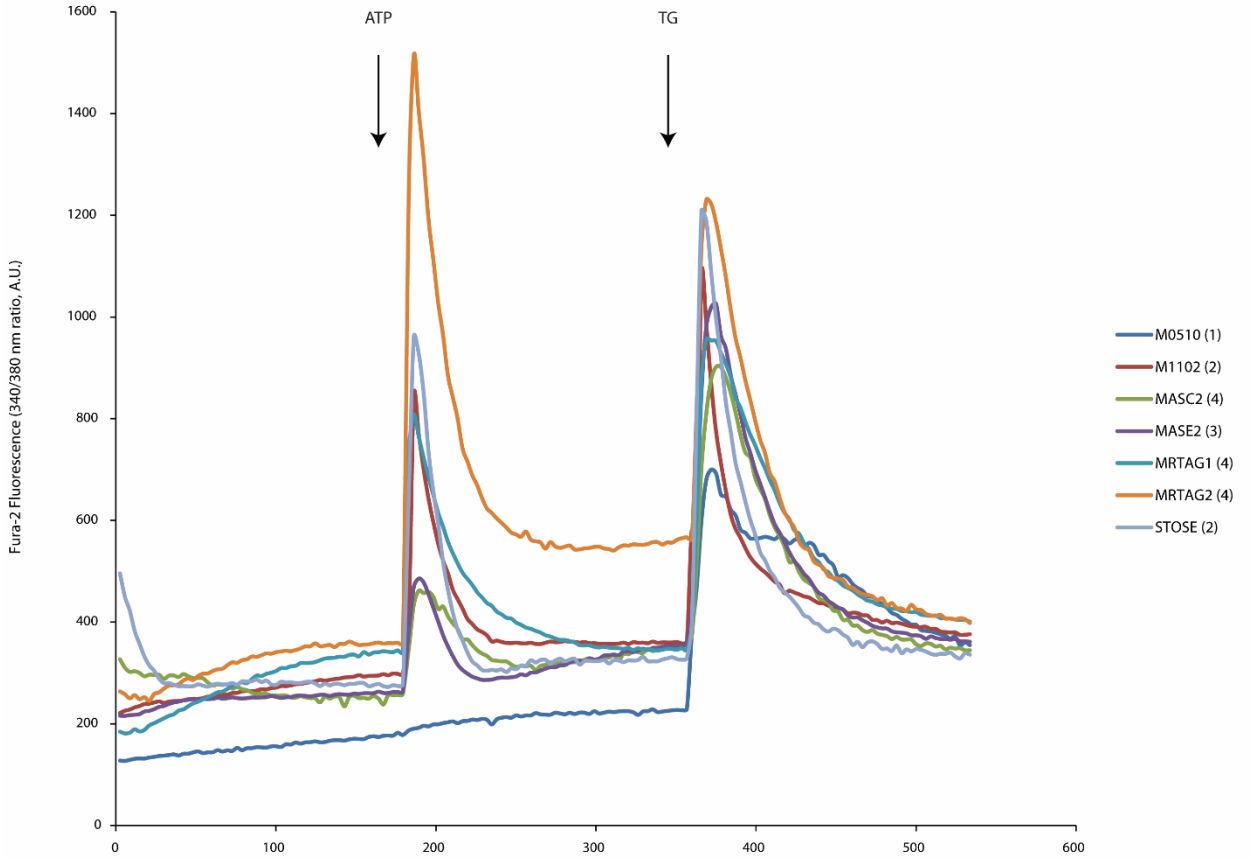

Figure AIII.4 Ca^{2+} signaling in ovarian cancer cell lines

Ca^{2+} signals induced by addition of adenosine triphosphate (ATP) and thapsigargin (TG) in M0510, M1102, MASC2, MASE2, MR TAG1, MR TAG2 and STose cell lines. Experiments were performed in Ca^{2+}-free buffer with 1 mM $CaCl_2$. Ca^{2+} measurements were performed by Daniel Prins.

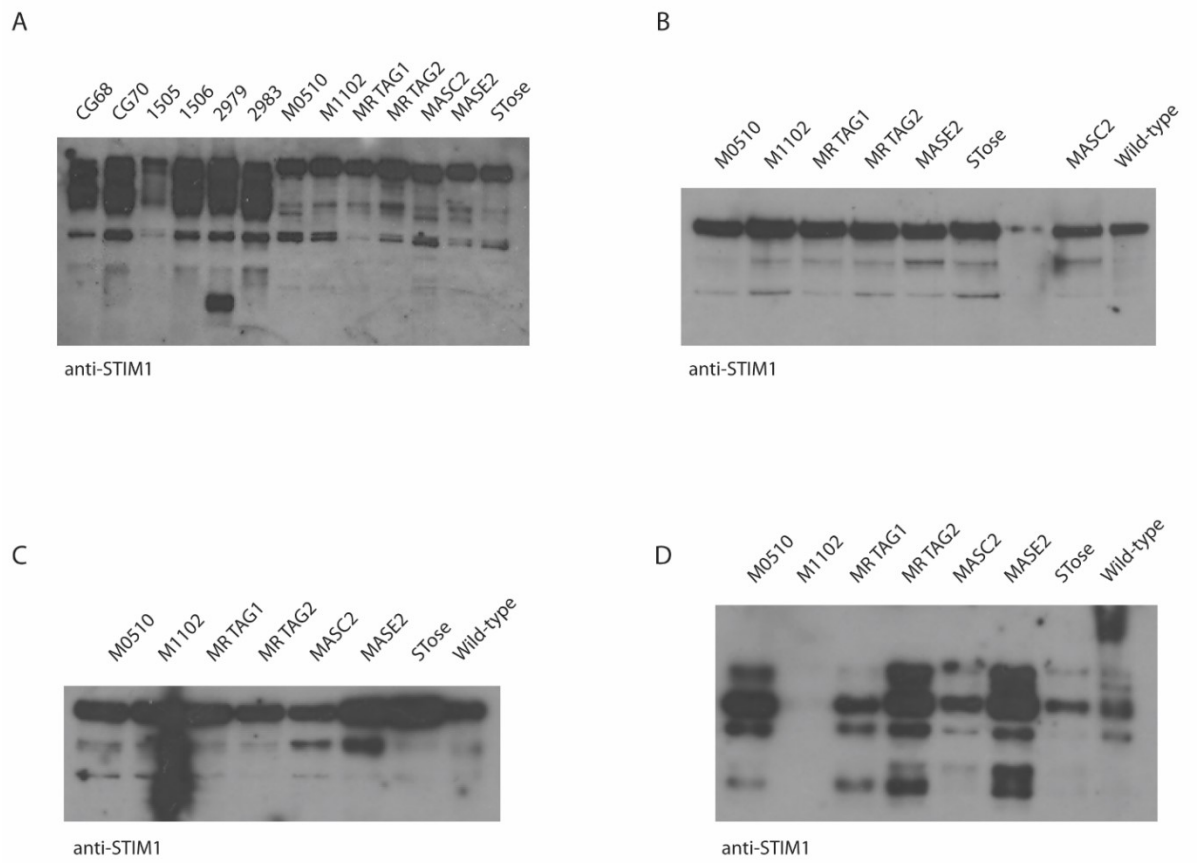

Figure AIII.5 STIM1 and STIM1 cleavage in ovarian cancer cell lines

A. Immunoblot of ovarian cancer tumors CG68, CG70, 1505, 1506, 2979 and 2983 and cells M0510, M1102, MASC2, MASE2, MR TAG1, MR TAG2 and STose, probed with anti-STIM1.

B. Immunoblot of ovarian cancer cells M0510, M1102, MASC2, MASE2, MR TAG1, MR TAG2 and STose, probed with anti-STIM1.

C. Immunoblot of ovarian cancer cells M0510, M1102, MASC2, MASE2, MR TAG1, MR TAG2 and STose treated with MG-132 (1 μM) for 24 hours, probed with anti-STIM1.

D. Immunoblot of apoptotic ovarian cancer cells (collected from the cultured media) from M0510, M1102, MASC2, MASE2, MR TAG1, MR TAG2 and STose cells treated with MG-132 (1 μM) for 24 hours, probed with anti-STIM1.

References

[1] I. Martins, O. Kepp, L. Galluzzi, L. Senovilla, F. Schlemmer, S. Adjemian, L. Menger, M. Michaud, L. Zitvogel, G. Kroemer, Surface-exposed calreticulin in the interaction between dying cells and phagocytes, Annals of the New York Academy of Sciences, 1209 (2010) 77-82.
[2] S.J. Gardai, K.A. McPhillips, S.C. Frasch, W.J. Janssen, A. Starefeldt, J.E. Murphy-Ullrich, D.L. Bratton, P.A. Oldenborg, M. Michalak, P.M. Henson, Cell-surface calreticulin initiates clearance of viable or apoptotic cells through trans-activation of LRP on the phagocyte, Cell, 123 (2005) 321-334.
[3] M. Wemeau, O. Kepp, A. Tesniere, T. Panaretakis, C. Flament, S. De Botton, L. Zitvogel, G. Kroemer, N. Chaput, Calreticulin exposure on malignant blasts predicts a cellular anticancer immune response in patients with acute myeloid leukemia, Cell death & disease, 1 (2010) e104.